NOTE TO USERS

University of Alberta

Analysis of Line Tension Measurements by the Conical Capillary Rise Method and the Study of the Behaviour of Droplets with Particles at Liquid-Liquid Interfaces

by

Samuel Oshoke Asekomhe 

A thesis submitted to the Faculty of Graduate Studies and Research in partial fulfillment of the requirements for the degree of

Master of Science

in

Chemical Engineering

Department of Chemical and Materials Engineering
Edmonton, Alberta

Spring, 2004

Your file Votre référence
ISBN: 0-612-96445-0
Our file Notre référence
ISBN: 0-612-96445-0

ABSTRACT

In order to explain better the role of solid particles in the stabilization of emulsions, understanding the placement and positioning of solid particles at liquid-liquid interfaces becomes pertinent. Using a model fluid system of silicone oil, and water with silica and glass beads as solid particles, the behaviour of a retracting drop of water/oil with particles at the interface was experimentally studied as a function of particle wettability, particle size, silicone oil viscosity and radius of the capillary introducing the drop. The behaviour of the particles and droplet was found to depend on the particle size, wettability, and the silicone oil viscosity while the droplet behaviour was not affected by the capillary diameter. One other factor that affects the positioning of particles at a fluid-fluid interface, which has often been neglected in emulsion studies, is the line tension acting at the three-phase contact line. In this study, we have also been able to improve the interpretation of line tension measurements from the capillary rise in a conical tube by including the effect of interface deformation due to gravity.

DEDICATION

"In loving memories of my beloved siblings: Blessing Asekomhe and Emmanuel Asekomhe. May your gentle souls rest perfectly in the Lord - Amen".

ACKNOWLEDGEMENT

My academic journey till date has been shaped and shared by countless others.

Just to mention a few.....

Special thanks to my supervisors Drs. Janet A. W. Elliott and Jacob H. Masliyah for their constant advice and immense support throughout my program.....thanks for always been there for me.

Thanks to the National Research Council of Canada (NRC) - Flight Research Laboratory and their staff for their immense support during the microgravity experience. Special thanks to Eric Vachon of the Canadian Space Agency. Also appreciated is the help of my research mates Colleen Chan (the microgravity "expert"), Raymond Chiang, Rick Dowell, and Amjad Ababneh. Not to forget the guys in the Oil sands group especially Jim Swarok and Leanne Swekla and of course the cryobiology guys.....thank you all for your support.

Special thanks to my dad, mum, my siblings, my cousins, aunties and uncles and my wife Opeyemi for their love, prayers, encouragement and understanding throughout this journey - how lucky am I to have you all as part of me...thanks for always been there and much love.

Thanks to Andrea Koenig - the department safety coordinator, the machine shop group, the computer support team and the other department support staffs for their support. I also would like to thank my friends for their support - Moruf, Sade, Folake, Folarin, Saheed, Tunde, Sunil, Danny, Paul, Segun, Jason, Wa'el and all those whose names are too numerous to mention. Thank you all for

your support. My profound gratitude to Isabelle Kelly and James Keene for their warmth and kindness - I cannot express how much I am grateful to you.

I would like to thank the Canadian Space Agency (CSA) and the Natural Sciences and Engineering Research Council of Canada (NSERC) Industrial Chair for Oil Sands Research for providing funding for this research.

Finally, all glory and gratitude to the Almighty God, Whose grace and love has enabled me to this day and to our Lord Jesus Christ - thank You for the sacrifice.

TABLE OF CONTENTS

CHAPTER 1: INTRODUCTION 1

1.1 Motivation 1

1.2 Literature Review 3

1.2.1 Emulsion Stability - Steric Stabilization 3

1.2.2 Role of Solid Particles in Emulsion Stability 5

1.2.3 Development of a Macroscopic Model Consisting of a Droplet with Adsorbed Solids 13

1.2.4 Role of Line Tension 14

1.3 Scope of Thesis 17

1.4 References 21

PART A: ANALYSIS OF LINE TENSION MEASUREMENTS BY THE CONICAL CAPILLARY RISE METHOD 24

CHAPTER 2: EFFECT OF INTERFACE DEFORMATION DUE TO GRAVITY 25

2.1 Introduction 25

2.2 The Conical Capillary Rise Method 29

2.3 Governing Equations for the Shape of the Interface in the Presence of Gravity 34

2.4 Numerical Implementation 40

2.5 Results and Discussion 42

2.6 Conclusions 47

2.7 References 48

PART B: STUDY OF THE BEHAVIOUR OF DROPLETS WITH PARTICLES AT THE LIQIUD-LIQUID INTERFACE 50

INTRODUCTION TO PART B 51

CHAPTER 3: MATERIALS AND METHODS 53

3.1 Introduction 53

3.2 Experimental Materials 53

3.2.1 Experimental Fluids 53

3.2.2 Solid Particles 54

3.2.3 Capillary Tubing 56

3.2.4 Syringes 56

3.2.5 Test Cells 56

3.3 Cleaning and Treatment Procedures **57**

3.3.1 Cleaning Procedure for Particles and Glassware 58

3.3.1.1 Treatment Procedure for Particles 58

3.3.1.2 Contact Angle of Particles 59

3.3.2 Cleaning Procedure for Capillary Tubes 59

3.3.3 Cleaning Procedure for Test Cells 60

3.4 Apparatus and Set-up **60**

3.5 Experimental Parameters **62**

3.6 Description of Forces Involved in Drop Behaviour **63**

3.7 References **70**

CHAPTER 4: GROUND-BASED EXPERIMENTS **72**

4.1 Ground-Based Experimental Observations **72**

4.2 Experimental Procedure **72**

4.3 Water-Droplet-in-Diluted-Bitumen System **73**

4.4 Water-Droplet-in-Silicone-Oil System **75**

4.4.1 Hydrophilic (45°) Particles in Water 75

4.4.1.1 Water Droplet with Hydrophilic (45°) Particles in 500 cSt Silicone Oil 76

4.4.1.2 Water Droplet with Hydrophilic (45°) Particles in 5 cSt Silicone Oil 78

4.4.2 Hydrophobic (125°) Particles in Water 79

4.4.2.1 Water Droplet with Hydrophobic (125°) Particles in 500 cSt Silicone Oil 79

4.4.2.2 Water Droplet with Hydrophobic (125°) Particles in 5 cSt Silicone Oil 82

4.5 Silicone-Oil-Droplet-in-Water System 85

4.5.1 Hydrophilic (45°) Particles in Oil 85

4.5.1.1 500 cSt Silicone Oil Droplet with Hydrophilic (45°) Particles in Water 86

4.5.1.2 5 cSt Silicone Oil Droplet with Hydrophilic (45°) Particles in Water 88

4.5.2 Hydrophobic (125°) Beads in Oil 89

4.5.2.1 500 cSt Silicone Oil Droplet with Hydrophobic (125°) Particles in Water 90

4.5.2.2 5 cSt Silicone Oil Droplet with Hydrophobic (125°) Particles in Water 91

4.6 Summary of Observations from Ground-Based Experiments 91

4.7 Discussion of Results from Ground-Based Experiments 92

4.7.1 Role of Particle Size 96

4.7.2 Role of Particle Wettability 97

4.7.3 Role of Viscous Effects in the Continuous Phase 97

4.8 Relation to Bitumen Studies 98

4.9 Conclusions from Ground-Based Experiments 99

4.10 References 100

CHAPTER 5: MICROGRAVITY EXPERIMENTS 101

5.1 Microgravity Experiments 101

5.1.1 Why Microgravity? 102

5.1.2 Experimental Procedures 102

5.2 Microgravity Experimental Observations 103

5.2.1 Observations from Microgravity Flight 1 104

5.2.2 Observations from Microgravity Flight 2 105

5.2.3 Observations from Microgravity Flight 3 106

5.2.4 Observations from Microgravity Flight 4 108

5.2.5 Observations from Microgravity Flight 5 109

5.2.6 Observations from Microgravity Flight 6 110

5.3 Discussion of Results from Microgravity Experiments 111

5.4 Conclusions on Microgravity Experiments 112

5.5 References 112

CHAPTER 6: CONCLUSIONS 113

6.1 Conclusions on the Analysis of Line Tension Measurements by the Conical Capillary Rise Method - The Effect of Interface Deformation Due to Gravity 114

6.2 Conclusions on the Experimental Study of the Behaviour of Droplets with Particles at the Liquid - Liquid Interfaces 115

6.3 Recommendations for Future Work 116

APPENDICES 118

A. Algorithm and Program for Numerical Solution 119

B. Experimental Pictures 123

C. Drop Detachment Calculations 130

LIST OF TABLES

2.1	Parameters used for this study	41
2.2	Average line tension values obtained from the results of this study	42
2.3	Average line tension values obtained from the work of Jensen and Li	43
2.4	Average line tension values obtained from ADSA and ACRACC	43
2.5	Comparison of the line tension values determined by various methods	47
3.1	Range of experimental parameters studied	63
3.2	Stages of drop behaviour and the forces operative in each stage	66

LIST OF FIGURES

1.1	Schematic representation of steric stabilization by particles	4
1.2	Schematic of components of crude oils and bitumen to be considered in a typical emulsion droplet and interfacial layer	5
1.3	Behaviour of a water droplet in diluted bitumen of different concentrations	10
1.4	Schematic of a small sphere at a liquid-liquid interface	16
2.1	Schematic of an axisymmetric sessile drop showing the three-phase contact line	28
2.2	The conical capillary tube	30
2.3	Force balance for a horizontal sessile drop showing the three-phase contact line	31
2.4	Force balance for a liquid rise in a conical crevice showing the three-phase contact line	31
2.5	Geometry of the conical capillary system	37
2.6	Variation of $\cos\theta$ with $(\cos\beta / R)$ for Dodecane (*FC722*)	44
2.7	Variation of $\cos\theta$ with $(\cos\beta / R)$ for Tetradecane (*FC722*)	45

2.8	Variation of $\cos\theta$ with $(\cos\beta / R)$ for Hexadecane (*FC722*)	46
3.1	Size (diameter) distribution for size #8 glass beads	55
3.2	Schematic of a test cell used for the experimental study	57
3.3	The pendant drop apparatus	61
3.4	Schematic of the original experimental set up	62
3.5	Schematic of a pendant drop with particles at the interface	64
3.6	Schematic of subsequent stages of a drop on contraction	65
4.1	Subsequent stages of drop retraction for a water droplet in 0.03% by volume bitumen diluted in 50:50 mixture of heptol	74
4.2	Schematic of a particle at an interface	76
4.3	Subsequent stages of drop retraction for a water droplet, with hydrophilic (45°) c.a. 13 (μm) diameter silica particles, in 500 cSt silicone oil	77
4.4	Subsequent stages of drop retraction for a water droplet, with hydrophilic (45°) c.a. 13 (μm) diameter silica particles, in 5 cSt silicone oil	78
4.5	Subsequent stages of drop retraction for a water droplet, with hydrophobic (125°) c.a. 13 (μm) diameter silica particles, in 500 cSt silicone oil	80

4.6 Subsequent stages of drop expansion for a water droplet, with hydrophobic (125°) c.a 13 (μm) diameter silica particles, in 500 cSt silicone oil (small capillary) 81

4.7 Subsequent stages of drop retraction for a water droplet, with hydrophobic (125°) 150 - 210 (μm) diameter glass beads, in 500 cSt silicone oil (small capillary) 82

4.8 Subsequent stages of drop retraction for a water droplet, with hydrophobic (125°) c.a. 13 (μm) diameter silica particles, in 5 cSt silicone oil (small capillary) 83

4.9 Subsequent stages of drop expansion for a water droplet, with hydrophobic (125°) c.a. 13 (μm) diameter silica particles, in 5 cSt silicone oil (large capillary) 84

4.10 Subsequent stages of drop retraction for a 500 cSt silicone oil droplet, with hydrophilic (45°) c.a. 13 (μm) diameter silica particles, in water 86

4.11 Subsequent stages of drop retraction for a 500 cSt silicone oil droplet, with hydrophilic (45°) 150 - 210 (μm) diameter glass beads, in water 88

4.12 Subsequent stages of drop retraction for a 5 cSt silicone oil droplet, with hydrophilic (45°) 150 - 210 (μm) diameter glass beads, in water 89

4.13 Subsequent stages of drop retraction for a 500 cSt silicone oil droplet, with hydrophobic (125°) 150 - 210 (μm) diameter glass beads, in water 90

5.1 Subsequent stages of drop retraction for a water droplet in microgravity with hydrophilic (45°) 150 - 210 (μm) diameter glass beads, in 500 cSt silicone oil 104

5.2 Subsequent stages of drop retraction for a water droplet in microgravity with hydrophobic (125°) 150 - 210 (μm) diameter glass beads, in 500 cSt silicone oil 107

5.3 Subsequent stages of drop retraction for a 500 cSt silicone oil droplet in microgravity with hydrophobic (125°) 150 - 210 (μm) diameter glass beads, in water 108

5.4 Subsequent stages of drop retraction for a 500 cSt silicone oil droplet in microgravity with hydrophilic (45°) 150 - 210 (μm) diameter glass beads, in water 110

B.1 Subsequent stages of drop retraction for a water droplet, with hydrophilic (45°) <105 (μm) diameter silica particles, in 500 cSt silicone oil 123

B.2 Subsequent stages of drop retraction for a water droplet, with hydrophilic (45°) 150 - 210 (μm) diameter glass beads, in 500 cSt silicone oil 123

B.3 Subsequent stages of drop retraction for a water droplet, with hydrophilic (45°) <105 (μm) diameter silica particles, in 5 cSt silicone oil 124

B.4 Schematic of subsequent stages of drop retraction for a water droplet, with hydrophilic (45°) 150 - 210 (μm) diameter glass beads, in 5 cSt silicone oil 125

B.5 Subsequent stages of drop retraction and expansion for a water droplet, with hydrophobic (125°) c.a. 13 (μm) diameter silica particles, in 500 cSt silicone oil (Large capillary) 126

B.6 Subsequent stages of drop retraction for a water droplet, with hydrophobic (125°) <105 (μm) diameter silica particles, in 500cSt silicone oil 126

B.7 Subsequent stages of drop retraction for a water droplet, with hydrophobic (125°) <105 (μm) diameter silica particles, in 5cSt silicone oil 127

B.8 Subsequent stages of drop retraction for a water droplet, with hydrophobic (125°) 150 - 210 (μm) diameter glass beads, in 5cSt silicone oil 128

B.9 Subsequent stages of drop retraction for a 500 cSt silicone oil droplet, with hydrophilic (45°) <105 (μm) diameter silica particles, in water 129

GLOSSARY OF TERMS

interface - the thermodynamic phase which separates the liquid-liquid or liquid-vapour phase

three - phase contact line - the line connecting the solid-liquid, liquid-vapour and solid-vapour interphases

microgravity - a reduced gravity condition simulated in a parabolic flight aircraft with near zero gravitational intensity

hydrophilic - contact angle less than 90^{o} (water loving)

hydrophobic - contact angle greater than 90^{o} (oil loving)

NOTATION

Bo	Bond number (defined in Equation 2.9)
D_{50}	Median particle diameter on a cumulative size distribution curve
F_B	Buoyancy force
F_{VD}	Drag force due to continuous phase viscosity
F_γ	Interfacial tension force
g	Magnitude of local acceleration due to gravity
H	Height of capillary liquid
H_m	Measured height of interface
h	Height of adsorbed particles on a drop
K_{gs}	Local geodesic curvature
N_p	Number of particles on a drop
R	Radius of the three-phase contact line
R_1, R_2	The principal radii of curvature
R_c	Capillary tube radius
R_d	Radius of a drop
R_m	Measured radius of the conical capillary at the point where the interface contacts the capillary
Var	Objective function (Equation 2.24)
V_d	Volume of a drop
V_{filled}	Volume of a drop filled with particles

V_p	Volume of a single particle
x, y z	Radial, axial and vertical coordinate of the conical capillary interface
x', y', z'	Non - dimensionalized coordinates of the conical capillary interface
Z_0	Initial height of interface on the axis of symmetry
Z_I	The capillary liquid height above the free interface

Greek Symbols

β	Cone angle (Figure 2.2)
θ	Equilibrium contact angle
θ_m	Contact angle corresponding to an infinitely large drop
σ	Line tension
γ	Interfacial or surface tension
φ	Turning angle (Figure 2.5)
ϕ	Correction factor (constant in Equation 3.2)
λ	Constant in Equation 2.20
μ	Viscosity of the continuous phase
ν	Average drop retraction velocity
$\Delta\rho$	Density difference
Δp	Pressure difference

Subscripts

sv	solid-vapour
sl	solid-liquid
lv	liquid-vapour
m	measured
I	interface
cp	continuous phase
d	droplet phase
p	particle

CHAPTER 1

INTRODUCTION

1.1 Motivation

Multiphase fluid systems are encountered in various applications and of particular importance are emulsions, which are encountered in many industries. Some important and familiar emulsions occur in the food processing industry, the petroleum industry, the cosmetic industry, and the pharmaceutical industry. In the petroleum industry for example, water-in-oil and oil-in-water emulsions are commonly encountered during the production of crude oil, the separation of fines from shale oil, and the extraction of bitumen from oil sands, and in many other oilfield operations. In oil sands processing, very stable water-in-oil and oil-in-water emulsions form during the extraction process used to recover bitumen from oil sands. In Canada, several oil sands operators use a variation of the Clark Hot Water Extraction process [1, 2]. The extraction process may be briefly described as follows: mined oil sands are digested in a hydrotransport pipeline or in a tumbler with the addition of hot water and small quantities of sodium hydroxide to facilitate bitumen liberation from the oil sand grains. The liberated bitumen droplets are recovered by air bubble attachment followed by flotation in a gravity-settling vessel where a bitumen rich froth rises to the top and is separated from most of the solids. The recovered froth consists approximately of 60% bitumen, 30% water and 10% solids by weight [3]. The froth is then diluted with naphtha, to reduce the bitumen froth viscosity, and then

centrifuged to remove most of the water and solids from the diluted bitumen. The bitumen-solvent product at this stage, which still contains about 2 - 3% residual water and 0.5% solids, is subsequently fed to the upgrading plant. The problem is that the residual water is usually in the form of very stable water-in-oil emulsion and resists coalescence under centrifugation. The residual water droplets also contain a significant amount of dissolved salts, mostly chlorides, which is carried to the downstream upgrading plant resulting in serious corrosion risks. Consequently, it is desirable to break the water-in-oil emulsion so as to coalesce the water droplets and to remove the aqueous phase prior to upgrading.

In addition, tailings are produced during the oil sands extraction process and contain water, solids and a small amount of bitumen in the form of stable oil-in-water emulsion. This represents a loss of oil and a potential environmental risk making it desirable that the tailings be treated to return them to their natural state. Hence it would be beneficial to break this oil-in-water emulsion both from the financial and environmental standpoint.

The major issue here is: what makes the emulsions so stable? Numerous studies have been done on such emulsions and their stability. There are several mechanisms by which emulsions may be stabilized including but not limited to steric stabilization by particles and electrostatic stabilization. It is understood that the positioning of particles at a fluid-fluid interface plays a crucial role in steric stabilization by particles. However, despite the large number of experimental and theoretical studies on the role of particles in emulsion stability, the stabilization

mechanism is not yet fully understood. Understanding how the emulsions' natural stabilizers and their environment can be modified to augment destabilization would be very beneficial.

1.2 Literature Review

A review of some previous emulsion studies, in particular related to emulsion stabilization and the role of solid particles in the stabilization process, is presented. The development of a macroscopic model of a solids-stabilized emulsion droplet by Chiang [4] is also discussed as a basis for this present study. Understanding the positioning of solid particles at liquid-liquid interfaces is pertinent to understanding emulsion stabilization by particles. One thermodynamic property which affects the placement of solid particles at a fluid - fluid interface is the line tension. A review of the role of line tension in the positioning of particles at interfaces is also presented.

1.2.1 Emulsion Stability - Steric Stabilization

In the process of crude oil production or bitumen extraction from oil sands, the formation of emulsions is inevitable. The degree of emulsification (amount of emulsion formed) depends on several factors including but not limited to: the energy of the process, the amounts of native surface-active components in the crude oil, and the physicochemical properties of the crude oil or bitumen, water and surfactants. The remarkable stability of emulsions is understood to result

from the presence of suitable interfacial barriers preventing coalescence of the dispersed droplets. For instance, the stability of water droplets formed during crude oil production and in bitumen extraction from oil sands is thought to be due to various species present in the crude oil or bitumen, which tend to adsorb at the interface [1]. Generally, crude oil and bitumen contain asphaltenes, resins, saturates, aromatics and fine solids. It has been suggested by many researchers [1] that the asphaltenes and/or solids form a steric sheath that covers the water droplets and offers steric stabilization against the coalescence of water droplets (as shown in Figure 1.1). Figure 1.2 shows a schematic of typical components of crude oil and bitumen to be considered in an emulsion droplet and the interfacial layer. Much of the research in emulsion stability, which focuses on the interfacial layer, describes the layer in terms of mechanical and rheological behaviour of the emulsion systems. The focus of this present study is primarily on the positioning of particles, such as silica and organic particles, at a liquid-liquid interface. This is relevant to understanding the role of solids particles present in crude oil and bitumen on emulsion stabilization.

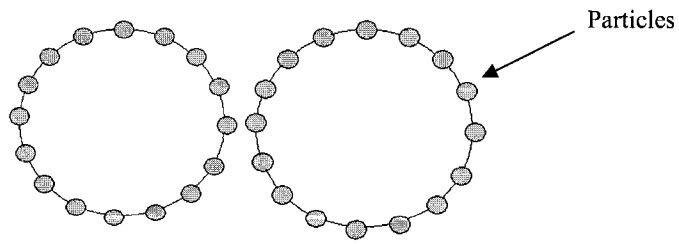

Fig.1.1: Schematic representation of steric stabilization by particles

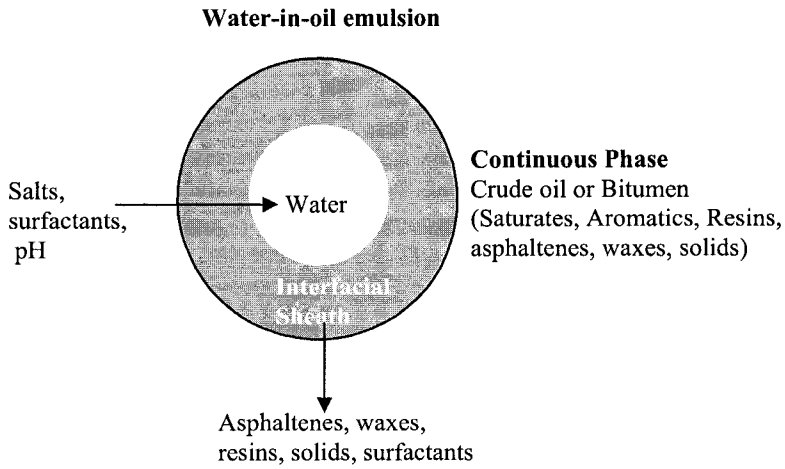

Fig.1.2: Schematic of components of crude oils and bitumen to be considered in a typical emulsion droplet and interfacial layer (adapted with modifications from Angle [5])

1.2.2 Role of Solid Particles in Emulsion Stability

The knowledge that solids can stabilize emulsions dates back to the beginning of the 20th century when Pickering [6] originally noted that particles of colloidal dimensions that are wetted more by water than by oil could act as an emulsifying agent for oil-in-water emulsions. Ramsden [7], in an earlier study, concluded that the stability of many emulsions could be attributed in part to "the presence of solid or highly viscous matter at the interfaces of the two liquids". Since then, several investigators have studied the stability of solids-stabilized emulsions.

Briggs [8] investigated the role of crystalline ferric oxide, carbon black, and silica in the stability of water-benzene and water-kerosene emulsions. He

observed that silica stabilized oil-in-water emulsions while carbon black stabilized water-in-oil emulsions. However, whenever appropriate quantities of silica and carbon black were mixed, the resulting mixture did not stabilize emulsions. He concluded that for finely divided solids to stabilize an emulsion, it was necessary for the solids to concentrate at the interfaces.

Finkle et al. [9] studied the stability of oil-in-water emulsions by linking the type of emulsions formed to the wettability of the particles. They reported that water-wet particles stabilized oil-in-water emulsions, while oil-wet particles stabilized water-in-oil emulsions. However, it was the experimental work of Schulman and Leja [10] that demonstrated conclusively the effect of particles' wettability on emulsion type. Using benzene, water and barium sulfate particles of various contact angles, measured through the aqueous phase in their studies, they concluded that if the contact angle at the oil-water-solid interface were slightly less than 90^{o}, the particles would tend to stabilize oil-in-water emulsions. Whereas, if the three-phase contact angle were slightly greater than 90^{o}, the particles stabilized water-in-oil emulsions. In the same experiment, Schulman and Leja also observed that the size of the particles used is an important factor in the emulsification process. They reported that the barium sulfate particles had to be less than one micron in diameter in order to obtain good emulsions.

Yan et al. [1] in a recent study on the roles of various bitumen components in the stability of water-in-diluted bitumen emulsion found that asphaltenes and fine solids were the main stabilizers of water-in-diluted bitumen emulsions. The two

components can stabilize water-in-diluted bitumen emulsions independently. Without either of them, the capacity of diluted bitumen to stabilize emulsified water decreases. They also found solids larger than 8 microns do not affect water-in-diluted bitumen emulsion stability while solids that were removed by 0.22 micron filter paper, but not removed with the 8 micron filter paper, are capable of stabilizing emulsions. They concluded that only solid particles in a certain size range were effective stabilizers.

Lucassen-Reynders and Tempel [11] studied the behaviours of emulsions prepared with paraffin oil, water, crystals of glycerol tristearate, and small amounts of surfactants. The concentrations of surfactants used were so low that there was no appreciable stabilizing effect in the absence of tristearate crystals. They observed that the stability of emulsions formed were maximum when both surfactant and crystals were used and concluded that emulsions may be stabilized by solid particles only if the particles are in a state of incipient flocculation. No emulsions could be formed if the system was either completely flocculated or completely deflocculated.

Gelot et al. [12] made an extensive investigation of the effect of various combinations of finely divided solids and surface-active agents on the stability of water-oil emulsions. They used carbon black, kaolinite, bentonite, toluene, water and various surfactants in their study and observed that kaolinite and bentonite, both hydrophilic particles, stabilized oil-in-water emulsions, while carbon black, which is hydrophobic, stabilized water-in-oil emulsions. They concluded that the

type of emulsion formed (water-in-oil or oil-in-water) is dependent on the type of solid used.

Several investigators studied the mechanism of particle stabilization by considering the thermodynamic aspects of the stabilization process. Tadros et al. [13] studied the mechanism by which solid particles stabilize emulsions by considering the free energies involved when a particle is displaced from the oil-water interface into either of the bulk phases. After free energy minimization, they concluded that particles would tend to remain at the interface when the equilibrium three-phase, oil-water-solid contact angle is 90^{o}. For coalescence to occur particles will have to be displaced into either of the bulk phases. This process requires additional energy and hence provides a barrier to coalescence.

Levine and Sanford [14] presented a very detailed theory of the energy of adsorption for solid particles at the oil-water interface, which included the interaction between particles and droplets; and concluded that in a stable emulsion, almost the entire oil-water interface must be covered with particles. Levine et al. [15] further presented both theoretical and experimental investigations of some of the physicochemical mechanisms governing the stability of colloid-stabilized oil-water emulsions. From their thermodynamic analysis on particle partitioning between the bulk phase and the oil-water interface, they concluded that, "an isolated spherical particle with an appropriate three-phase contact angle is trapped in a deep energy well at the interface of an oil-water emulsion droplet". As a consequence of these large adsorption energies,

the equilibrium partitioning of particles between the interface and the bulk phase requires that the particles form a close packed two-dimensional structure at the oil-water interface.

Denkov et al. [16] presented an analysis for a possible mechanism by which colloidal particles stabilized emulsions in which they reported that the capillary pressure arising from the deformation of the liquid interface around the adsorbed particles when the liquid is squeezed out of the thin film could be a major factor controlling the drainage of the liquid films trapped between coalescing emulsion droplets. Their analysis was done for a monolayer of particles pressed between the interfaces of two emulsion droplets.

Dabros et al. [17] recently proposed that emulsification requiring very little input energy can be induced at an oil-water interface that is initially in a state of equilibrium. This new mechanism of emulsification involves destabilization, through contraction, of local interfacial regions. Using diluted bitumen and water, a micropipette was used to form a water droplet in the oil phase and the droplet was allowed to age, after which it was subjected to area contraction by retracting the droplet into the micropipette by suction. They observed that in solutions with low concentrations of bitumen, the interface between the water droplet and diluted bitumen crumples like a paper bag while in solutions with higher bitumen concentration, the formation of smaller emulsion droplets from the parent emulsion droplet was observed with the droplet remaining spherical upon retraction (See Figure 1.3).

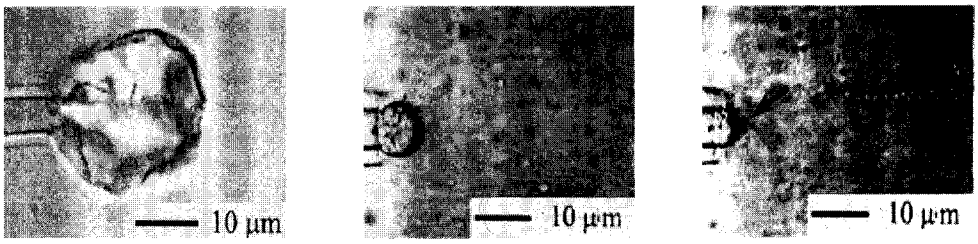

(a) Crumpling at low bitumen concentration

(b) 'Dimpling' at high bitumen concentration

(c) small emulsion droplet forms

Fig.1.3: Behaviour of a water droplet in diluted bitumen of different concentrations (adapted with permission from Dabros et al. [17])

They proposed a new mechanism of emulsification involving destabilization, through area contraction, of local interfacial regions. Although this phenomenon was observed, the role of particles at the interface in this mechanism of emulsification is not well understood.

Some researchers have attributed the stabilization of solids-stabilized emulsions to the formation of complex structures at the oil-water interface. Tsugita et al. [18] obtained an oil-water emulsion using a combination of sodium montmorillonite and polar organic compounds such as glycerol monopalmitate and ethylene glycol monostearate. They found that the complexes formed between the particles and the organic compounds, surrounded the oil droplets and that the droplets were fixed by a network structure formed by the interaction of sodium montmorillonite platelets in the aqueous phase. Menon and Wasan [19] reported that the stability of water-in-oil emulsion stabilized by colloidal clay particles depended on the formation of a network of complex structures at the oil-water interface. Such structures sustained the particles at the oil interface. The

stability of the emulsions formed depended on the strength of the interfacial network of particles.

Blair [20] suggested that solid materials found in petroleum oils, such as clays, sands and minerals, contribute to the stability of crude oil-brine emulsions. He attributed the principal source of stability to the formation of a condensed and viscous interfacial film at the oil-water interface, which prevents emulsion droplets from coalescing. Bartell and Niederhauser [21] investigated the physical characteristics of the interfacial film formed between crude petroleum oils and water. They found that the interfacial films possessed considerable strength, because they could be repeatedly contracted and expanded by advancing and receding a drop of crude oil suspended from a glass tip in water. However they concluded that, in as much as the formation of the interfacial films was accompanied by an appreciable lowering of the interfacial tension of the oils, these films were formed by an adsorption process. Reisberg and Dosscher [22] in their study on the interfacial behaviour of crude oil-water systems, using the crude oil from Ventura County, California, concluded that the interfacial tension of the oils could be affected by aging, contraction and expansion of the interface, and the pH of the aqueous phase.

Menon and Wasan [23] in a review of the factors affecting the stability of solids-stabilized emulsions concluded that, for solids-stabilized emulsions, some of the factors affecting the stability of these emulsions include the particles' wettability, solids concentration, and particle size. The adsorption of natural

surface active components such as asphaltenes from crude oil and bitumen onto mineral surfaces renders the particles hydrophobic. These hydrophobic particles are partially responsible for the stability of water-in-oil emulsions. Thus in addition to acting as emulsifying agents, asphaltenes convert otherwise water-wet particles into oil-wet particles, which then act as emulsifying agents for water-in-oil emulsions.

Other investigators have also studied the effect of pH of the aqueous phase as well as the effect of temperature on the stability of emulsions. Johansen et al. [24] performed an extensive study on the effect of pH on the stability of water-in-crude oil emulsions. Using brines containing sodium, calcium, potassium, magnesium, barium, and chloride as the aqueous phase, they reported that emulsions were most stable at very high and very low pH values. Intermediate values appeared to cause instability. Strassner [25] made similar conclusions in his study on the effect of pH on interfacial films and stability of crude oil-water emulsions. Johansen et al. also found that emulsions were more stable at low temperature than at high temperature. At high temperatures, the viscosity of the continuous phase decreased substantially, hence facilitating collisions between aqueous drops. Destabilization will result if these enhanced collisions result in increased coalescence. They then concluded that "an important individual parameter governing the stability of crude oil-water emulsions appears to be crude oil viscosity".

1.2.3 Development of a Macroscopic Model Consisting of a Droplet with Adsorbed Solids

It is well known that one of the factors affecting the stability of emulsions is the presence of fine particles, which adsorb at the fluid interface. However, due to the small size of these particles, most of the studies on solid-stabilized emulsions have been at the microscopic level. By reducing the gravitational force exerted on the droplets and particles, it is possible to enlarge the emulsion droplet system such that the particles on the interface can be observed optically.

Such an enlarged model of a solids-stabilized emulsion droplet was developed by Chiang [4] using silicone oil, de-ionized water and glass beads. Silicone oil of 500 centistokes (488 mPa.s) and glass beads with approximately 150 - 210 micron diameters were used in their studies. A drop of one liquid phase, representing the dispersed phase, is formed in the other liquid phase, the continuous phase, with beads introduced through the dispersed phase by means of a capillary tube. The droplet is then subjected to retraction and the behaviour of the droplet is captured by means of a camera. Ground based as well as microgravity experiments were performed with the model. The microgravity experiments were performed aboard a modified Falcon 20 aircraft, which produces near-zero gravity environments, by flying in a parabolic path. Chiang observed that the model system exhibited similar coalescence behaviour to the well known behaviour of solids-stabilized emulsion systems. The model system also showed that when hydrophobic beads start from the water phase, they do not

get to the interface spontaneously but rather an additional energy is required to force the beads on to the interface. They attributed the behaviour of beads at the interface to the combined effects of line tension, van der Waals forces, and film drainage.

In this present study, the enlarged model system developed by Chiang [4] will be used. However, the present studies further investigate the effect of various particle sizes, the size of the capillary tube introducing the droplet and the silicone oil viscosity, on the behaviour of the droplet during retraction and expansion.

1.2.4 Role of Line Tension

One phenomenon contributing to the positioning of small solid particles at fluid-fluid interfaces, and hence emulsion stabilization by particles, that has often been neglected in emulsion studies is the line tension that exists in the three-phase contact line.

Yan et al. [26] performed a study on water-in-oil emulsions stabilized by fine solids of different hydrophobicities with model organic solvents. The fine solids used in their study included kaolinite clay particles treated with asphaltenes, hydrophilic and hydrophobic colloidal silica, hydrophobic polystyrene latex microspheres, as well as fumed silica dry powder treated with silanization. Light mineral oil (Bayol - 35), decane and toluene were used as organic solvents. They observed that hydrophilic colloidal silica particles could only stabilize

oil-in-water emulsions for a short period of time. And if hydrophobic particles (colloidal silica or polystyrene latex microspheres) were suspended in the aqueous phase prior to emulsification, they could only produce oil-in-water emulsions. They also observed that only particles with intermediate hydrophobicities could produce very stable water-in-oil emulsions. They concluded that the stability and type of emulsions stabilized by solids depend not only on the hydrophobicity of the particles but the phase they reside in prior to emulsification.

Chiang and Elliott [27, 28] attributed the inability of hydrophobic particles, which start in the aqueous phase prior to emulsification, to stabilize water-in-oil emulsions to the combined effect of line tension and van der Waals forces. They concluded "when hydrophobic particles start in the water phase, they can behave similarly to hydrophilic particles, and stabilize oil-in-water emulsions rather than water-in-oil emulsions, due to the combined effect of line tension and van der Waals forces". Aveyard et al. [29] in their studies on the wettability of spherical particles at liquid surfaces have shown that the ability of a particle to enter a liquid interface and the contact angle established after entry are dependent on the existence and magnitude of the line tension of the three-phase contact line.

Line tension is the one-dimensional analogue of surface tension acting to minimize the length of a three-phase line (Fig.1.4). The existence of a positive line tension in the three-phase contact line around a solid spherical particle

resting in a fluid-fluid interface can influence the contact angle or the wettability of the fluid interface with the solid particle. If the particle is small and line tension is sufficiently large, the particle can become thermodynamically unstable in the interface or can be prevented from entering the interface because significant activation energy exists for entry.

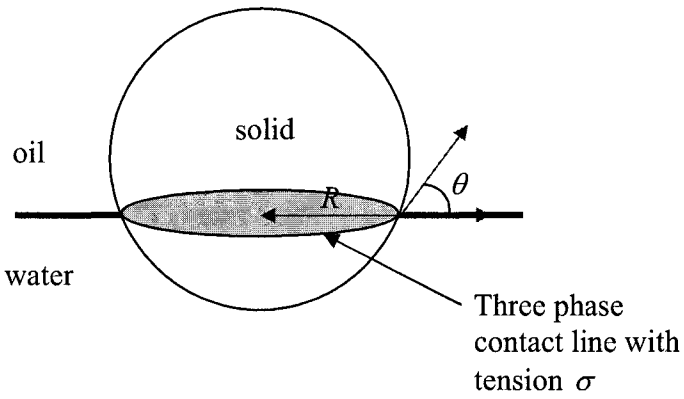

Fig.1.4: Schematic of a small sphere at a liquid-liquid interface

The magnitude of line tension and a method whereby it can be reliably measured are still under debate. Recently, Jensen and Li [30] proposed a method of measuring line tension which involves observing the height to which a liquid rises in a conical capillary tube (Conical Capillary Rise method) and converting the measured data into line tension. Here, capillary rise (caused by the balance between surface forces and the weight of a column of fluid) causes fluid to rise in a capillary with an inverted conical shape, while line tension retards the rise. In converting the measured height to a value of line tension, Jensen and Li assumed the interface meniscus to be spherical (assuming gravity effects do not play a

role). However in order to measure line tension, one requires a system that is large enough to enable measurements and in such systems, gravitational effects can not be ruled out. Ward and Sasges [31, 32] have recently shown, both theoretically and experimentally, that gravitational effects play a large role in determining fluid behaviour in right cylindrical capillaries.

In this present study, the work of Jensen and Li is generalized to include the effect of interface deformation due to gravity on the interpretation of line tension measurements inferred form the conical capillary method.

1.3 Scope of Thesis

From the brief review presented above, it is evident that solids-stabilized emulsions have been the subject of extensive study. The following concepts appear to be well established:

1. It is essential to have particles at the interface before any solids-stabilization can take place for solids-stabilized emulsions. The ability of these particles to transfer to the interface and remain there in a state of mechanical equilibrium depends largely on the properties of the fluids and /or the solids involved.
2. Water-wet particles tend to stabilize oil-in-water emulsions while oil-wet particles stabilize water-in-oil emulsions.

3. The formation of a rigid and protective interfacial film, possessing certain interfacial rheological properties, appears to be of fundamental importance to the stability of the emulsions.
4. Only colloidal particles (of the order of a few microns and less) can effectively act as emulsion stabilizers.
5. Line tension plays a significant role in the placement of colloidal particles at fluid interfaces and hence in the stability of solids-stabilized emulsions

However, despite the large number of studies on the role of solid particles in emulsion stability, the mechanism by which these particles stabilize emulsions is not yet fully understood. Questions about the nature and activity of the interfacial film of solid particles involved in the protective skin associated with bitumen-water emulsions, and the positioning and behaviour of these particles, when the emulsion droplet is subjected to, for instance, contraction, expansion and shearing of the interface, require better understanding.

Using a model emulsion drop system, in which the interfacial adsorbed particles can be controlled, will provide useful information which can be linked to the behaviours of real emulsion systems. It is believed that understanding how these particles position themselves at the interface and the behaviour of the droplet when subjected to shearing will be critical to understanding the behaviour of emulsion systems in general. A fundamental understanding of the behaviours

of emulsions and factors governing the stability of emulsions in general is essential and of economic importance not only to the oil industry but other related industries.

The goals of this thesis are:

- *Theoretically determine the impact of interface deformation due to gravity on the interpretation of line tension measurements performed in the laboratory*. In this thesis, the work of Jensen and Li [30] on the conical capillary rise method of line tension measurement is generalized to include the effect of deformation of the liquid-vapour interface due to gravity. A thermodynamic formulation is derived for the equilibrium of a curved interface in a conical capillary under the effect of gravity. The governing equations for the shape of the interface in the presence of gravity are developed. From these equations and from the geometry of the conical capillary system, a method for predicting the shape of the curved interface is developed which includes an iterative scheme to find two boundary conditions, which are not known a priori.

- *Observe and explain the behaviour of droplets with adsorbed particles, during retraction and expansion, both in the presence of gravity and in reduced gravity*. Here liquid droplets of silicone oil, water and/or diluted bitumen along with solid glass beads or silica particles are studied. A pendant drop of a one liquid phase in another continuous liquid phase,

with solids placed at the liquid-liquid interface, is subjected to both expansion and retraction and the behaviours of the drop and particles observed as a function of: the particles' wettability, particle size, capillary size, and silicone oil viscosity, using a video camera. The observed behaviours are then compared to known behaviours of solids - stabilized emulsion droplets.

The thesis has been structured into two parts as follows: Part A discusses the analysis of line tension measurement by the conical capillary rise method and the impact of interface deformation due to gravity on the interpretation of line tension measurements by the conical capillary rise method. In chapter 2, the governing equation for the equilibrium shape of a curved interface in a conical capillary tube under the effect of gravity, and a method for predicting the shape of the curved interface are developed.

Part B describes the study on the behaviour of droplets with particles at the interfaces. Chapters 3 through 5 report an experimental study of droplets with adsorbed particles during retraction and expansion. In Chapter 3, the materials used for the experimental study as well as the preparation procedures and experimental techniques are presented. The ground based experiments and observations are given in Chapter 4 while Chapter 5 reports the microgravity experiments and observations. In Chapter 6, the conclusions made from both the theoretical line tension and experimental droplet studies are outlined.

1.4 References

[1] Z. Yan, J.A.W. Elliott, and J. H. Masliyah, J. Colloid Interface Sci., 220 (1999) 329-337.

[2] G. Gu, Z. Xu, K. Nandakumar, and J. H. Masliyah, Fuel, 81 (2002) 1859-1869.

[3] J. Czarnecki, "Water-in-oil emulsions in recovery of hydrocarbons from oil sands", in J. Sjoblom (Ed.), Encyclopedic Handbook of Emulsion Technology, Chapter 3, (2001), 59-70.

[4] R. Chiang, "Development of a macroscopic model of solids-stabilized emulsion", M. Sc. Thesis, University of Alberta, Fall (2003).

[5] C. W. Angle, "Chemical demulsification of stable crude oil and bitumen emulsions in petroleum recovery - A review" in J. Sjoblom (Ed.), Encyclopedic Handbook of Emulsion Technology, Chapter 24, (2001), 541-594.

[6] S. U. Pickering, J. Chem. Soc., 91 (1907) 2001.

[7] W. Ramsden, Proc. R. Soc. (London), 72 (1903) 156.

[8] T. R. Briggs, J. Ind. Eng. Chem., 13 (11) (1921) 1008.

[9] P. Finkle, H. D. Draper and J. H. Hildebrand, J. Am. Chem. Soc., 45 (1923) 2780.

[10] J. H. Schulman and J. Leja, Tran. Faraday Soc., 50 (1954) 589.

[11] E. H. Lucassen-Reynders, and M. Van der Tempel, J. Phys. Chem., 67 (1) (1962) 731.

[12] A. Gelot, W. Friesen and H. A. Hamza, Colloids Surface, 12 (1984) 271.

[13] T. F. Tadros and B. Vincent, in P. Becher (Ed.), Encyclopedia of Emulsion Technology (1983), P. 129.

[14] S. Levine and E. Sanford, Can. J. Chem. Eng., 58 (1985) 622.

[15] S. Levine, B. Bowen and S. Partridge, Colloids Surfaces, 38 (1989) 325.

[16] N. D. Denkov, I. B. Ivanov, and P. A. Kralchevsky, J. Colloid Interface Sci., 150 (2) (1992) 589

[17] T. Dabros, A. Yueng, J. Masliyah and J. Czarnecki, J. Colloid Interface Sci., 210 (1999) 222.

[18] A. Tsugita, S. Takemoto, K. Mori and Y. Otami, J. Colloid Interface Sci., 95, (1983) 551.

[19] V. B. Menon and D. T. Wasan, Sep. Sci. Technol., 23, (1988) 2131.

[20] C. M. Blair, Chem. Ind., 20 (1960) 538.

[21] F. E. Bartell and D. O. Niederhauser, "Film forming constituent of crude petroleum oils", American Petroleum Institute progress report on Fundamental research on occurrence and recovery of petroleum, (1946-1947), P. 57-80.

[22] J. Reisberg and T. M. Doscher, "Interfacial Phenomena in crude oil systems", Producers monthly, November, (1956), P. 43-51.

[23] V. B. Menon and D. T. Wasan, Colloids Surfaces, 23 (1987) 353.

[24] E. J. Johansen, M. I. Skjarvo, Toreirlund, J. Sjoblom, H. Soderlund and G. Bostrom, Colloids Surfaces, 34 (1988) 353.

[25] J. E. Strassner, J. Pet. Technol., March (1968), 303.

[26] N. Yan, M. R. Gray, and J. H. Masliyah, Colloids Surfaces A: Physicochem. Eng. Aspects, 193 (2001) 97.

[27] R. Chiang and J. A. W. Elliott, "A macroscopic studies of solids-stabilized emulsion droplet", Paper presented at the NSERC Oil sands technical forum, University of Alberta, Dec. 5th (2002).

[28] R. Chiang and J. A. W. Elliott, "A macroscopic solids-stabilized emulsion droplet analogue in microgravity", 6th Japan - Canada workshop on space technology, Hamamatsu, Japan, November 18 - 20, (2002).

[29] R. Aveyard, B. D. Beake, and J. H. Clint, J. Chem. Soc., Faraday Trans., 92 (1996) 4271.

[30] W. C. Jensen and D. Li, Colloids Surfaces A: Physicochem. Eng. Aspects, 156 (1999) 519.

[31] C. A. Ward and M. R. Sasges, J. Chem. Phys., 109(9), (1998), 3651.

[32] C. A. Ward and M. R. Sasges, J. Chem. Phys., 109(9), (1998), 3661.

PART A:

ANALYSIS OF LINE TENSION MEASUREMENTS BY THE CONICAL CAPILLARY RISE METHOD

CHAPTER 2

EFFECT OF INTERFACE DEFORMATION DUE TO GRAVITY

2.1 Introduction

Over the last decade and indeed the last century, many studies on the wetting characteristics of solid surfaces have been performed not only from fundamental aspects but also from practical ones. The measurement of interfacial tension of fluid interfaces as well as the contact angle formed between the fluid interface and a restricting wall remains of key importance in surface and colloidal science.

One fundamental thermodynamic property of key importance in surface science, which has attracted much study, is the line tension in a three-phase equilibrium system. Analogous to surface tension for a two-dimensional surface, line tension may be defined as the one-dimensional excess energy per unit length of a three-phase contact line or alternatively, as the tensile force acting in a one-dimensional three-phase contact line (directed tangentially to the contact line) and tending to minimize the length in much the same way as the surface tension tends to minimize the surface area [1, 2].

The major content of this chapter has been published as: S. O. Asekomhe and J. A. W. Elliott, "The Effect of Interface Deformation Due to Gravity on Line Tension Measurements by the Capillary Rise in a Conical Tube" in the Journal of Colloids and Surfaces A: Physicochemical and Engineering Aspects, Vol. 220, Issue 1-3, June 2003, Pgs. 271-278.

Gibbs' pioneering work on the thermodynamics of three-phase systems remains the fundamental basis for line tension analysis. He noted that the three-phase contact line plays an important role in three-phase systems, and that this contact line should be treated in a manner similar to that in which surfaces of discontinuity are treated [1]. Essential progress in the experimental as well as the theoretical analysis of line tension problems has been achieved in recent years and details can be found in [3]. Unfortunately, despite these advances, the sign, magnitude and significance of line tension remains as contentious and controversial as ever.

Various techniques have been employed in the determination and study of line tension for solid-liquid-vapour systems; however none of these techniques has measured line tension directly. The line tension was either determined based on contact angle measurements or investigation of the size dependence of the contact angle of liquid drops (or gas bubbles) on a solid surface [4 - 6] and the examination of a profile in the vicinity of the three-phase contact line [7, 8].

The most popular and perhaps the most controversial technique is based on the examination of the drop size dependence of contact angle and calculation of the line tension from the modified Young's equation, which is the mechanical equilibrium condition for a three-phase sessile drop system on an ideal horizontal solid surface:

$$\cos\theta = \cos\theta_{\infty} - \left(\frac{\sigma}{\gamma_{IV}}\right)\left(\frac{1}{R}\right)$$

where

$$\cos\theta_{\infty} = \frac{\gamma_{SV} - \gamma_{SI}}{\gamma_{IV}} \qquad (2.1)$$

Here, R is the radius of the three-phase contact line, σ is the line tension, θ is the equilibrium contact angle and θ_{∞} is the contact angle corresponding to an infinitely large drop i.e., $R = \infty$. γ_{IV}, γ_{SV} and γ_{SI} are the interfacial tensions of the liquid-vapour, solid-vapour and solid-liquid interfaces respectively.

For a given solid-liquid-vapour system, $\cos\theta_{\infty}$ is a constant and if $\left(\frac{\sigma}{\gamma_{IV}}\right)$ is also taken as constant, then Equation (2.1) indicates a linear relationship between the cosine of the contact angle ($\cos\theta$) and the reciprocal of the radius (R) of the three-phase contact line (as shown in Figure 2.1).

The line tension can thus be calculated from the slope of a plot of $\cos\theta$ vs. $\left(\frac{1}{R}\right)$. The technique described, otherwise known as the sessile drop method, has been used experimentally to measure the line tension of various solid-liquid-vapour systems and the line tension values were mostly positive and of the order of $1\mu Jm^{-1}$ [4, 6, 9].

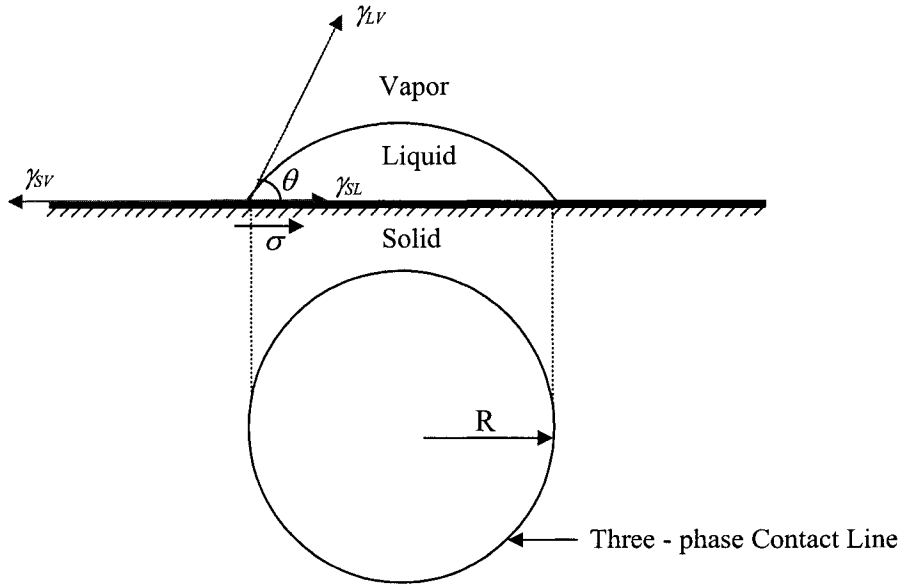

Fig.2.1: Schematic of an axisymmetric sessile drop showing the three - phase contact line

A substantial difficulty, however, arises from the measurement of such an extremely small quantity as line tension, which requires measurements at very small R requiring very high accuracy approaching the resolution limit of the instruments used. Also difficulties associated with the correct determination of line tension may result from non-equilibrium conditions [10]. The drop size dependence of contact angle is also generally small; as a result, highly sophisticated instruments and techniques are required for accurate measurements. One such technique is the automated Axisymmetric Drop Shape Analysis (ADSA) method combined with digital image analysis and processing [6, 9, 11]. The ADSA method has since become a useful technique for determining line

tensions. It is a fairly accurate and highly sophisticated method involving drop shape analysis and digital image analysis, however it is relatively expensive.

2.2 The Conical Capillary Rise Method

The modified Young equation, Equation 2.1, is only applicable to a horizontal solid surface. In modelling multi-phase systems, it is often necessary to consider inclined surfaces or surfaces of revolution such as that shown in Figure 2.2. For such surfaces of revolution, the modified Young equation is not applicable. For a three-phase line in contact with an inclined solid surface, the curvature $\left(\frac{1}{R}\right)$ in the mechanical equilibrium condition, Equation (2.1), should be replaced by the local geodesic curvature K_{gs} [2], that is,

$$\cos\theta = \cos\theta_{\infty} - \left(\frac{\sigma}{\gamma_{lv}}\right) K_{gs} \tag{2.2}$$

where the local geodesic curvature of the three-phase line, K_{gs}, can be understood as the local curvature of the three-phase line in the plane of the solid surface [2]. The derivation of the modified Young equation as well as the specific form of K_{gs}, from thermodynamics, for an inclined solid surface is generally quite involved and moreover there still exist some disagreement as to the validity of some of the thermodynamic assumptions and arguments. However if one thinks

in terms of a simple force balance at a reference point on the three-phase contact line one can understand the derivation of the modified Young equation.

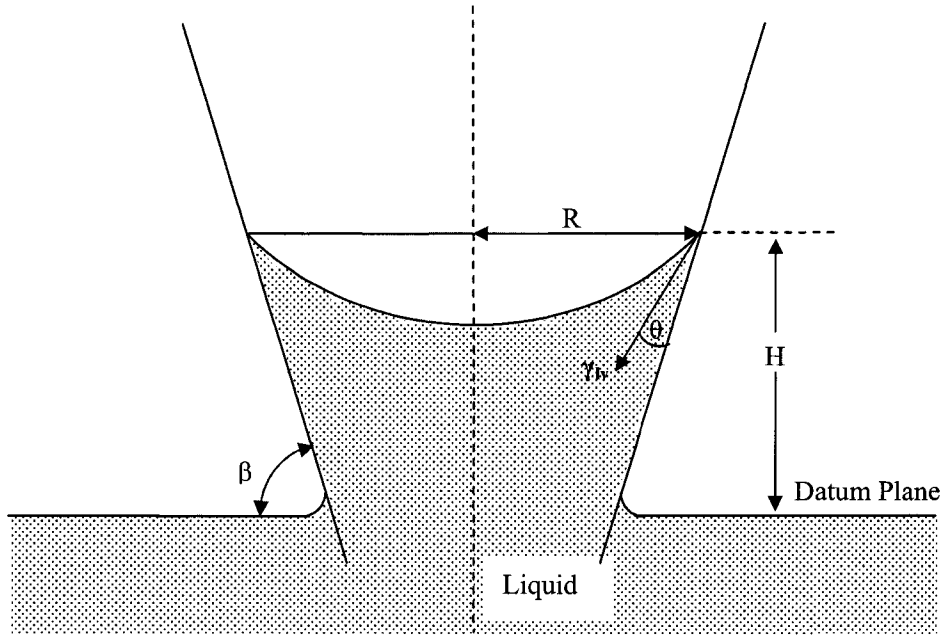

Fig.2.2: The conical capillary tube

Consider first the force balance for a sessile drop on a horizontal solid surface as shown in Figure 2.3. The equilibrium of forces at the reference point (Figure 2.3) requires that:

$$\gamma_{lv}\cos\theta+\gamma_{SL}+\frac{\sigma}{R}=\gamma_{sv} \tag{2.3}$$

Rearranging implies:

$$\cos\theta=\frac{\gamma_{sv}-\gamma_{sl}}{\gamma_{sv}}-\frac{\sigma}{\gamma_{lv}}\frac{1}{R} \tag{2.4}$$

This is the same as the modified Young equation for a horizontal sessile drop, Equation 2.1.

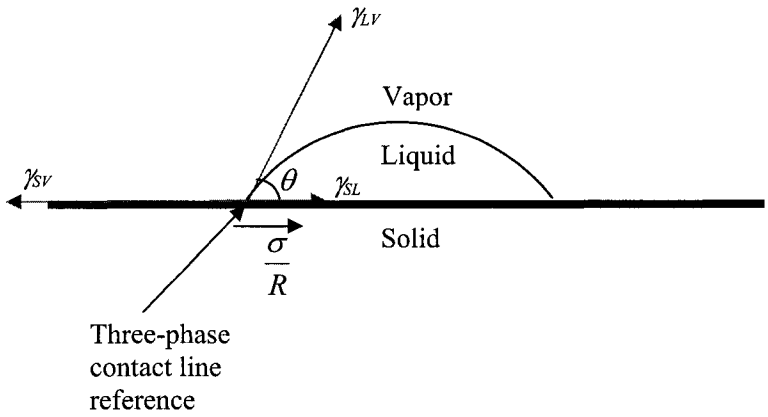

Fig.2.3: Force balance for a horizontal sessile drop showing the three-phase contact line

Similarly, a simplified derivation of the specific form of K_{gs} for an ideal solid surface of revolution, such as the conical crevice of Figure 2.2, is shown below.

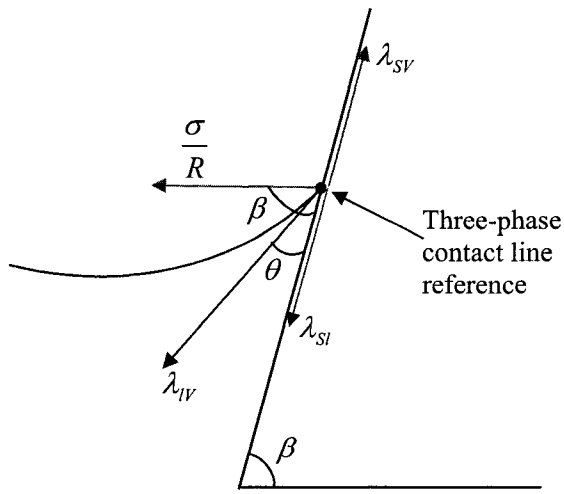

Fig.2.4: Force balance for a liquid rise in a conical crevice showing the three-phase contact line

The equilibrium of forces at the reference point (Figure 2.4) requires that:

$$\gamma_{lV}\cos\theta+\frac{\sigma}{R}\cos\beta+\gamma_{Sl}=\gamma_{SV} \tag{2.5}$$

Rearranging implies:

$$\cos\theta=\frac{\gamma_{SV}-\gamma_{Sl}}{\gamma_{LV}}-\frac{\sigma}{R\gamma_{lV}}\cos\beta \tag{2.6}$$

That is:

$$\cos\theta=\cos\theta_{\infty}-\frac{\sigma}{\gamma_{lV}}\left(\frac{\cos\beta}{R}\right) \tag{2.7}$$

Equation 2.7 is the modified Young equation for a solid of revolution such as the conical capillary tube of Figure 2.2.

It has been suggested to use this mechanical equilibrium condition, Eq. (2.7), to determine line tension. Li and Lin [2] concluded that line tension could be determined from a single capillary height measurement. Recently, Jensen and Li [13] developed a relatively cheap and simple method based on the use of a simple conical capillary tube and Equation 2.7. The method involves measuring the height of capillary rise and the radius of the three-phase contact line at various locations along the conical tube, see Figure 2.2. The line tension was then determined from the slope of the linear relationship between $\cos\theta$ and $\cos\beta/R$. In reference [13], the contact angle, θ, was calculated from the measured height of capillary rise and the radius of the three-phase contact line using the following relationship, which assumes a spherical interface:

$$\theta = \beta - \sin^{-1}\left(\frac{\Delta\rho g H R}{2\gamma_{lv}}\right) \tag{2.8}$$

where $\Delta\rho$ is the density difference between the bulk phases, g is the magnitude of the local acceleration of gravity, H is the height of the capillary liquid, and γ_{lv} is the liquid surface tension.

The conical capillary technique gave line tension values of the same order of magnitude as those reported in the literature using other methods; however the line tension values obtained by the conical capillary method were larger. The authors attributed this discrepancy to the assumption of a spherical liquid-vapour interface (neglecting gravity) in their model as well as possible non-equilibrium effects.

The Bond number (the ratio of the gravitational force to the surface tension force) provides a reasonable estimate of whether gravitational effects will deform the liquid-vapour interface from spherical. The Bond number, Bo is given by:

$$Bo = \frac{g\Delta\rho R_m^{\,2}}{\gamma_{lv}} \tag{2.9}$$

where g and $\Delta\rho$ are as defined before and R_m is the measured radius of the conical capillary at the point where the interface contacts the capillary. The necessary condition for assuming a spherical interface is for the Bond number to

be small compared to unity (i.e. $Bo <<< 1$). Bond numbers were calculated for the conical capillary system [13] and they ranged from 0.1 to 0.9; which clearly are not all small compared to unity.

The objective of this theoretical study is to take advantage of the relative simplicity of the conical capillary technique and attempt to improve the accuracy of the line tension values inferred from laboratory data obtained using the conical capillary technique. Herein, the effect of the deformation due to gravity on the shape of the liquid-vapour interface is included in the conical capillary analysis.

2.3 Governing Equations for the Shape of the Interface in the Presence of Gravity

Consider a three-phase system consisting of a solid surface and two homogenous fluid phases separated by a curved interface as depicted by the conical capillary geometry of Figure 2.2. The pressure difference across the curved interface is described by the Laplace equation:

$$\Delta P = \gamma_{lv}\left(\frac{1}{R_1}+\frac{1}{R_2}\right) \tag{2.10}$$

where γ_{lv} is the liquid surface tension, R_1 and R_2 are the two principal radii of curvature and ΔP is the pressure difference across the interface.

In the absence of external forces, other than gravity, and for small elevations, the pressure difference across the interface is a linear function of the elevation above the free interface[1]:

$$\Delta P = (\Delta\rho) g z_I \tag{2.11}$$

where z_I is the distance from the free interface, which is assumed to be flat at the datum plane. Equating (2.10) and (2.11) yields

$$(\Delta\rho) g z_I = \gamma_{IV}\left(\frac{1}{R_1}+\frac{1}{R_2}\right) \tag{2.12}$$

By the methods of Bashforth and Adams [14] and Sasges and Ward [15, 16], and assuming an axisymmetric interface, the interface may be parameterized in terms of a turning angle, φ, as shown in Figure 2.5. Note that for an axisymmetric interface, the two radii of interface curvature, R_1 and R_2 are equal on the axis of symmetry.

[1] For the elevations relevant to the conical capillary rise technique, the assumption that the linearization of the exponential elevation dependence of the vapour phase pressure does not introduce any error was verified.

For the axisymmetric interface,

$$R_2 = \frac{x_I}{\sin\varphi} \tag{2.13}$$

The differential geometry of the interface, as shown in Figure 2.5, yields the differential relationships:

$$dx_I = R_1(\varphi)\cos\varphi d\varphi \tag{2.14}$$

$$dz_I = R_1(\varphi)\sin\varphi d\varphi \tag{2.15}$$

Substituting Eqs. (2.13) - (2.15) into Eq. (2.12), and rearranging yields:

$$dx_I = \frac{\cos\varphi d\varphi}{\frac{\Delta\rho g z_I}{\gamma_{IV}} - \frac{\sin\varphi}{x_I}}$$

$$dz_I = \frac{\sin\varphi d\varphi}{\frac{\Delta\rho g z_I}{\gamma_{IV}} - \frac{\sin\varphi}{x_I}} \tag{2.16}$$

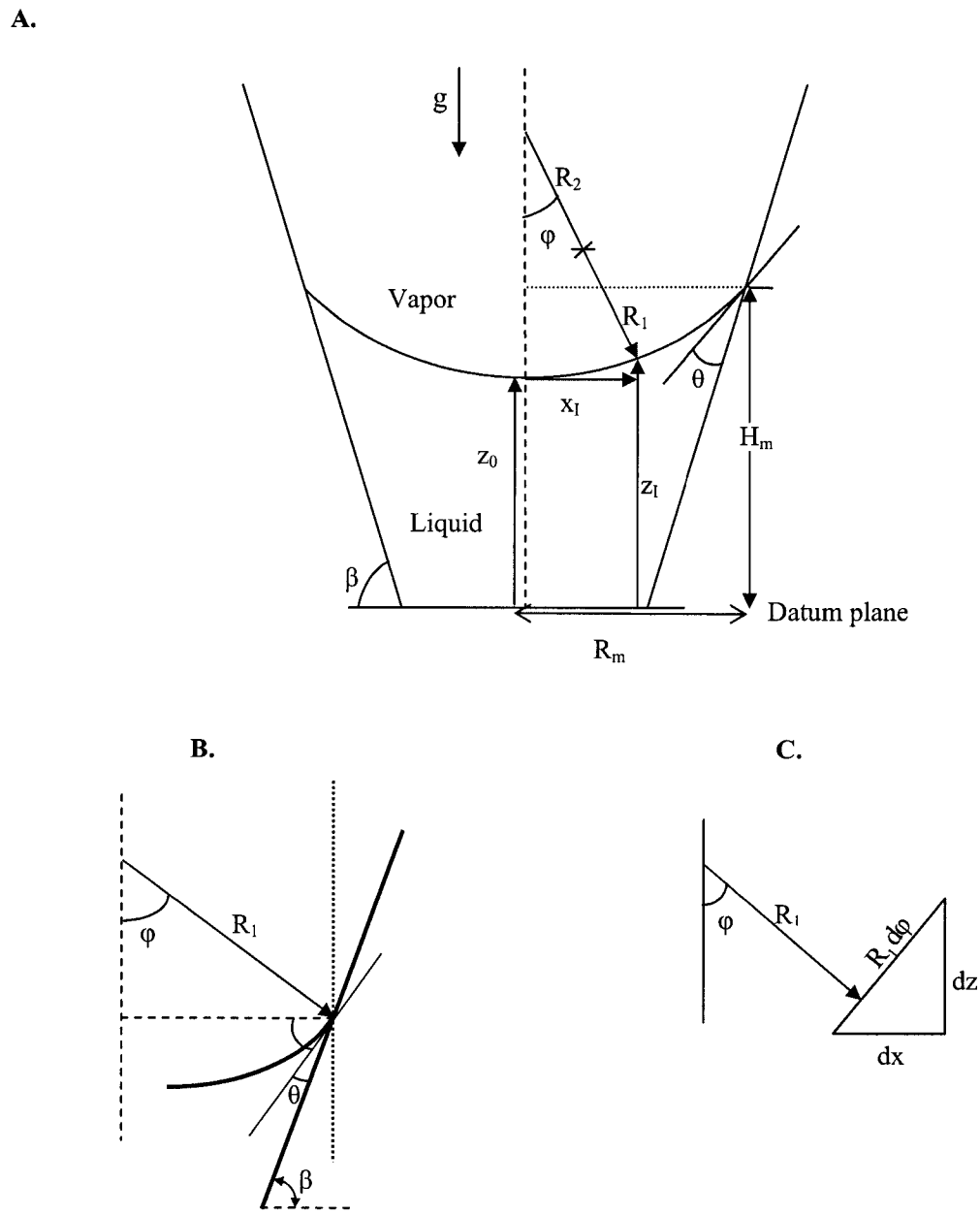

Fig.2.5: Geometry of the conical capillary system. (A) General geometry of the capillary and the liquid-vapour interface. (B) Geometry of the interface. (C) Differential geometry of the interface.

Using the experimentally measured radius of the conical capillary, R_m, as the characteristic length of the system, Equation (2.16) can be written as:

$$dx' = \frac{\cos\varphi d\varphi}{\frac{\Delta\rho g z' R_m^{\,2}}{\gamma_{IV}} - \frac{\sin\varphi}{x'}}$$

$$dz' = \frac{\sin\varphi d\varphi}{\frac{\Delta\rho g z' R_m^{\,2}}{\gamma_{IV}} - \frac{\sin\varphi}{x'}} \qquad (2.17)$$

where x' and z' are the non-dimensionalized radial and vertical coordinates of the interface respectively:

$$x' = \frac{x_I}{R_m} \; ;$$

$$z' = \frac{z_I}{R_m} \qquad (2.18)$$

Introducing the constant λ defined as:

$$\lambda = \frac{\Delta\rho g R_m^{\,2}}{\gamma} \qquad (2.19)$$

Eq. (11) can be written as:

$$dx' = \frac{\cos\varphi d\varphi}{\lambda z' - \frac{\sin\varphi}{x'}}$$

$$dz' = \frac{\sin\varphi d\varphi}{\lambda z' - \frac{\sin\varphi}{x'}} \qquad (2.20)$$

with the initial boundary conditions,

$$\varphi = 0, \quad x' = 0 \quad z' = z_0 \tag{2.21}$$

where z_0 is the height of the interface on the axis of symmetry as shown in Figure 2.5 (A). The shape of the fluid interface can thus be determined by integrating Equation (2.20) numerically from the initial boundary conditions φ = 0 ($x' = 0$ and $z' = z_0$) to the final boundary conditions, $\varphi = (\beta - \theta)$, where β and θ are as defined before. Since the initial interface height, z_0 and the liquid contact angle, θ, are not known *a priori*, these parameters have to be hypothesized. The maximum calculated value of the interface radius must equal the measured cone radius, and the maximum calculated value of the interface height must equal the measured interface height, z_m for the guessed contact angle:

$$x'(\beta - \theta) = 1, \tag{2.22}$$

$$z'(\beta - \theta) = z_m = \frac{H_m}{R_m}, \tag{2.23}$$

where H_m is the experimentally measured interface height. If the conditions in Eqs. (2.22) and (2.23) are not satisfied; new values of z_0 and θ must be chosen. Using the initial conditions in Eq. (2.21), the differential equations for the interface, Eq. (2.20), may be integrated iteratively until the boundary conditions,

Eqs. (2.22) and (2.23) are simultaneously satisfied. Thus for a given measured radius, R_m and height, H_m, and a given λ, the liquid contact angle, θ, can be determined. Finally using Equation (2.7), the line tension, σ, can be determined from the slope of the linear relationship between $\cos\theta$ and $(\cos\beta / R)$.

2.4 Numerical Implementation

To determine accurate values of z_0 and θ, the error between the calculated endpoint values of the hypothesized interface [x' and z' at $\varphi = (\beta - \theta)$] and the measured interface endpoint values need to be minimized. An objective function, Var, is thus defined as:

$$Var = \left[1 - x'(\beta - \theta)\right]^2 + \left[z_m - z'(\beta - \theta)\right]^2 \tag{2.24}$$

The minimization of the objective function, Var, leads to the solution of a nonlinear equation that is solved by the direct search method. The numerical integration was performed using the classical higher order Runge-Kutta method with adaptive step sizes. Details of these mathematical techniques can be found elsewhere [17]. A *Matlab* script (See Appendix A) was developed to implement the numerical integration and the script utilized the standard differential equation solver (*ODE45*), which uses the fourth-and fifth-order Runge-Kutta algorithms with adaptive step size to attain higher accuracy [18]. The minimization of the

objective function was achieved via the built-in Matlab package (*FMINSEARCH*), which uses the *Nelder-Mead* simplex (direct search) method for unconstrained multidimensional optimization.

The values for the density difference, $\Delta\rho$, between the bulk phases, the magnitude of the local acceleration of gravity, g, the liquid surface tension, γ_{lv}, the cone angle, β, and the experimentally measured values of the cone radius, R_m, and the height of liquid interface, H_m, are required for computation. The experimental data from Jensen [19] and Jensen and Li [13] for dodecane, tetradecane, and hexadecane (in air) in glass conical capillaries treated with *FC722* were used for this work. Additional parameters are given in Table 1. Initial guesses for the liquid contact angle, θ, with the solid wall and the height of the interface on the axis of symmetry are also required. (Initial guesses and accuracy parameters required by the numerical packages were varied and found not to affect the results).

Table 2.1: Parameters used for this study. **Ref. [19]**

Liquid	$\Delta\rho$ (kg/m^3)	γ_{lv} (mJm^{-2})	g (m/s^2)
Dodecane	748	25.44	9.81
Tetradecane	762.8	26.7	9.81
Hexadecane	773	27.6	9.81

2.5 Results and Discussions

Using the same data and parameters utilized by Jensen and Li [13] in their analysis, a numerical solution of the shape of the liquid-vapour interface was obtained. For the systems studied in ref. [13], plots of $\cos\theta$ versus $(\cos\beta / R)$ are given in Figures (2.6) - (2.8). The filled circles represent the results of this work (which assumes a non-spherical liquid-vapour interface) while the open squares corresponds to the reported work of Jensen and Li [13]. As seen from Tables 2.2 and 2.3, although the regression coefficients of the best-fit lines for this study are lower than those of the previously determined slopes, the regression coefficients are above 0.70 and are statistically acceptable. The line tensions of the various systems were calculated from the slope of the best-fit lines, as discussed in the theory section, and predicted values are as shown in Table 2.2. No analysis was made for the Decane system in this work as a result of error in the data presented by Jensen [19], which were not mathematically consistent.

Table 2.2: Average line tension values obtained from the results of this study

Liquid	Solid Surface	Line Tension (μJm^{-1})	θ_∞ (degree)	Regression Coefficient, r
Dodecane	FC722	3.1	69.7	0.78
Tetradecane	FC722	2.9	73.2	0.72
Hexadecane	FC722	2.4	74.4	0.80

Table 2.3: Average line tension values obtained from the work of Jensen and Li [13, 19]

Liquid	Solid Surface	Line Tension (μJm^{-1})	θ_∞ (degree)	Regression Coefficient, r
Dodecane	FC722	6.8	68.1	0.94
Tetradecane	FC722	5.7	72.1	0.90
Hexadecane	FC722	4.5	73.5	0.91

Table 2.4: Average line tension values obtained from ADSA [6, 9, and 11] and ACRACC [20]

Liquid	Solid Surface	Line Tension (μJm^{-1})	θ_∞ (degree)	Regression Coefficient, r
Dodecane	FC721[a]	2.1	69.9	0.98
Dodecane	FC721[b]	2.1	63.6	0.87
Tetradecane	FC725[b]	3.3	65.4	0.84
Hexadecane	FC725[b]	3.7	69.5	0.83

Ref. [a] ADSA.
Ref. [b] ACRACC.

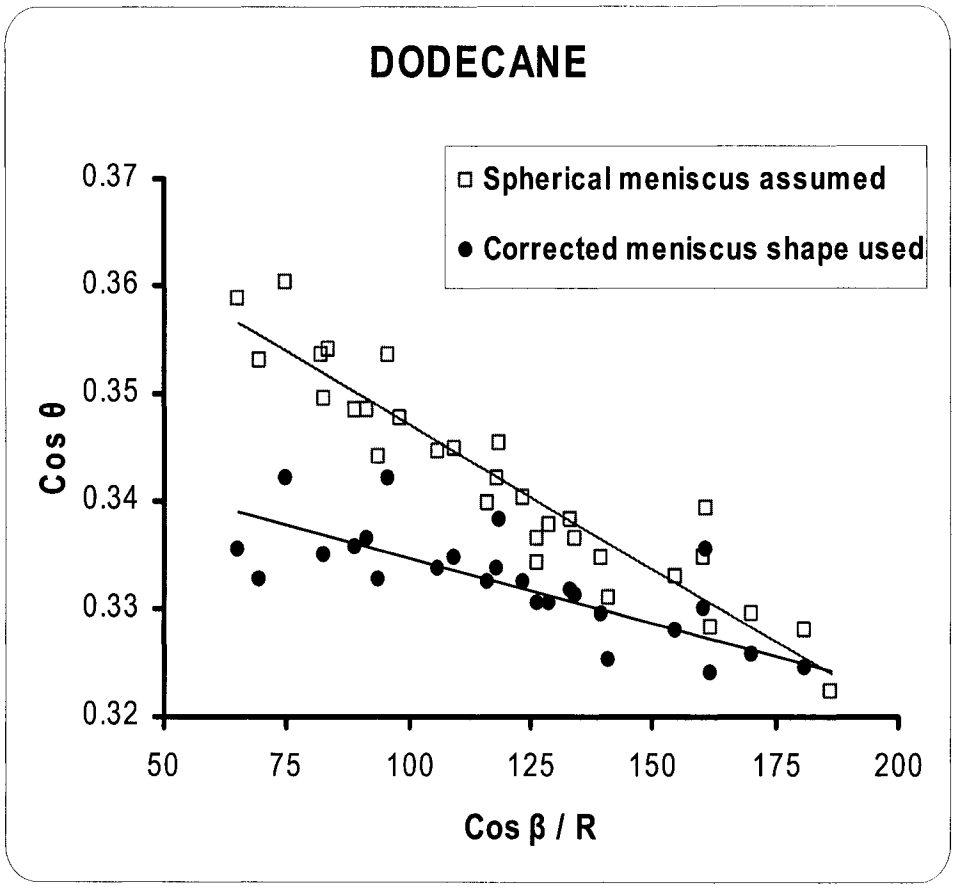

Fig.2.6: Variation of $\cos\theta$ with $(\cos\beta / R)$ for Dodecane (*FC722*).

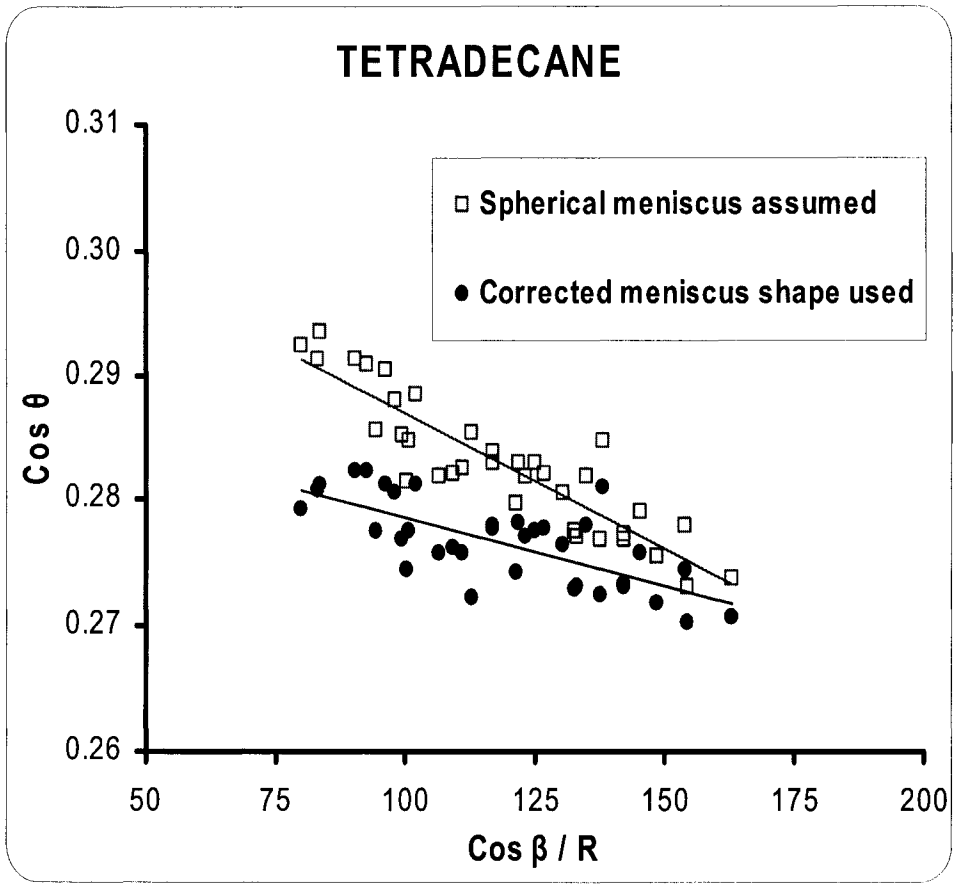

Fig.2.7: Variation of $\cos\theta$ with $(\cos\beta / R)$ for Tetradecane (*FC722*).

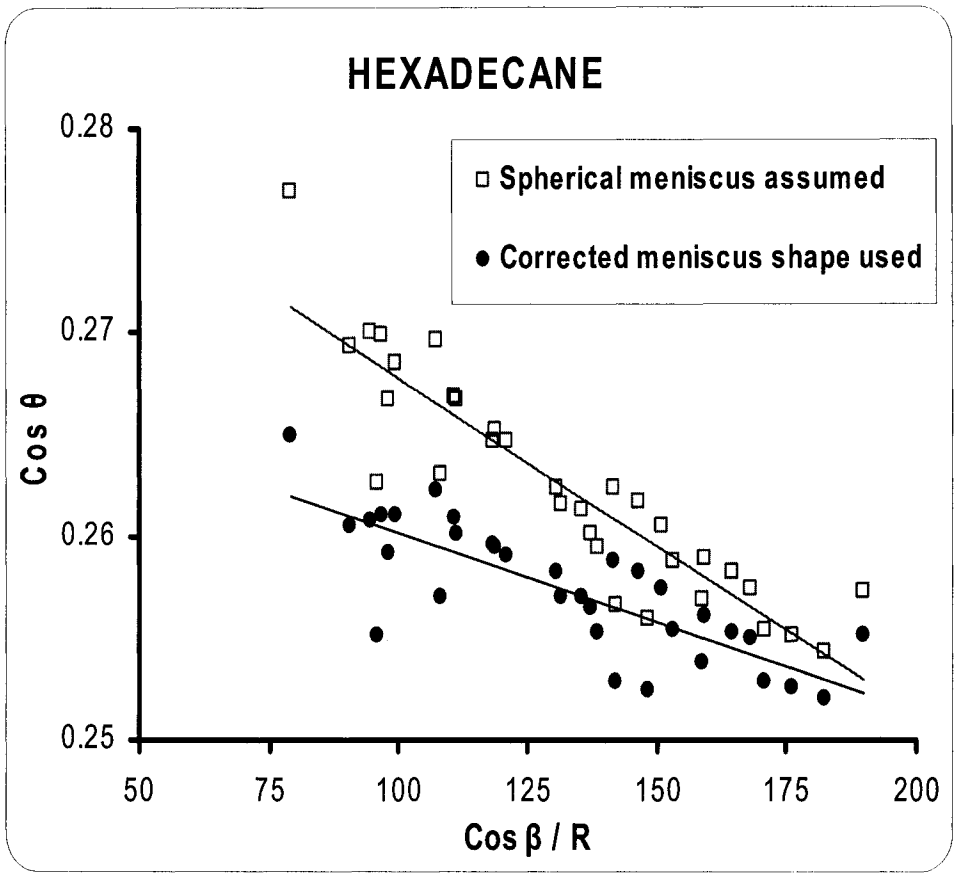

Fig. 2.8: Variation of $\cos\theta$ with $(\cos\beta / R)$ for Hexadecane (*FC722*).

2.6 Conclusions

Table 2.5 shows a comparison of the obtained line tension values, when gravity effect on interface deformation is included in the analysis, and the previously determined line tension values of Jensen and Li [13] with those determined by other sophisticated techniques such as the ADSA and the analysis of the capillary rise around a conical cylinder (ACRACC technique) [20] for similar solid-liquid systems, see Table 2.4.

Table 2.5: Comparison of the line tension values determined by various methods

Liquid	Solid Surface	Line Tension from Jensen and Li [12,19] (μJm^{-1})	Line Tension from this work (μJm^{-1})	Line Tension from ADSA [6,9,11] / ACRACC [20] (μJm^{-1})
Dodecane	FC722	6.8	3.1	
Dodecane	FC721			2.1
Dodecane	FC721			2.1
Tetradecane	FC722	5.7	2.9	
Tetradecane	FC725			3.3
Hexadecane	FC722	4.5	2.4	
Hexadecane	FC725			3.7

As seen from Table 2.5, the values of the line tension obtained via the method of Jensen and Li [13, 19] are of the same order of magnitude but larger than those

of ADSA and ACRACC for similar systems. However by including the effect of the deformation due to gravity on the shape of the liquid-vapour interface in the conical capillary analysis, as has been done in this work, the line tension values inferred from the experimental data of the conical tube method were not only reduced by about fifty percent (50%) but compare better with those of ADSA and ACRACC. The conical capillary method of determining line tension has been advanced and provides a simple, less expensive and reliable means of measuring line tension.

2.7 References

[1] J. W. Gibbs, "The Scientific Papers", Vol. 1, Dover, New York, 1961.

[2] F.Y.H. Lin and D. Li, Colloids Surfaces A: Physicochem. Eng. Aspects, 87 (1994) 93 -100.

[3] J. Drelich, Colloids Surfaces, 116 (1996) 43.

[4] J. Gaydos and A.W. Neumann, J. Colloid Interface Sci., 120 (1987) 76.

[5] J. Drelich and J.D.Miller, J.Colloid Interface Sci., 164 (1994) 489.

[6] D. Duncan, D. Li, J.Gaydos and A.W.Neumann, J. Colloid Interface Sci., 169(1995) 256.

[7] Z. Zorin, D. Platikanov and T. Kolarov, Colloids Surfaces, 22 (1987) 147.

[8] Y. Rotenberg, L. Boruvka, and A.W. Neumann, J. Colloid Interface Sci., 93 (1) 169.

[9] D. Li, and A.W. Neumann, Colloids Surfaces, 43(1990) 195.

[10] A. S. Dimitrov, A.D. Nikolov, P.A. Kralchevsky and I.B. Ivanov, J.Colloid Interface Sci., 151(1992) 462.

[11] D. Li, Colloid Surfaces A: Physicochem. Eng. Aspects, 116 (1996) 1.

[12] H. B. Callen, "Thermodynamics and an introduction to thermostatic", Wiley, New York, 2ed, 1985

[13] W. C. Jensen and D. Li, Colloids Surfaces A: Physicochem. Eng. Aspects, 156 (1999) 519.

[14] F. Bashforth and J.C.Adams, "An Attempt to test the Theories of Capillary Action", Cambridge Univ. Press and Deighton Bell & Co, Cambridge, 1883.

[15] C. A. Ward and M. R. Sasges, J. Chem. Phys., 109(9), (1998), 3651.

[16] C. A. Ward and M. R. Sasges, J. Chem. Phys., 109(9), (1998), 3661.

[17] M. J. Maron, "Numerical Analysis: A Practical Approach", Macmillan Publishing Company, New York/London, 2ed, p.403, 1987.

[18] S. C. Chapra, and R.P. Canale, "Numerical methods for Engineers", McGraw-Hill, New York, 2ed., 1988.

[19] W. C. Jensen, M.Sc. Thesis, University of Alberta, 1997.

[20] Y. Gu, D. Li, and P. Cheng, J. Colloid Interface Sci., 180 (1996) 212.

PART B:

STUDY OF THE BEHAVIOUR OF DROPLETS WITH PARTICLES AT A LIQUID-LIQUID INTERFACE

INTRODUCTION TO PART B

The behaviour of a pendant drop of one liquid phase (dispersed phase) in another liquid phase (the continuous phase) with solid particles at the interface is observed by means of a camera, as the interfacial area of the drop is varied by retraction and expansion. Liquid phases of silicone oil, water and/or diluted bitumen along with solid glass beads or silica were studied. Droplet behaviour was observed as a function of the size of particles, the wettability of the particles, the viscosity of the silicone oil, and the radius of the capillary introducing the droplet.

It is important to understand how the solid particles position themselves at the interface depending on their size, contact angles and the starting phase. When the droplet is retracted, what happens to the solid particles when there is no more interface left? Do the particles leave the interface as the droplet area diminishes? Does the droplet lose its spherical shape or deform as the interfacial area changes? These are questions of interest in this experimental study and an attempt is made to explain the observed behaviours as a way of understanding better how droplets with particles on their interfaces behave. A theoretical description of various stages of a pendant drop, with adsorbed particles, subjected to contraction is also presented.

Ground based as well as microgravity experiments were performed in this study. The microgravity experiments were performed aboard a Falcon 20 parabolic aircraft, provided by the National Research Council of Canada (made

possible through an agreement with the Canadian Space Agency), which provides near zero gravity environments.

This part of the thesis (Part B) is made up of Chapters 3 through 6. In Chapter 3, the materials and methods used in the study of the behaviour of droplets at a liquid-liquid interface are described. As well, a description of the forces involved in the behaviour of a detaching droplet is given. In Chapter 4, ground-based experiments and the experimental observations are discussed. Here, the knowledge gained from the study of liquid-in-liquid droplet behaviour using a model liquid-liquid system of silicone oil and water with solid particles is extended to real bitumen systems. In Chapter 5, the reduced gravity experiments and results are discussed.

Conclusions of both the theoretical line tension studies and the studies of the behaviour of droplets at a liquid-liquid interface are summarized in Chapter 6.

CHAPTER 3

MATERIAL AND METHODS

3.1 Introduction

In this chapter, the experimental materials are described as well as the cleaning and treatment procedures used in the experimental study. The experimental observations will be presented in subsequent chapters. A description of the forces involved in the behaviour of a detaching droplet is also presented in this chapter.

3.2 Experimental Materials

The materials used for the experimental studies include: silicone oil, water, diluted bitumen, glass beads, silica particles, syringes, plastic and stainless steel capillary tubes. Test cells made of plexiglass were used to contain the fluid. The experimental materials are described in detail below.

3.2.1 Experimental Fluids

Two different kinds of silicone oil fluids were used for the experimental study and both fluids were Dow Corning 200 (*DC 200*) fluids. For the initial ground based experiments and the microgravity experiments, the 500 centistokes (500 cSt) fluid was used while the 5 centistokes (5 cSt) fluid was used for subsequent ground-based experiments. The *DC 200* / 500 cSt fluid, with viscosity of 488

mPa.s, is the more viscous silicone oil and has a specific gravity of 0.975. The *DC 200* / 5 cSt fluid is the less viscous silicone oil and has a viscosity of 4.58 mPa.s and a specific gravity of 0.915.

Ultra-filtered, deionized and double distilled water was used as the aqueous phase in all experiments. The distilled water used for the ground-based experiments was obtained from an Elix Millipore water purification system while the distilled water used for the microgravity experiments was purchased from Fischer Scientific.

The bitumen used in this study was extracted from Canada's Athabasca deposit. The particular sample used for the study is Coker feed bitumen, supplied by Syncrude Canada Ltd, which is a heavy form of crude oil. The density of the bitumen ranged approximately between 1006 - 1022 kg/m^3 [1]. To attain workable viscosities, the bitumen was diluted in a solvent that is 50:50 by volume of n-heptane and toluene (known as *heptol*). Both the n-heptane and toluene were *HPLC* grades with no further purification, supplied by Fisher Scientific.

3.2.2 Solid Particles

The solid particles used in this study include glass beads and silica particles. The glass beads were supplied by Manus Abrasive System Inc. Beads of size #8 (mesh size 80) with an approximate size distribution of 150 - 210 μm diameters were used. The beads were manufactured from a high-grade optical crown glass, lead-free, soda lime type with minimum silica content of 68%. The glass beads

have a specific gravity of approximately 2.5. The beads' size distribution is as shown in Figure 3.1.

Crystalline silica particles in the form of quartz of various grades were also used for this experimental study. Two different sizes of silica particles, supplied by Unimin Corporation were used: silica particles with diameters <105 μm and silica particles D_{50} (median particle diameter on a cumulative size distribution curve) circa 13 μm. The silica particles have a specific gravity of approximately 2.65.

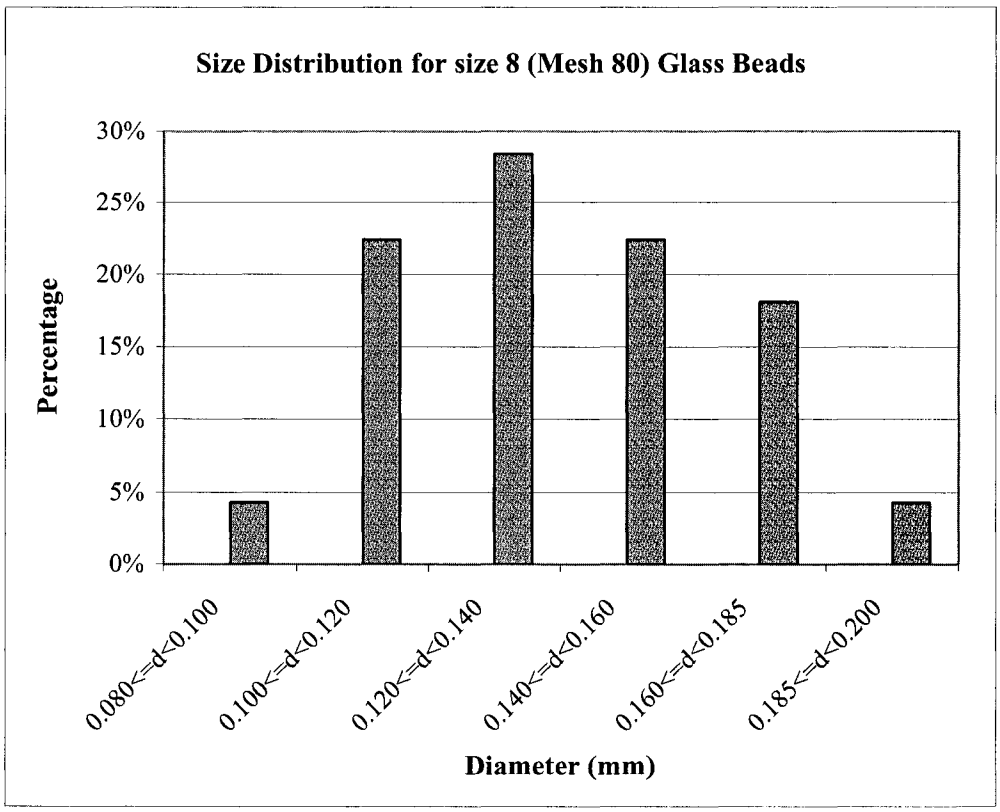

Fig.3.1: Size (diameter) distribution for size #8 glass beads [Ref: Manus Abrasive System Inc.]

3.2.3 Capillary Tubing

Stainless steel tubing attached to plastic capillary tubes were used in the experimental study. Two sizes of stainless steel tubing: *AT 3010 1/8" x 0.085 ID (304 SS)* stainless steel tubing and *AT 3000 1/16" x 0.030 ID (316 SS)* stainless steel tubing, obtained from Fisher Scientific, were used. The stainless steel tubings (each 50 ft long) were cut into smaller pieces each 12cm in length and were cleaned. The smaller tubings have approximately a diameter of 0.159cm (OD) x 0.076cm (ID) while the larger tubings have approximately a diameter of 0.318cm (OD) x 0.216cm (ID). Fischer Scientific *TYGON S-50-HL* 1/16" (ID) x 1/8" and 1/8" (ID) x 1/16" plastic tubings were also used in this study. Glass tips, approximately 0.159cm outer diameter and 2cm in length, cut from a glass capillary were also used in the design of the experimental apparatus.

3.2.4 Syringes

Disposable *B-D Luer-Lok* 20ml syringes were used for injecting the solid particles and the dispersed phase into the test cells while a 10ml Luer-Lok gas tight syringe was used in the particles treatment procedure for introducing trimethylchlorosilane. The syringes were obtained from Fisher Scientific.

3.2.5 Test Cells

Test cells, made of plexiglass and glass panels were used to contain the liquids for this experiment. A schematic of a test cell is as shown in Figure 3.2. The test

cells designed by Chiang et al. [2] were used for both the ground-based and microgravity experiments. One fluid phase is contained in the test cell and droplets of the other fluid phase were formed in the test cells by means of the capillary tubes.

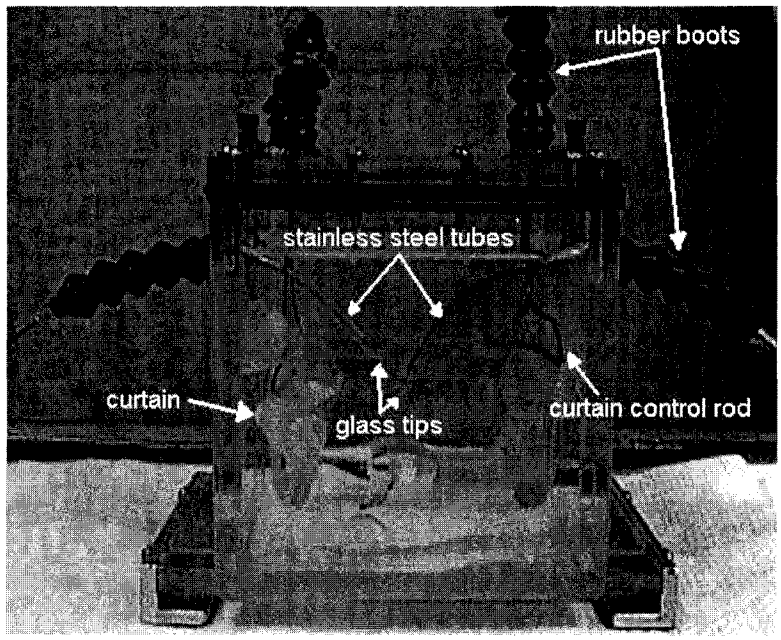

Fig.3.2: Schematic of a test cell used for the experimental study (Reprinted with permission from Chiang [2])

3.3 Cleaning and Treatment Procedures

The materials used for this experimental study were cleaned and treated using procedures similar to those of Blake et al. [4] and Chiang and Elliott [2, 3]. Detailed descriptions of the procedures are as discussed below.

3.3.1 Cleaning Procedures for Particles and Glassware

All glassware including jars, beakers, glass plates, and syringes used for this experiment were cleaned repeatedly using a mixture of sulfuric acid with no Chromix. Approximately 20ml of each type of solid particles (glass beads or silica particles) were then poured into a clean glass jar and soaked in the acid mixture for about 24hrs. A piece of glass slide, approximately one-third of a slide, was soaked along side the particles in each jar so that the contact angle on a flat plate could be determined. After washing in the acid mixture, the particles and glass slides were rinsed thoroughly with distilled water, repeatedly, until no noticeable yellow colour remained. The particles and slide in the glass jars were then dried at about 100°C and between 80 - 90 kPa in a vacuum drier for 24hrs.

3.3.1.1 Treatment Procedure for Particles

After the cleaning procedure, about half of the cleaned jar of solid particles and glass slides were treated with a mixture of approximately 80ml toluene and appropriate amounts of trimethylchlorosilane, TMCS (> 98 Sigma-Aldrich). For this study, for each particle size and jar, 5 ml or 10ml of TMCS were used for treatment and the methylation time was approximately 60minutes. After 60minutes, the glass jars of particles and slides were then thoroughly washed with toluene and the washing repeated about 6 times to remove all the TMCS. The jar of particles was then dried in a vacuum drier at conditions similar to the cleaning procedure above.

3.3.1.2 Contact Angle of Particles

The contact angles of the particles were indirectly estimated by measuring the contact angle of a droplet of water, on glass slides, which had the same treatment with the particle, in silicone oil. The contact angles were then determined both by geometric observation (using a ruler and a protractor) and the use of a drop shape analyzer - LIA program. The contact angles of the clean untreated particles were found to be approximately 45^{o} which means that they are hydrophilic while the particles treated with 5ml and 10 ml TMCS have approximate contact angles of 125^{o} and $140^{o}+$ respectively. The treated particles are essentially hydrophobic.

3.3.2 Cleaning Procedure for Capillary Tubes

In order to minimize contamination, all materials that came into contact with the experimental fluids, i.e., the stainless steel capillary tubes and the glass tips were cleaned as follows: the tubes were soaked in toluene for approximately 10minutes after which they were thoroughly brushed on the outside for approximately 3minutes and allowed to dry. A syringe was then used to force about 50ml of distilled water through the tubes and the tubes allowed to dry on the counter. The glass tips were soaked in dish washing detergent and shaken thoroughly for 5minutes after which a syringe was used to force distilled water through the glass tips.

3.3.3 Cleaning Procedure for Test Cells

The test cells were made from plexiglass and glass panels which are held together by glues and thus cannot be cleaned with common solvents or acids. The following describes the cleaning procedure for the test cells. The cells were rinsed in hot tap water for approximately 3minutes after which the cells were scrubbed with a flask brush in dish washing detergent for 3minutes. The cells were again washed in hot tap water and then cleaned in an ultrasonic cleaner (Fisherbrand FS20) with a fisherbrand ultrasonic cleaning solution for approximately 15minutes. Finally, the cells were rinsed in distilled water and allowed to dry, placed upside down, overnight on the counter.

3.4 Apparatus and Set-up

A pendant drop apparatus was used throughout this study for observing droplet behaviours. The complete set-up of the apparatus is as shown diagrammatically in Figure 3.3. The apparatus consists basically of a test cell which holds the continuous phase; a syringe through which the droplet is formed and a lighting source - a halogen lamp (Leica Model). A Sony digital camcorder (Model DCR-TRV530), with an LCD display, was used to capture and record the behaviour of the droplet. The image was then processed and analyzed via a computer. A Fisher laboratory jack stand was used to elevate and secure the test cell.

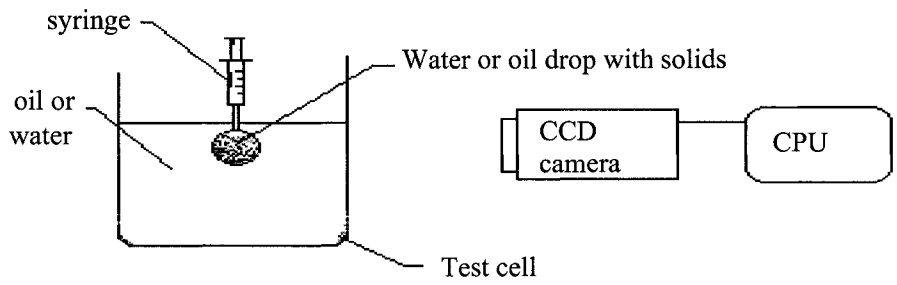

Fig.3.3: The pendant drop apparatus

The pendant drop apparatus was chosen for this experimental study because of the simplicity of the set-up and since it permits an interface to age almost independently under static conditions and affords a method for varying the interfacial area by distension or retraction of the drop. In the pendant drop technique, a liquid droplet is formed in another continuous liquid phase with solid particles introduced through the droplet phase and allowed to age for a finite time. The drop is then contracted by application of suction while a camera captures the change in the geometry of the drop as well as behaviours of the particles. The drop is thereafter filled out to its initial size while its behaviour is captured once again by the camera.

In order to meet both the requirements of the ground based and microgravity experiments, a steel frame was designed and built to house the components. Figure 3.4 shows a diagram of the experimental set-up and the frame. The original apparatus and frame was designed by Chiang and a detailed description of the initial design of the experimental apparatus is presented in [2]. For this

present study, the original apparatus was modified to include a tilt adapter to allow for better focusing of the camera.

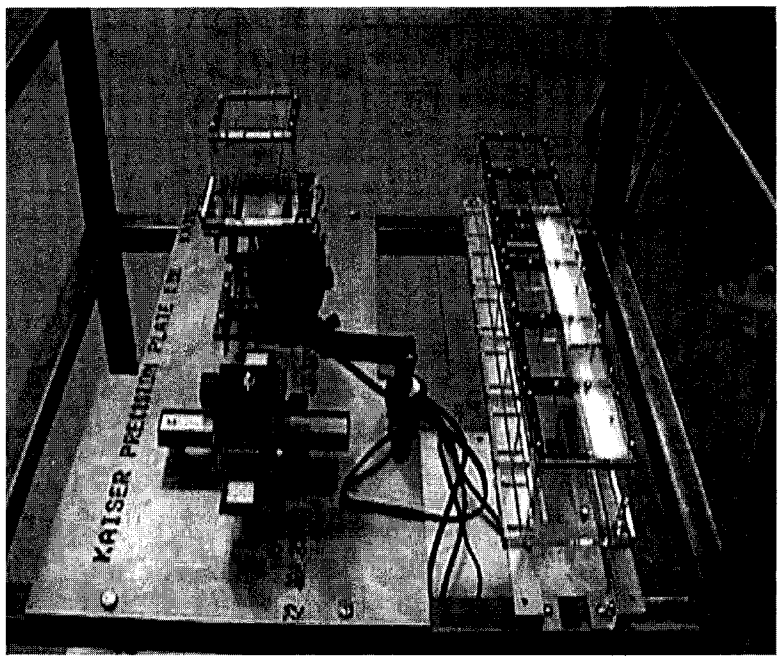

Fig.3.4: Schematic of the original experimental set up (Reprinted with permission from Chiang [2])

3.5 Experimental Parameters

Using the pendant drop technique, parametric studies were performed. The behaviour of a droplet was observed as a function of particle sizes, the wettability of the particles, the silicone oil viscosity and the radius of the capillary introducing the droplet. Glass beads with average diameter of 150 - 210 μm and silica particles less than 105 μm in diameter and approximately 13 μm in

diameter were used for the experimental study. The silicone oils used for the experiments were both DC 200 fluids with viscosities of 4.58 mPa.s (less viscous oil) and 488 mPa.s (more viscous oil), respectively. The capillary tubes used for the experimental study had internal diameters of 0.076cm (small capillary) and 0.216cm (large capillary), respectively. Both hydrophilic (45°) particles and hydrophobic (125° and 140°+) particles were used for this study. Table 3.1 indicates the range of variables studied.

Table 3.1: Range of experimental parameters studied

Serial Number	Parameter	Magnitude of parameter		
1	Particle size (μm)	150-210	<105	13
2	Particle wettability (°)	45	125	140^{+}
3	Silicone oil viscosity (mPas)	4.58 mPa.s	488 mPa.s	-
4	Capillary diameter (cm)	0.318 (OD) x 0.216 (ID)	0.159 (OD) x 0.076 (ID)	-

3.6 Description of Forces Involved in Drop Behaviour

Consider a static pendant drop of one liquid phase (dispersed phase) in another continuous liquid phase, suspended from the tip of a capillary tube, with the

droplet surface covered with particles as shown schematically in Figure 3.5. Depending on the surface property of the particles (contact angle of particle), the interfacial particles would be either placed more in the droplet phase or in the surrounding phase. When the droplet is subjected to contraction and expansion, various behaviours of the droplet and particles are expected. The emulsion droplet either gets sucked into the capillary, detaches from the capillary tip or deforms on contraction. The expected behaviour of the drop gives rise to two predictive questions: (1) the condition for detachment and (2) the prediction of the shape of the drop as the interfacial area diminishes. In this study, the focus will be on the conditions for drop detachment from the tip of the capillary. No theoretical description is provided for predicting the shape of the drop during retraction.

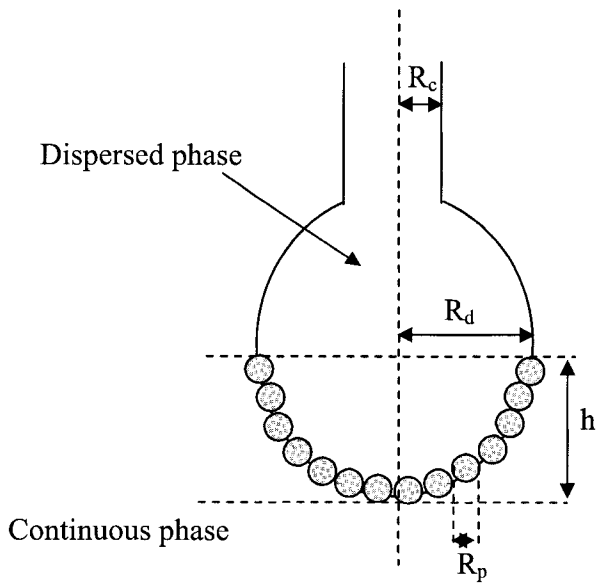

Fig.3.5: Schematic of a pendant drop with particles at the interface

When the static droplet is subjected to retraction, we expect the droplet interfacial area to reduce and the droplet may become unstable (as evidenced by a necking near the capillary tip) and eventually detach from the capillary. The droplet remains either spherical on retraction, deforms due to the effect of gravity or crumples due to the effect of the particles at the interface. The various stages of interest in the drop behaviour thus include: the static drop stage, the retraction stage and the detachment stage of the drop. Figure 3.6 shows the subsequent stages of drop detachment due to retraction and Table 3.2 indicates the forces operative in each stage of drop behaviour.

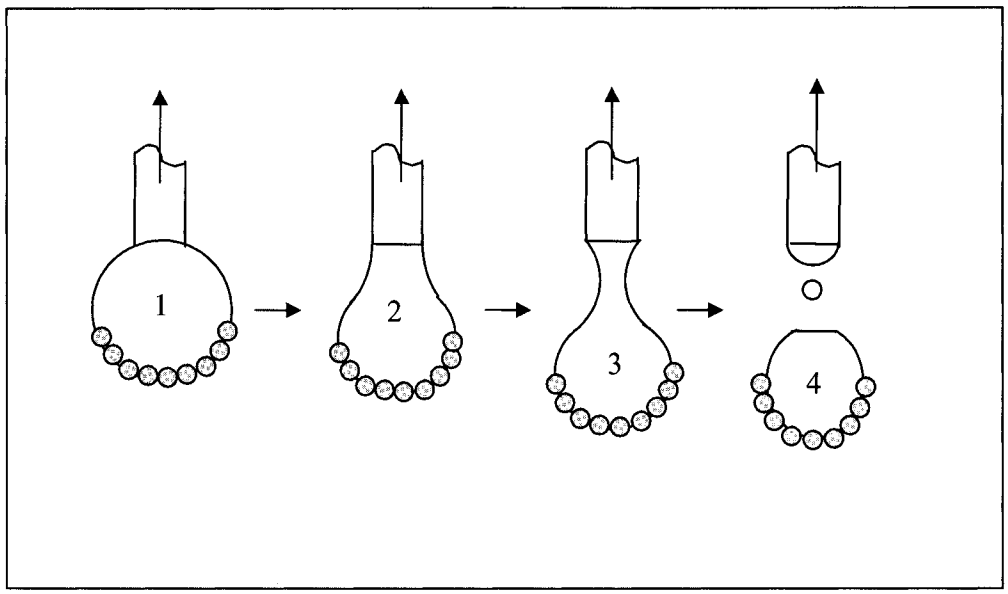

Fig.3.6: Schematic of subsequent stages of a drop on contraction

Table 3.2: Stages of drop behaviour and the forces operative in each stage

Static drop stage	Retraction stage	Detachment stage
Downward force	Downward force	Downward force
(a) Buoyancy force	(a) Buoyancy force	(a) Buoyancy force
	(b) Drag force	(b) Drag force
Upward force	Upward force	Upward force
(a) Interfacial tension	(a) Interfacial tension	(a) Interfacial tension
	(b) Force due to inertia of moving fluid	(b) Force due to inertia of moving fluid

There are four major forces which act on the drop during the static drop stage and the stages of retraction and drop detachment. The buoyancy force due to the density difference between the two fluids and between the particles and the fluids and the drag force exerted by the continuous phase act to separate the drop from the capillary tip while the interfacial tension force at the capillary tip and the inertia force associated with fluid flowing into the capillary act to keep the drop on the capillary tip. When the detachment force exceeds the retaining force, the drop begins to detach from the capillary tip.

To analyze the droplet detachment, the following assumptions will be made:

1. The water droplet is covered with particles in an ordered hexagonal closed packed arrangement.
2. The particles will be assumed to have a contact angle of 90°, that is half of a particle is inside the water droplet.
3. Drop retraction and expansion were performed at relatively very small velocity (very slowly) and thus the force due to inertia is assumed negligible.
4. An average retraction/expansion velocity of 7.330 x 10^{-5} m/s is assumed for calculation of the drag force. This average velocity value was obtained by analyzing the time for retraction and expansion (using the centre point of the drop as reference) for each experiment and taking an average value.
5. The change in interfacial tension during necking is negligible.

For the static stage of the drop, the attachment of the drop to the capillary tip is determined by a balance between the downward buoyancy force and the force due to interfacial tension. The interfacial tension force, F_γ , is given by [5]:

$$F_\gamma = f(\gamma, R_c) = 2\pi R_c \gamma \phi\left(\frac{R_c}{V_d^{1/3}}\right) \tag{3.1}$$

where γ is the interfacial tension, R_c is the radius of the capillary, V_d is the volume of the drop and $\phi\left(\frac{R_c}{V_d^{1/3}}\right)$ is a correction factor suggested by Harkins and

Brown [6] for the shape of the drop. It is assumed that ϕ really determines the shapes of the hanging drop and that it is the shape of the drop that determines the fraction of the drop that detaches. Various forms of the correction factor ϕ have been proposed in literatures. Wilkinson [7] proposed a simple polynomial for obtaining accurate values for the correction factor which is given by:

$$\phi\left(\frac{R_c}{V_d^{1/3}}\right) = z(0.50832 + z(1.5257 + z(-1.2462 + z0.60642))) - 0.0115 \qquad (3.2)$$

where,

$$z = \frac{R_c}{V_d^{1/3}} \qquad (3.3)$$

The buoyancy force F_B is a combination due to the fluids buoyancy and the buoyancy between the particles and the fluids, and is given by:

$$F_B = (\rho_p - \rho_{cp})0.5V_pN_pg + (\rho_p - \rho_d)0.5V_pN_pg + (\rho_d - \rho_{cp})V_dg \qquad (3.4)$$

where V_p is the volume of a particle, V_d is the volume of the droplet phase, N_P is the number of particles on the drop, and ρ_p, ρ_{cp} and ρ_d are the densities of the particle, the continuous phase and the droplet phase respectively. The volumes of a drop and a particle are given by:

$$V_d = \frac{4}{3}\pi R_d^3 \qquad (3.5)$$

$$V_p = \frac{4}{3}\pi R_p^3 \qquad (3.6)$$

To estimate the maximum number of particles in a drop and on its surface, N_p; the volume of the drop assumed to be filled by particles to a height h on the drop, is given by [8]:

$$V_{filled} = \frac{1}{3}\pi h^2(3R_d - h) \tag{3.7}$$

Assuming a *hexagonal closed packing fraction* of particles, that is, seventy four percent (74%) of the spherical cap is filled with particles [9], then, the number of particles is:

$$N_p = \frac{0.74V_{filled}}{\frac{4}{3}\pi R_p^{\ 3}} \tag{3.8}$$

One other force, which comes to play, as the drop area is reduced is the drag force, F_{VD} due to the continuous phase viscosity. This force is given by:

$$F_{VD} = 6\pi\mu R_d v \tag{3.9}$$

where μ is the viscosity of the continuous phase and v is the average retraction velocity. For liquids of low viscosity, μ is very small and the drag force may be neglected in the drop detachment analysis.

When the static drop stage is passed and the drop volume is reduced by suction, the downward buoyancy force plus the new viscous force overcomes the force due to interfacial tension and the drop becomes unstable (evidenced by a necking instability) and falls off the capillary.

It will be necessary to understand the effect of buoyancy, due to the difference in density between the continuous phase and the dispersed phase, as well as the continuous phase viscosity on drop detachment. For this present study, the drop retraction and expansion was done relatively slowly (at very low velocity) and thus the inertia forces will be neglected in the analysis. The observed behaviour of a droplet at different stages of drop detachment will thus be explained based on the above force interplay.

3.7 References

[1] F. W. Camp, "The tar sands of Alberta, Canada", Cameron Engineers, Inc., Colorado, 3ed., p. 23, 1976.

[2] R. Chiang, "Development of a macroscopic model of solids-stabilized emulsion", M. Sc Thesis, University of Alberta, Fall 2003.

[3] R. Chiang and J. A. W. Elliott, "A macroscopic solids-stabilized emulsion droplet analogue in microgravity", The 6th Japan-Canada workshop on space technology, Hamamatsu, Japan, Nov. 18-20, 2002.

[4] P. Blake and J. Ralston, "Controlled methylation of quartz particles", Colloids and Surfaces, 15 (1985) 101.

[5] E. V. L. Narasinga Rao, R. Kumar and N. R. Kuloor, "Drop formation studies in liquid-liquid systems", Chemical Engineering Science, 21 (1966) 867.

[6] W. D. Harkins and F. E. Brown, J. Am. Chem. Soc., 41 (1919) 499.

[7] M. C. Wilkinson, J. Colloid Interface Sci., 40 (1972) 14.

[8] M. R. Spiegel and John Liu, "Theory and problems of mathematical handbook of formulas and tables - Schaum's outline series", Mc Graw - Hill publishing company Inc., USA, 2ed., 1998.

[9] W. D. Callister, "Material science and engineering - an introduction", J. Wiley publishing company, New York, 6ed., 2003.

CHAPTER 4

GROUND-BASED EXPERIMENTS

4.1 Ground-Based Experimental Observations

This chapter describes the experiments performed in the laboratory. The first set of experiments involved the diluted bitumen-water system and subsequent experiments involved the silicone-oil-water system. The diluted bitumen-water experiments were performed to investigate the existence of interfacial skins which have been found on bitumen-oil-water emulsion droplets as well as the behaviour of the droplet when subjected to contraction and expansion. The model silicone-oil-water-particle system was then studied with emphasis on the positioning of the particles at the liquid-liquid interface as well as the behaviour of the droplet when subjected to retraction and expansion. A detailed description and experimental observations are presented below.

4.2 Experimental Procedure

A drop of one liquid phase (either oil or water) is formed in a continuous phase of another immiscible liquid by injecting the liquid drop through a syringe and a capillary tube. The drop is then allowed to age (i.e allowed to stand for about 15 minutes) for a finite time after which it is subjected to retraction and/or expansion. The drop is first retracted and then expanded to its initial size and the behaviour of the droplet is captured throughout by means of a camera. The

following sections describe the experimental observations from the ground-based studies.

4.3 Water-Droplet-in-Diluted-Bitumen System

Experiments involving a water droplet in diluted bitumen (diluted in a 50:50 mixture of n-heptane and toluene, otherwise known as heptol mixture) were performed to confirm the existence of interfacial skins present on water-in-diluted-bitumen emulsion droplets subject to area contraction reported in literature [1] and discussed in chapter 1. A water droplet, approximately 3mm in diameter, was formed in diluted bitumen and allowed to age (stand) for various finite times after which it was subjected to retraction and the behaviour of the drop captured by means of a camera.

Experiments were performed for diluted bitumen concentrations of 0.001 percent (less than 0.01 percent) and 0.03 to 0.125 percent (greater than 0.01 percent) by volume bitumen. For bitumen concentrations less than 0.01 percent, no noticeable change (droplet remained spherical and showed no evidence of a skin) was observed in the behaviour of the water droplet as well as the interface on retraction for all observation times.

For diluted bitumen concentration greater than 0.01 percent by volume bitumen; a water droplet was formed in the diluted bitumen on the tip of a capillary tube and allowed to age for 15minutes after which the droplet was subsequently retracted by means of a syringe thus reducing the interfacial area.

The retraction experiment was then repeated for aging times of 30minutes and 45minutes respectively.

Figure 4.1 shows the retraction behaviour of a water droplet in 0.03 percent diluted bitumen which was allowed to age for 15minutes as captured by the video camera. From the video, it is clearly seen that the droplet was initially spherical in shape and then loses it spherical shape as retraction is initiated and finally crumples, with some observed necking, as retraction continues. Similar crumpling was also observed for water droplets that were allowed to age for 30 and 45minutes respectively.

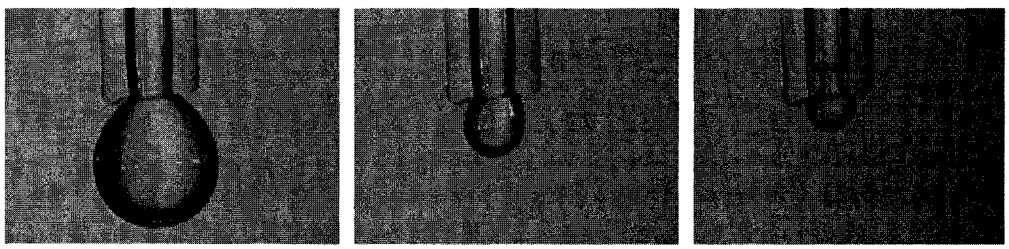

(a) Water droplet in diluted bitumen

(b) Water droplet upon application of suction

(c) Droplet loses its spherical shape

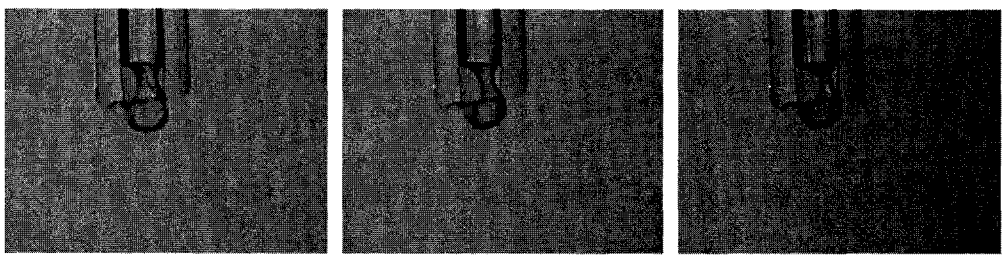

(d) Droplet appears to crumple

(e) Crumpling and necking continues

(f) Water droplet crumples upon suction

Fig.4.1: Subsequent stages of drop retraction for a water droplet in 0.03% by volume bitumen diluted in 50:50 mixture of heptol

4.4 Water-Droplet-in-Silicone-Oil System

Experiments were then performed to observe the behaviour of water droplets, with adsorbed solid particles, in silicone oil on reduction of the interfacial area by retraction. A water droplet of approximately 3mm in diameter, with solid particles, was injected by means of a syringe and capillary into a silicone oil continuous phase. The droplet was allowed to stand for about 10minutes. The droplet of water with solid particles was then consecutively retracted and expanded into the capillary thus reducing and expanding the interfacial area respectively. The drop behaviour was captured by means of a video camera.

Experiments were performed for both the less viscous (*5 cSt* - 4.58 mPa.s) and more viscous (*500 cSt* - 488 mPa.s) silicone oil fluids. Three kinds of solid particles were used for the experiments: 13 micron diameter silica particles, < 105 micron diameter silica particles and 105 - 210 micron diameter glass beads. Both untreated, hydrophilic (45°) and treated, hydrophobic (125° and 140°) particles were used. Large capillaries {0.318 OD x 0.216 ID} as well as small capillaries {0.159 OD x 0.076 ID} were used for the experiments. The following section discusses the experimental observations for water droplets, with hydrophilic and hydrophobic particles, in silicone oil systems.

4.4.1 Hydrophilic (45°) Particles in Water

Untreated hydrophilic particles were injected with water into a continuous phase of silicone oil. 13 (μm) diameter silica particles, < 105 (μm) diameter silica

particles and 105 - 210 (μm) diameter glass beads were used in the experiment. The hydrophilic particles were expected to stay mostly in the water phase, i.e., **sticking-in** the water droplet as depicted in Figure 4.2. The water droplet with particles was allowed to stand for 10 minutes after which it was retracted into the capillary and the droplet behaviour captured on a video camera. Sections 4.4.1.1 and 4.4.1.2 describe the observed behaviours of the drop as captured by the camera.

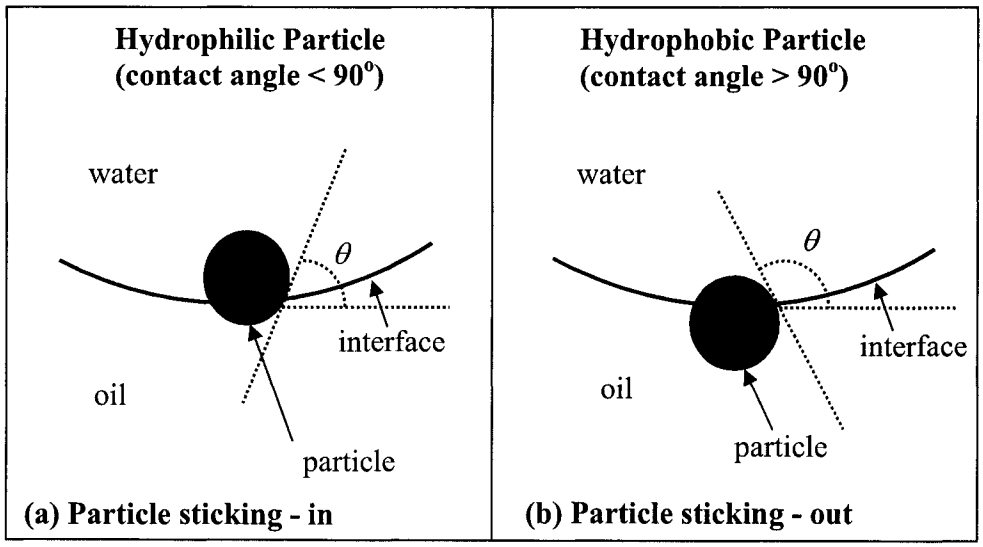

Fig.4.2: Schematic of a particle at an interface

4.4.1.1 Water Droplet with Hydrophilic (45°) Particles in 500 cSt Silicone Oil

Figure 4.3 shows the behaviour of a water droplet in 500 cSt silicone oil with hydrophilic (45°) c.a. 13 (μm) diameter silica particles subject to retraction. From

the video it is seen that the droplet was initially spherical and remained spherical on retraction and the particles were eventually sucked in with water into the capillary with further retraction.

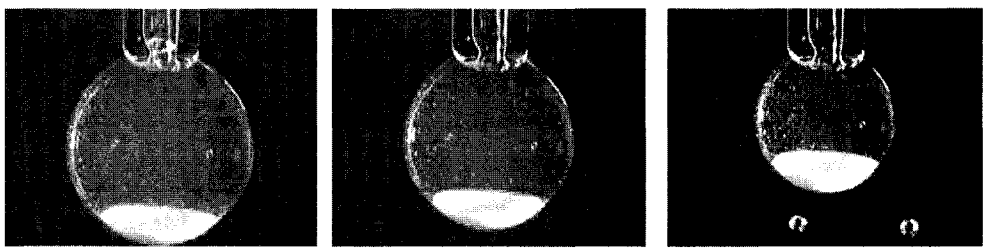

(a) Particles injected with water (b) Water droplet remain spherical on retraction (c) Droplet continues to remain spherical

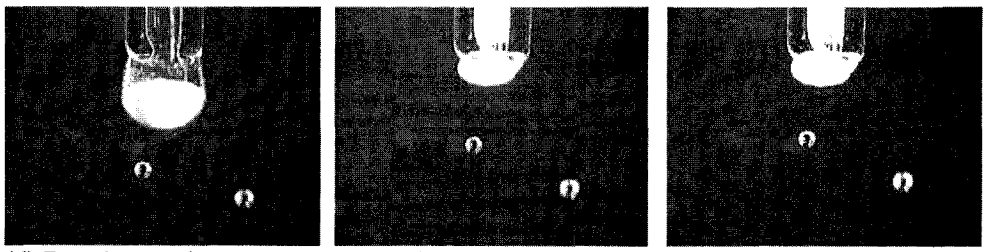

(d) Droplet continues to remain spherical (e) Particles sucked in with water (f) Particles sucked in with water upon suction

Fig.4.3: Subsequent stages of drop retraction for a water droplet, with hydrophilic (45°) c.a. 13 (μm) diameter silica particles, in 500 cSt silicone oil

The droplet remaining spherical on retraction may be due to the particles not running out of interface as well as the fewer number of particles on the droplet. The same results were observed for water droplet in 500 cSt silicone oil with hydrophilic silica particles of diameter < 105 (μm) in size and 105 - 210 (μm) diameter glass beads. See Appendix B.1 and B.2 respectively.

4.4.1.2 Water Droplet with Hydrophilic (45°) Particles in 5 cSt Silicone Oil

Figure 4.4 shows the behaviour of a water droplet in 5 cSt silicone oil with hydrophilic (45°) c.a. 13 (μm) silica particles subject to retraction. As with the case of hydrophilic particles in the more viscous silicone oil (section 4.4.1.1), it is seen that the droplet was initially spherical and appeared to remain spherical on retraction and the particles were eventually sucked in with water into the capillary with further retraction.

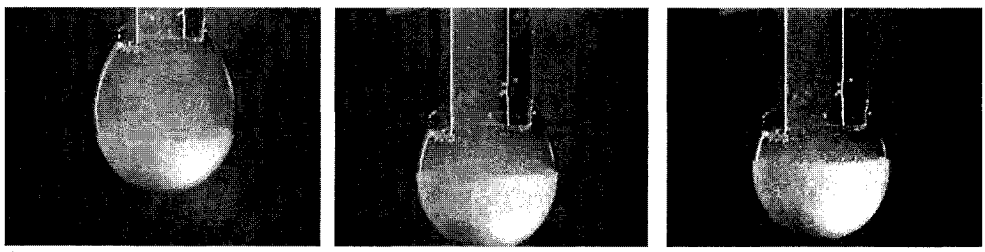

(a) Particles injected with water (b) Water droplet remain spherical on retraction (c) Droplet continues to remain spherical

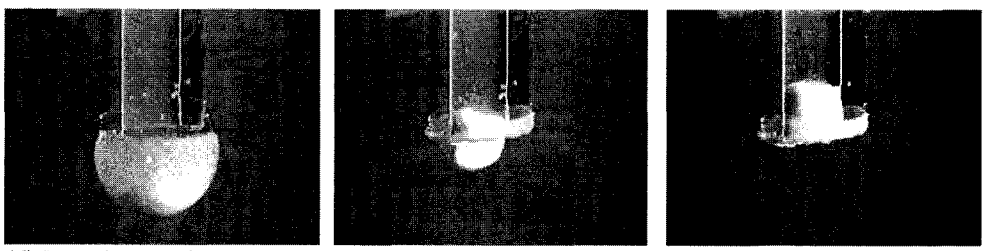

(d) Droplet continues to remain spherical (e) Particles sucked in with water (f) Particles sucked in with water upon suction

Fig.4.4: Subsequent stages of drop retraction for a water droplet, with hydrophilic (45°) c.a. 13 (μm) diameter silica particles, in 5 cSt silicone oil (large capillary)

The same results were observed for a water droplet in 5 cSt silicone oil with hydrophilic silica particles of diameter < 105 (μm) in size and 105 - 210 (μm) diameter glass beads. See Appendix B.3 and B.4 respectively.

4.4.2 Hydrophobic (125°) Particles in Water

Treated hydrophobic particles were then injected with water into a continuous phase of silicone oil. The hydrophobic particles were expected to stay mostly in the oil phase, i.e., **sticking-out** of the water droplet as depicted in Figure 4.2. The water droplet with particles was allowed to stand for 10 minutes after which it was retracted into the capillary and successively injected out of the capillary and the droplet behaviour captured on a video camera. Sections 4.4.1.1 and 4.4.1.2 show the observed behaviours of the drop as captured by the camera.

4.4.2.1 Water Droplet with Hydrophobic (125°) Particles in 500 cSt Silicone Oil

Figures 4.5 show the behaviour of a water droplet in the more viscous 500 cSt silicone oil with hydrophobic (125°) c.a. 13 (μm) diameter silica particles subject to retraction. From the video it is seen that the particles are clearly on the interface of the water droplet (sticking out). The droplet was initially spherical and upon retraction crumpled like a paper bag.

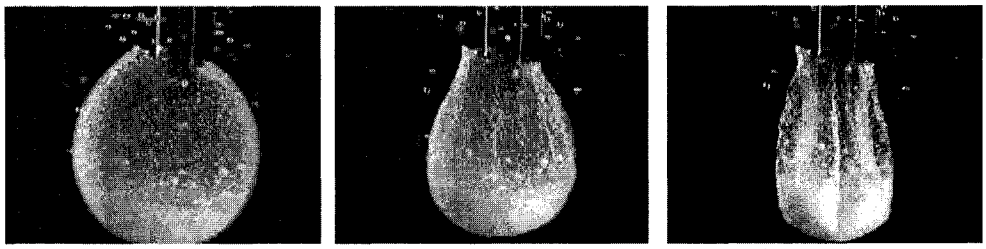

(a) Particles injected with water (b) Water droplet starts to crumple on retraction (c) Droplet continues to crumple on retraction

(d) Droplet continues to crumple on retraction (e) Crumpling clearly visible (f) Drop completely crumpled like a paper bag

Fig.4.5: Subsequent stages of drop retraction for a water droplet, with hydrophobic (125°) c.a. 13 (μm) diameter silica particles, in 500 cSt silicone oil

However, when the retracted water droplet of particles was subsequently expanded by injecting water and particles out of the capillary, it is observed that the droplet assumes its original spherical shape as shown in Figure 4.6. As seen in Figures 4.6 (c) and 4.6 (d), there also appeared to be an interesting observation involving the coalescence of droplets. The same retraction and expansion experiment, for the 13 (μm) hydrophobic silica particles, was repeated with the larger size capillary tube and similar experimental results were observed. See Appendix B.5.

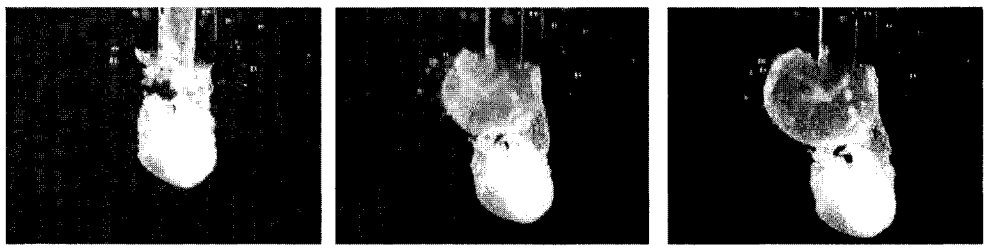

(a) Crumpled droplet after retraction (b) Water droplet slowly being expanded (c) Droplet continues to expand to original shape

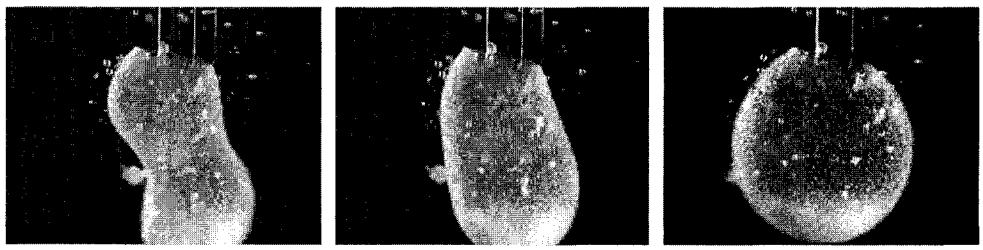

(d) Droplet continues to expand (e) Water droplet continues to expand (f) Droplet back to original shape

Fig.4.6: Subsequent stages of drop expansion for a water droplet, with hydrophobic (125°) c.a. 13 (μm) diameter silica particles, in 500 cSt silicone oil (small capillary)

Similar interface crumpling was observed for the larger < 105 (μm) diameter silica particles (see Appendix B.6) although crumpling was not clearly as visible as compared to the 13 (μm) diameter hydrophobic silica particles. For the 105 - 210 (μm) diameter glass beads (Figure 4.7), drop deformation rather than interface crumpling was observed with a characteristic necking accompanied by drop detachment from the tip of the capillary as retraction continued.

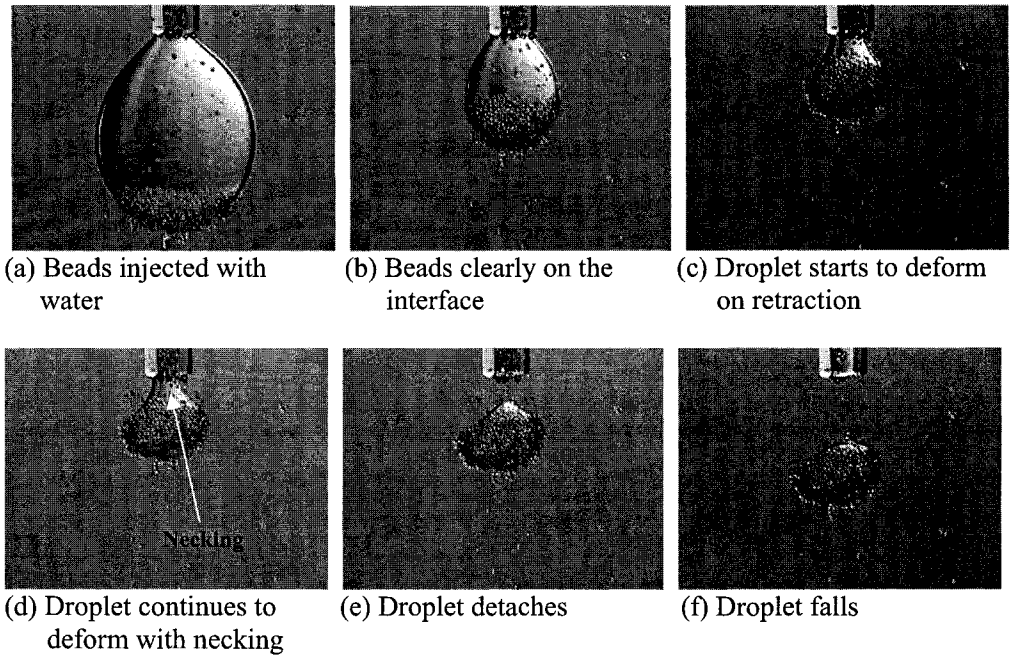

(a) Beads injected with water (b) Beads clearly on the interface (c) Droplet starts to deform on retraction

(d) Droplet continues to deform with necking (e) Droplet detaches (f) Droplet falls

Fig.4.7: Subsequent stages of drop retraction for a water droplet, with hydrophobic (125°) 150 - 210 (μm) diameter glass beads, in 500 cSt silicone oil (small capillary)

The droplet detached from the tip of the capillary, with some necking instability, while some particles were observed to fall off the interface of the drop as the interfacial area of the drop is reduced by retraction. The particles appeared to fall off not as individual particles but as smaller water droplets with particles.

4.4.2.2 Water Droplet with Hydrophobic (125°) Particles in 5 cSt Silicone Oil

Experiments involving water droplets with adsorbed hydrophobic particles were also performed using the less viscous (5 cSt) silicone oil. Figures 4.8 show the

behaviour of a water droplet in 5 cSt silicone oil with hydrophobic (125°) c.a. 13 (μm) silica particles subject to retraction. From the video, as with the more viscous 500 cSt silicone oil (section 4.2.2.1), it is seen that the particles are clearly on the interface of the water droplet (sticking out). The droplet was initially spherical and upon retraction crumpled like a paper bag.

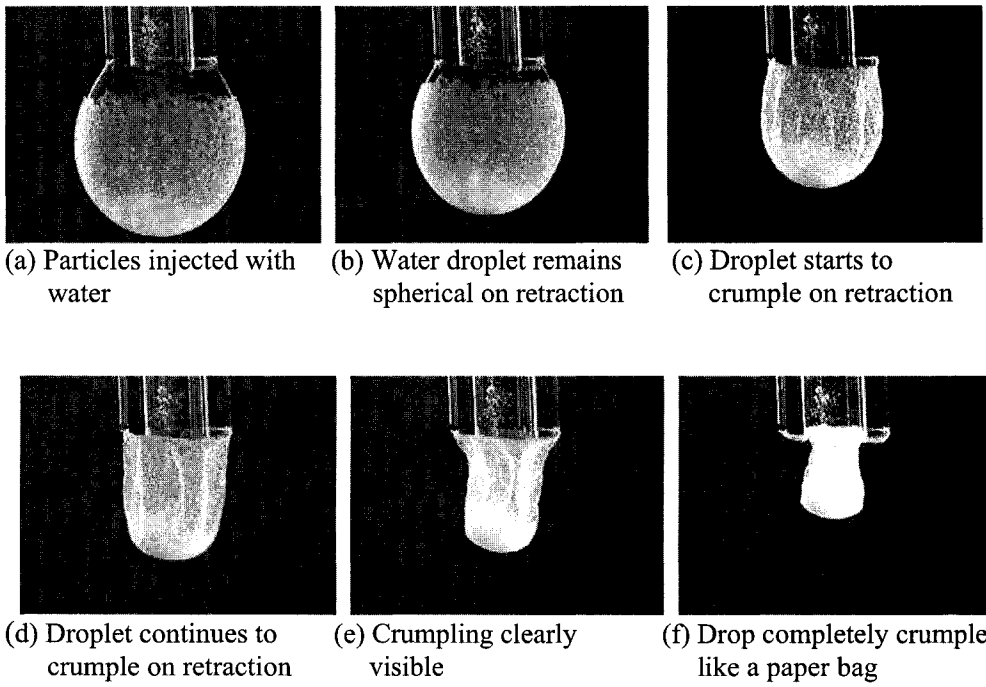

(a) Particles injected with water

(b) Water droplet remains spherical on retraction

(c) Droplet starts to crumple on retraction

(d) Droplet continues to crumple on retraction

(e) Crumpling clearly visible

(f) Drop completely crumpled like a paper bag

Fig.4.8: Subsequent stages of drop retraction for a water droplet, with hydrophobic (125°) c.a. 13 (μm) diameter silica particles, in 5 cSt silicone oil (small capillary)

The crumpled water droplet was thereafter expanded by injecting out of the capillary by means of a syringe. Figure 4.9 shows the droplet as it expands to its original shape.

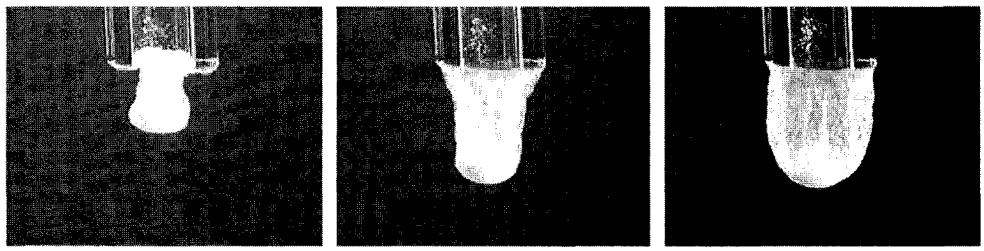

(a) Crumpled droplet after retraction (b) Water droplet slowly being expanded (c) Droplet continues to expand to original shape

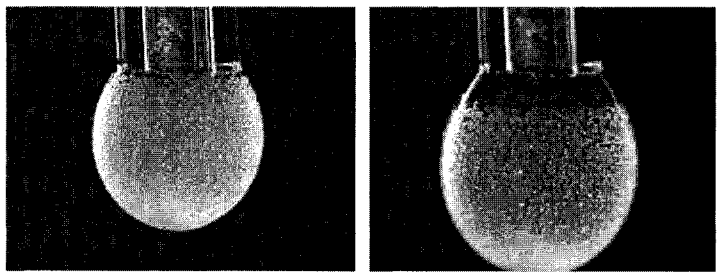

(d) Droplet continues to expand (e) Droplet back to its original shape on expansion

Fig.4.9: Subsequent stages of drop expansion for a water droplet, with hydrophobic (125°) c.a. 13 (μm) diameter silica particles, in 5 cSt silicone oil (large capillary)

Similar interface deformation was also observed for larger particles: < 105 (μm) diameter silica particles and 105 - 210 (μm) diameter glass beads. However, unlike the case of the 13 (μm) diameter silica particles (section 4.2.2.1); a droplet with beads attached was observed to fall off, from the tip of the capillary on retraction. See Figures in Appendix B.7 and B.8. Although it was observed in most of the experiments that the particles fall off the tip of the capillary upon retraction, the necking instability noticed in section 4.2.2.1 with the more viscous 500 cSt silicone oil was not observed for the less viscous 5 cSt silicone oil. It is imperative to however mention that one or two isolated cases of

drops with necking were observed for water droplets in 5 cSt silicone oil. The number of particles on such droplets could have accounted for such cases. It is suspected that the observed necking instabilities may likely be due to the weight of particles and/or the viscosity of the silicone oil continuous phase. This assumption will be further investigated in a subsequent section.

4.5 Silicone-Oil-Droplet-in-Water System

Experiments were also performed involving silicone oil droplets in water with particles of varying hydrophobicity. By switching the droplet and continuous phases, we expect the droplet behaviour to be mirror images of similar systems for water droplets in silicone oil. Emphasis was placed on the behaviour of hydrophilic (45^{o}) particles so as to understand better the crumpling and detachment behaviours noticed for water-in-oil systems. Both the 500 cSt and the 5 cSt silicone oil fluids were used in these experiments. All experiments for silicone oil in water were performed with the small size capillary. The following sections discuss the observed behaviours of a silicone oil droplet in water.

4.5.1 Hydrophilic (45^{o}) Particles in Silicone Oil

Untreated, hydrophilic (45^{o}) c.a. 13 (μm) diameter silica particles were first injected with silicone oil to form a droplet in water. The silicone oil droplet was allowed to stand for 10mins after which it was subjected to retraction by sucking oil into the capillary by means of a syringe. The experiment was thereafter

repeated with larger size particles: < 105 (μm) diameter silica particles and 150 - 210 (μm) diameter glass beads. Due to the hydrophilic nature of the particles, they were expected to be protruding more into the water phase, i.e. sticking - out of the silicone oil droplet. Sections 4.5.1.1 and 4.5.1.2 show the behaviour of the silicone oil droplet, subjected to retraction, as captured by a video camera.

4.5.1.1 500 cSt Silicone Oil Droplet with Hydrophilic (45°) Particles in Water

Figures 4.10 show the behaviour of a 500 cSt silicone oil droplet, with c.a. 13(μm) diameter hydrophilic silica particles, in water on retraction. As seen from the video, it appears that the particles were clearly in the oil phase contrary to their thermodynamically favoured position (the water phase). This is particularly an interesting observation and a likely explanation is that the particles are not able to cross the interface. Also the droplet remained spherical on retraction with the particles completely sucked into the capillary tube.

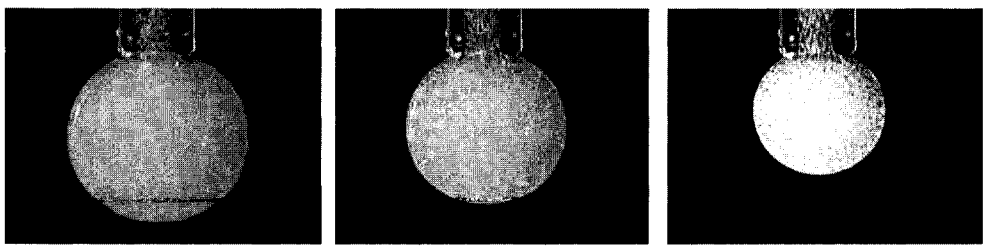

(a) Particles injected with silicone oil

(b) Oil droplet remains spherical on retraction

(c) Droplet continues to remain spherical

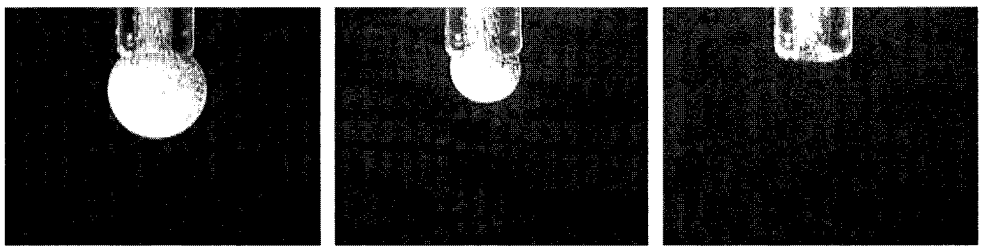

(d) Droplet continues to remain spherical

(e) Droplet continues to remain spherical

(f) Drop completely sucked in with silicone oil

Fig.4.10: Subsequent stages of drop retraction for a 500 cSt silicone oil droplet, with hydrophilic (45°) c.a. 13 (μm) diameter silica particles, in water

Similar silicone-oil-droplet-in-water experiments were also performed with larger size particles. For hydrophilic silica particles of size < 105 (μm) diameter as depicted in Appendix B.9, it is seen that some of the particles appear to be somewhat on the interface although not clearly visible. And on retraction, the droplet deforms from its spherical shape. As the particles' size becomes larger, it appears they are able to get to the interface as seen in Figure 4.11 for glass beads of size 150 - 210 (μm) diameter. The droplet also deforms from its spherical shape and the beads are sucked into the capillary on retraction. The inability of the smaller hydrophilic particles to get to the interface may possibly be due to line tension effects [2, 3, and 4]. This will be further investigated in a subsequent section.

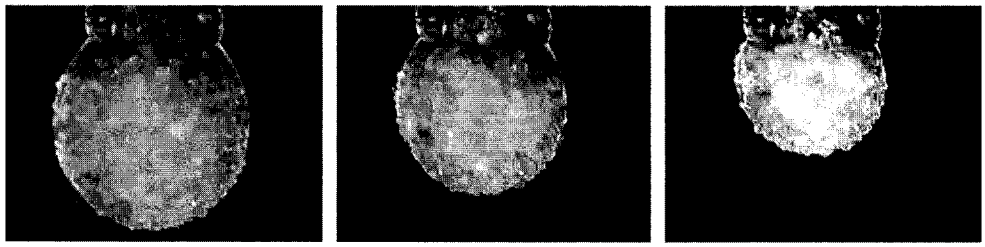

(a) Particles injected with silicone oil (b) Oil droplet remains spherical on retraction (c) Droplet continues to remain spherical

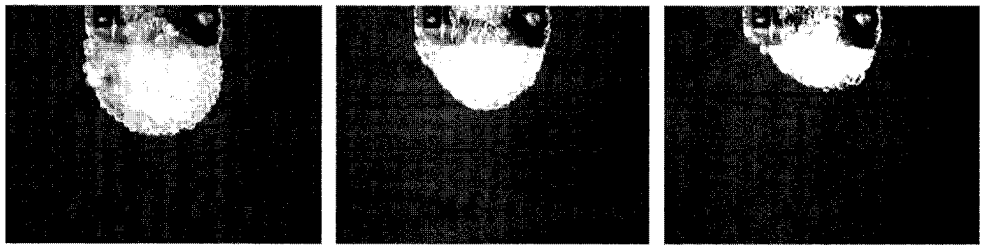

(d) Droplet appears to deform (e) Droplet continues to deform (f) Beads sucked in with silicone oil

Fig.4.11: Subsequent stages of drop retraction for a 500 cSt silicone oil droplet, with hydrophilic (45°) 150 - 210 (μm) diameter glass beads, in water

4.5.1.2 5 cSt Silicone Oil Droplet with Hydrophilic (45°) Particles in Water

Similar experimental results to section 4.5.1.1 were observed for the less viscous 5 cSt silicone oil droplets in water with hydrophilic particles. Figures 4.12 show the behaviour of a 5 cSt silicone oil droplet, with hydrophilic (45°) 150 - 210 (μm) diameter glass beads, in water.

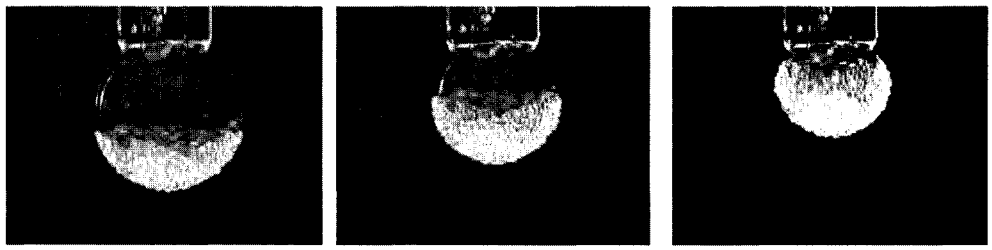

(a) Particles injected with silicone oil

(b) Oil droplet remains spherical on retraction

(c) Droplet continues to remain spherical

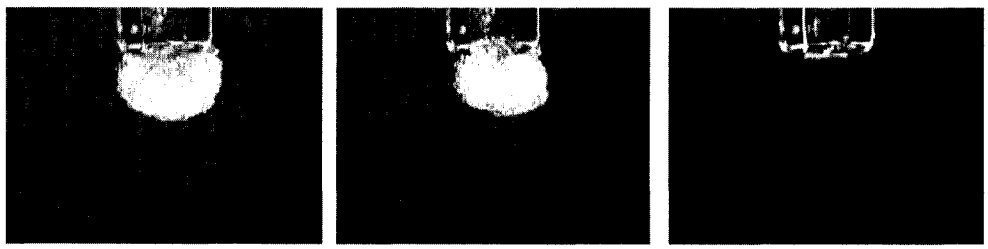

(d) Droplet appears to deform

(e) Droplet continues to deform

(f) Drop fall off the tip of the capillary

Fig.4.12: Subsequent stages of drop retraction for a 5 cSt silicone oil droplet, with hydrophilic (45°) 150 - 210 (μm) diameter glass beads, in water

4.5.2 Hydrophobic (125°) Particles in Silicone Oil

Treated hydrophobic particles were then injected with 500 cSt silicone oil into a continuous water phase. The hydrophobic particles were expected to stay mostly in the oil phase, i.e., **sticking-in** the oil droplet. The silicone oil droplet with particles was allowed to stand for 10 minutes after which it was retracted into the capillary and the droplet behaviour captured on a video camera.

4.5.2.1 500 cSt Silicone Oil Droplet with Hydrophobic (125°) Particles in Water

Figure 4.13 shows the behaviour of a silicone oil drop, with hydrophobic 150 - 210 (μm) diameter glass beads, in a continuous water phase. From the video, it is clear that the beads are all in the oil phase and the droplet remained spherical while the beads get sucked in through retraction.

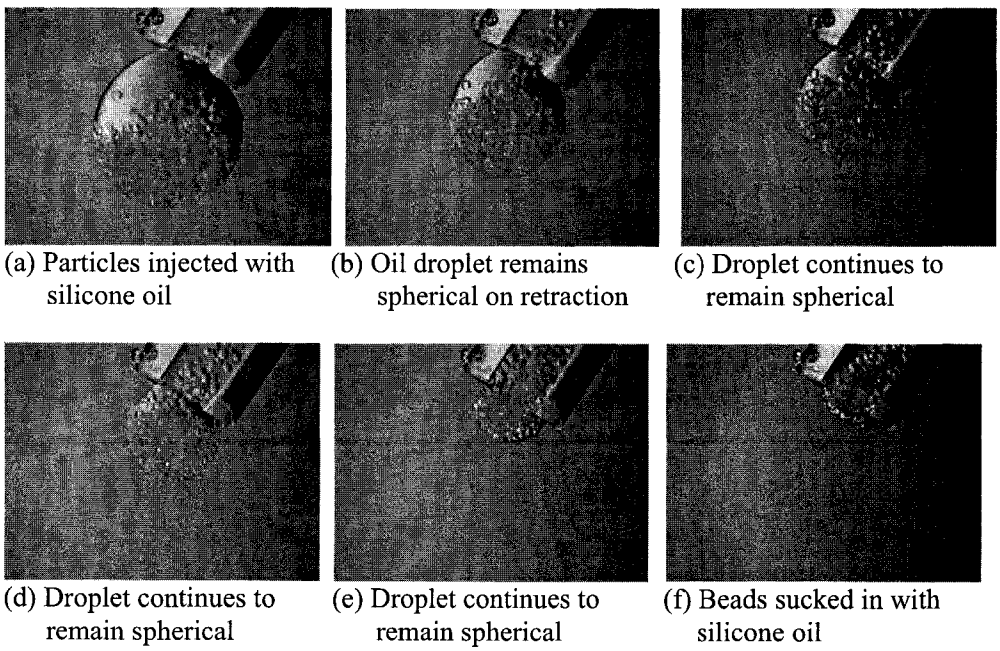

(a) Particles injected with silicone oil
(b) Oil droplet remains spherical on retraction
(c) Droplet continues to remain spherical
(d) Droplet continues to remain spherical
(e) Droplet continues to remain spherical
(f) Beads sucked in with silicone oil

Fig.4.13: Subsequent stages of drop retraction for a 500 cSt silicone oil droplet, with hydrophobic (125°) 150 - 210 (μm) diameter glass beads, in water

The same result was observed for a 500 cSt silicone oil drop in water with the smaller 13(μm) diameter and the < 105(μm) diameter silica particles.

4.5.2.2 5 cSt Silicone Oil Droplet with Hydrophobic (125°) Particles in Water

Similar experimental results in section 4.5.2.1 were observed for the less viscous 5 cSt silicone oil droplets in water with hydrophobic particles. For all three particles, the particles were clearly in the silicone oil droplet and on retraction; the silicone oil droplet remained spherical while the particles were completely sucked into the capillary with oil.

4.6 Summary of Observations from Ground-Based Experiments

From the results of the ground based experimental studies in sections 4.3 through 4.5, the following experimental observations can be summarized:

1. The capillary diameter has no effect on the behaviour of the droplet.
2. For the water-in-silicone-oil-droplet experiments, interface crumpling was observed mainly for hydrophobic particles and the crumpling effect was more pronounced (visible) with the smallest (13 micron diameter) particles.
3. The necking instability accompanied by droplet detachment was observed for the larger particles and the more viscous (500 cSt) silicone oil while no necking instability was observed for the less viscous (5 cSt) silicone oil with larger particles although drop detachment occurred.

4. The observed necking instability and subsequent drop detachment may likely be due to the viscous drag effect in the more viscous silicone oil (since necking was prevalent for the more viscous 500 cSt oil) and/or the weight of the particles (as no necking was observed for the smallest, 13 micron diameter particles for both silicone oils).

5. For silicone-oil-droplet-in-water experiments with hydrophilic (45^{o}) particles, we expect the particles to be at the interface and sticking more into the aqueous phase. However for the cases of silicone oil droplet in water with the smaller hydrophilic particles, the particles appeared to mostly be in the oil phase rather than the water phase as expected with only a very few particles reaching the interface. As such, the particles behaved more like hydrophobic particles. This may be explained as possibly due to the effect of line tension, which prevents the particle from reaching the interface or their thermodynamically favoured position, as discussed by previous researchers in the literature [2, 3, and 4].

4.7 Discussion of Results from Ground-Based Experiments

In order to understand better the positioning of solid particles at the liquid-liquid interface, it is pertinent to explain some of the experimental observations from the ground based studies such as: the observed interface crumpling, the necking instabilities, droplet detachment and the inability of the smaller hydrophilic

particles, starting from the oil phase, to reach the interface for the silicone-oil-in- water systems.

From the experimental results, the necking instability was observed for water droplets in both silicone oils with only hydrophobic particles and was found to be profound with the smaller 13 micron diameter silica particles. By expanding the crumpled droplet, it was also observed that the droplet regained its initial shape indicating that the interface crumpling was reversible. This observation is consistent with previous studies of the behaviour of real bitumen water interfacial skins [5].

The observed necking and drop detachment can be explained if one considers the force interplay on the drop, at the tip of the capillary, at the time of detachment. Using the analysis described in Section 3.6 and Equations 3.1 through 3.9, the role of buoyancy (due to the density difference between the drop and the continuous phase) as well as the viscous drag (due to the continuous phase viscosity) on drop detachment can be explained.

Consider the retraction of a water droplet in the more viscous (500 cSt) silicone oil with adsorbed hydrophobic 150 - 210 micron diameter glass beads (Figure 4.7). For an approximate water droplet diameter of 3mm, a capillary radius of 0.038cm (small capillary), an average retraction velocity of 7.33mm/s, average particle radius of 90 microns, silicone oil density of 975kg/m3, silicone oil viscosity of 488mPa.s and an interfacial tension of 21.1mN/m (Ref: Dow Chemicals); the calculated values of the forces acting on the droplet at the point

of detachment indicate an interfacial tension force of 5.12 μN, a buoyancy force of magnitude equal to 15.0 μN and a viscous drag of magnitude equal to 1.01 μN. (Detailed calculations are as shown in Appendix C).

As discussed in section 3.6, the condition for the drop to remain attached to the tip of the capillary requires that the interfacial tension force be greater than the summation of both the buoyancy force and the force due to the viscous drag. However a comparison of the magnitude of the forces calculated above showed that the buoyancy force is far greater than the interfacial tension force and may thus have been responsible for the drop detaching from capillary tip.

The explanation of the likely detachment due to the effect of gravity however still does not explain the necking instability observed with the more viscous silicone oil but not with the less viscous silicone oil. By considering the force interplay on a water droplet, with same attached 150 - 210 micron diameter glass beads, but now in the less viscous silicone oil (5 cSt), it is seen (Appendix C) that although the buoyancy force still far exceeds the interfacial tension force (likely cause of detachment), the force due to the viscous drag nevertheless has reduced from a magnitude of few μN (micro-Newton) calculated for the more viscous silicone oil to nN (nano-Newton). This difference in viscous drag magnitude may be responsible for the necking instability which was observed for the larger hydrophobic (150 - 210) micron diameter glass beads in the more viscous silicone oil.

The inability of the smaller hydrophilic particles, starting from the oil phase, to reach the interface for the silicone oil in water systems may be related to the effect of line tension. As discussed in Chapter 1, the effect of line tension on the positioning of a particle at a liquid interface becomes pronounced as the radius of the particles becomes very small - usually of the order of nano-meter [2].

In recent studies on a macroscopic model of solid stabilized emulsion droplet using silicone oil, water and glass beads, Chiang et al. [3] observed that regardless of the starting phase, hydrophilic glass beads got to the interface and were able to obtain their thermodynamic favourable position. However, when hydrophobic particles start from the water phase, they do not reach the interface spontaneously and thus do not attain their thermodynamically favourable position. They attributed the inability of the hydrophobic particles getting to their thermodynamically favoured position as being due to an energy barrier resulting from the effect of line tension at the interface.

Although, the existence of this energy barrier due to line tension, which prevents particles from reaching the interface, was not observed by Chiang et al. for hydrophilic particles, the size of the particles used for their studies were larger than those for which the same observations were made in this study. As line tension increases as the size of the particles reduces, it is possible that the inability of the smaller (13 micron diameter) silica particles, starting from the oil phase, to get to the interface may be due to the existence of line tension at the interface.

Based on the above observations and discussions, this study of the behaviour of solid particles at a liquid-liquid interface will be summarized under the following headings: the role of particle size, role of particle wettability and the role of viscous effects in the continuous phase. Finally the model experimental study will be linked to known behaviours of real bitumen emulsion studies.

4.7.1 Role of Particle Size

Yan et al. [6] in their study of the roles of various bitumen components in the stability of water-in-diluted bitumen emulsions concluded that only solid particles in a certain size range were effective stabilizers. Also in a review of the factors affecting the stability of solids-stabilized emulsions, Tambe et al. [7] reported that emulsion stability increased with a decrease in particle size until a critical particle size was reached.

From the ground based experiments performed in this study, it was seen that the retracting droplet behaved differently with the size of the attached particles. For this model study, three different particle sizes were used including 13 micron diameter silica particles, less than 105 micron diameter silica particles and 150 - 210 micron diameter glass beads. Interface crumpling was clearly observed with the smallest (13 micron diameter) silica particles while interface deformation (jamming) rather than crumpling was observed with the larger (150 - 210) micron diameter glass beads. Drop detachment was also observed for the larger particles

while no drop detachment was observed for experiments involving the smallest (13 microns) particles.

Hence, it can be concluded that the behaviour of a retracting liquid-in-liquid pendant drop with adsorbed solids depends on the size of the particles involved.

4.7.2 Role of Particle Wettability

Water-wet particles are known to stabilize oil-in-water emulsions while oil-wet particles stabilize water-in-oil emulsions. Thus the wettability of the particle is expected to play a role in the behaviour of emulsion droplet.

From the model ground based experimental studies; it was observed that the retracting droplet behaved differently depending on the hydrophobicities of the adsorbed particles. Only liquid-in-liquid droplets with hydrophobic particles exhibited the interface crumpling while no crumpling was seen for hydrophilic particles.

It may thus be concluded that interface crumpling observed for a liquid-in-liquid droplet, with attached particles, subjected to shearing is due to the hydrophobic nature of the adsorbed interfacial particles.

4.7.3 Role of Viscous Effects in the Continuous Phase

Not much is known regarding the role of the continuous phase viscosity in emulsion studies. From the ground based model droplet studies, it was observed that some necking instability occurred, prior to droplet detachment, for water

droplets in the more viscous silicone oil with larger hydrophobic particles at the interface. An analysis of the forces acting on the droplet at the point of detachment showed that the buoyancy forces due to the density difference between the fluid as well as the viscosity of the continuous phase contribute to this necking behaviour.

Hence, one can conclude that the behaviour of a liquid-in-liquid drop, with adsorbed particles, depends on the viscosity of the continuous phase.

4.8 Relation to Bitumen Studies

Based on the traditional understanding of the behaviour of solids-stabilized bitumen emulsions systems; hydrophilic particles are known to stabilize oil-in-water emulsions while hydrophobic particles stabilize water-in-oil emulsions. Also, solid materials found in bitumen, such as clays, sands, minerals and asphaltenes (which can be thought of as nano-particles), have been known to contribute to the stability of bitumen emulsions by forming an interfacial film or "skins", at the bitumen-oil-water interface that prevents the emulsion droplets from coalescing. The existence of these interfacial films or "skin" has also been investigated by repeatedly contracting and expanding a drop of water suspended from a glass tip in the bitumen. However, the properties and mechanisms by which these interfacial films are formed as well as other known stabilization behaviours of bitumen emulsions are still not yet fully understood.

From the ground-based experiments performed using a model emulsion droplet of silicone oil, water and solid glass and silica particles in this study, it would appear that the interfacial "skins" observed in bitumen emulsions system (manifested by an interfacial crumpling, when these droplets are subjected to shearing) can be attributed to the hydrophobic nature of the adsorbed entities. It has also been seen that the interfacial crumpling observed in bitumen emulsions is reversible.

4.9 Conclusions from Ground-Based Experiments

The following conclusions can be made from the ground based experimental study with the model emulsion drop system:

1. The behaviour of a retracting liquid-in-liquid pendant droplet with adsorbed particles depends on: the size of the particles, their wettability, the viscous effects in the continuous phase and is independent of the radius of the capillary introducing the droplet.
2. The observed necking instability, prior to droplet detachment, can be explained by an analysis of the forces (buoyancy or gravitation force, interfacial tension force and the viscous drag) acting on the droplet at the time of detachment.
3. Interface crumpling observed in real bitumen emulsion systems may be attributed to the very small size and the hydrophobic nature of the interfacial adsorbed entities such as asphaltenes and fine solids.

4.10 References

[1] T. Dabros, A. Yueng, J. Masliyah and J. Czarnecki, J. Colloid Interface Sci., 210 (1999) 222.

[2] R. Aveyard, B. D. Beake, and J. H. Clint, J. Chem. Soc., Faraday Trans., 92 (1996) 4271.

[3] R. Chiang, "Development of a macroscopic model of solids-stabilized emulsion", M. Sc Thesis, University of Alberta, Fall 2003.

[4] R. Chiang and J. A. W. Elliott, " A macroscopic solids-stabilized emulsion droplet analogue in microgravity", The 6th Japan-Canada workshop on space technology, Hamamatsu, Japan, Nov. 18-20, 2002.

[5] F. E. Bartell and D. O. Niederhauser, "Film forming constituent of crude petroleum oils", American Petroleum Institute progress report on Fundamental research on occurrence and recovery of petroleum, 1946-1947, P. 57-80.

[6] Z. Yan, J.A.W. Elliott, and J. H. Masliyah, J. Colloid Interface Sci., 220 (1999) 329-337.

[7] E. Tambe and M. M. Sharma, Advances in Colloids and Interface Sci., 52 (1994) 1 - 63

CHAPTER 5

MICROGRAVITY EXPERIMENTS

5.1 Microgravity Experiments

As discussed in Chapter 1, it is well known that the presence of solid nano-sized particles affects the stability of emulsions. However, it is difficult to make direct observations of these particles' behaviour because of their dimensions. By reducing the gravitational force exerted on the droplets and particles, it is possible to enlarge the emulsion droplet system such that the particles on the interface can be observed optically. Such a macroscopic model was developed by Chiang et al. [1] using silicone oil, water and glass beads of extreme hydrophobicities.

Although this enlarged model will not be affected by all the same forces that affect nano-scale particles, the model could however be used to study systems where interfacial forces dominate and can give information about the role of geometry in the behaviour of particles at interfaces.

These reduced gravity experiments were performed aboard a modified Falcon 20 parabolic aircraft provided by the National Research Council of Canada (NRC) and the Canadian Space Agency (CSA). The aircraft provides a near-zero gravity environment by flying on a parabolic path. The aircraft started the parabolic flight path by initiating a shallow dive, and then pulled-up into a nose high attitude. The aircraft then travelled in a parabolic path the same as a projectile travelling through air. During this time of approximately 20 seconds, the aircraft and the objects inside the cabin experienced near weightlessness (on

the order of 0.02-*g*). The near weightless condition ended when the aircraft pulled-out of the parabolic path. During the entry into and exit from the parabolic motion, the aircraft experienced an increased g-load of approximately 2.0 to 2.5-*g*'s for approximately 10 seconds. Six flights of four parabolas with typically 0.02-*g* for 20 seconds were available for these experiments.

5.1.1 Why Microgravity?

In this present study, reduced gravity experiments were performed using the model system developed by Chiang et al. but with glass beads of intermediate hydrophobicities. It was necessary to investigate some of the observed behaviours in the ground based studies, such as the necking instabilities and the drop detachment discussed in Chapter 4, in an environment where surface forces dominate over gravitational forces such as in a reduced gravity environment. The role of gravitational force and viscous drag on the observed behaviours of the droplet, as discussed in Chapter 4, can then be better understood. Experiments were conducted with same glass beads (hydrophilic 45° and hydrophobic 125° beads) used in the previous ground based studies. The following sections describe the experimental procedures and the observations from microgravity.

5.1.2 Experimental Procedures

The same experimental apparatus used for the ground based experiments was used in the reduced gravity studies. However, due to the nature of the reduced

gravity experiments, the plexiglass test cells containing the fluids were tightly sealed before each flight. Two stainless steel capillary tubes, each attached to a syringe, were used to introduce the droplet phase to allow for effective control of the droplet (See Figure 3.2 in Chapter 3). For each experiment, a very small drop with particles about 1mm in size is formed during the 2.0-*g* pull up to prevent the droplet falling off the capillary tip due to the increased g-load. During the 20*s* of reduced gravity, the droplet size is increased to approximately 8mm and subsequently subjected to retraction by sucking into the capillary by means of a syringe. A CCD camera is used to capture the behaviour of the drop during this process.

For the microgravity experiments, only the large glass beads (150 - 210 microns in diameter), the more viscous 500 cSt silicone oil and the smaller stainless steel capillary tubes were used in the experimental studies.

5.2 Microgravity Experimental Observations

Six flights of four parabolas each were conducted in the reduced gravity experiments. Four of the flights involved a water droplet in silicone oil while two involved a silicone oil droplet in water. A new and cleaned test cell was used every time for each flight. Below is a description of the experimental observations for each flight.

5.2.1 Observations from Microgravity Flight 1

A water droplet in 500 cSt silicone oil with hydrophilic (45°) 150 - 210 (μm) diameter glass beads was used for the first flight. Two stainless steel capillaries, each attached to a syringe, were used to introduce the droplet and particles. It was expected that the beads would protrude more into the water phase from the interface (sticking-in) because of their hydrophilic nature.

The first parabola (*parabola 1*) was conducted to see if the experimental set-up and the personnel on the flight will be able to withstand the adverse conditions of the microgravity environment.

For the second parabola (*parabola 2*), a water droplet of approximately 6mm in diameter was formed in microgravity with the beads completely in the water droplet. Figures 5.1 show the observed behaviour of the water droplet in micro-gravity. From the figure, it is seen that the water droplet was initially spherical and the beads clearly in the water droplet. On retraction, the droplet continued to remain spherical while the water droplet and beads were completely sucked into the capillary.

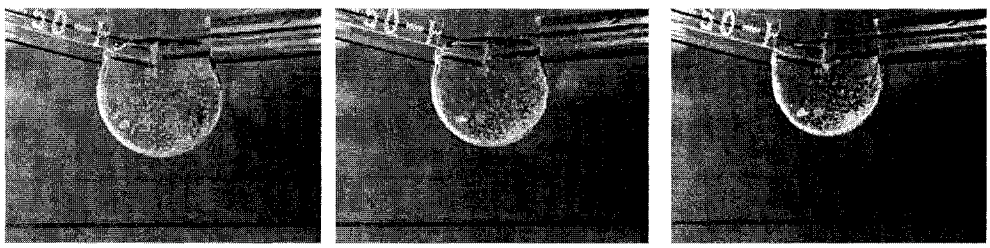

(a) Beads injected with water

(b) Water droplet remains spherical on retraction

(c) Droplet continues to remain spherical

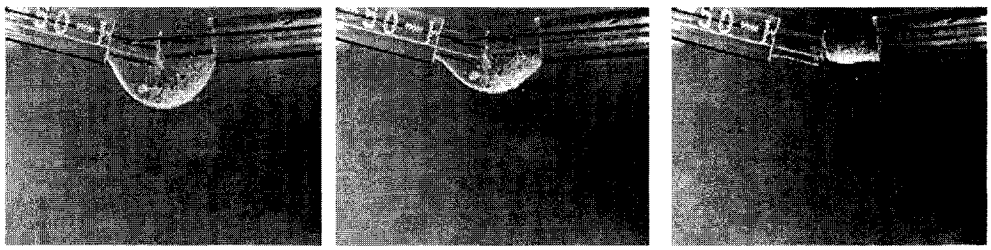

(d) Droplet continues to remain spherical

(e) Droplet continues to retract

(f) Beads sucked in with water

Fig.5.1: Subsequent stages of drop retraction for a water droplet in microgravity with hydrophilic (45°) 150 - 210 (μm) diameter glass beads, in 500 cSt silicone oil.

It is important to mention here that it was difficult to get a large number of beads on the droplet during microgravity. It was also observed that the beads were collected on one side of the water droplet while the water droplet formed was attached to the sides of the capillary tubes and may have affected the shape and behaviour of the droplet. Similar experimental observations were noted for the third and fourth parabolas (*parabola 3 and 4*).

5.2.2 Observations from Microgravity Flight 2

For the second flight, similar experiments with water droplets in 500 cSt silicone oil was used, however with hydrophobic (125°) 150 - 210 (μm) diameter glass beads. The beads were expected to protrude more into the oil side of the interface and sticking-out of the water droplet. In order to prevent the droplet sticking to the side of the capillary tubes, a single capillary tube attached to a syringe was used henceforth.

For the first parabola (*parabola 1*), a water droplet of approximately 6mm in diameter was formed in microgravity and attempts to retract the droplet and particles in microgravity failed as the particles tend to form a cake, which made retraction difficult. It was also observed that the beads were not at the interface as expected but rather in the water phase, behaving more like hydrophilic beads. This may likely be due to the fact that the beads were soaked in the water phase for at least 2hrs prior to the microgravity flight. As a result of the problems encountered sucking in the beads, parabolas 2, 3 and 4 for the second flight were suspended.

5.2.3 Observations from Microgravity Flight 3

A repeat of the experiments in section 5.2.2 was conducted during the third flight using a new test cell with a modified drop injection. An experiment involving a water droplet in 500 cSt silicone oil with hydrophobic (125^{o}) 150 - 210 (μm) diameter glass beads was performed.

For the first parabola (*parabola 1*), a water droplet of approximately 4mm in diameter was formed in microgravity. Figure 5.2 showed the behaviour of the droplet when subjected to retraction.

(a) Beads injected with water (b) Water droplet remains spherical on retraction (c) Droplet continues to remain spherical

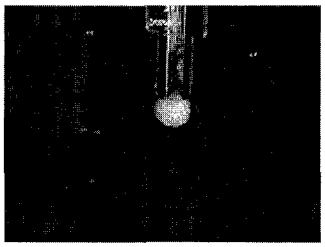

(d) Droplet continues to remain spherical with beads sucked in.

Fig.5.2: Subsequent stages of drop retraction for a water droplet in microgravity with hydrophobic (125°) 150 - 210 (μm) diameter glass beads, in 500 cSt silicone oil.

From Figure 5.2, it is seen that the beads are not clearly on the interface but rather in the water droplet contrary to expectation. This again may be due to the fact that the beads were soaked in water for more than 2hrs prior to the microgravity experiment. The droplet was observed to remain spherical on retraction and the beads were sucked to the tip of the capillary as retraction continued.

The same experiments were performed during the second and third parabolas and similar observations were noted. For the fourth parabola, no conclusive observation was made as the camera focus was lost during the experiment.

5.2.4 Observations from Microgravity Flight 4

For the fourth flight, silicone oil droplet in water experiments were performed with hydrophobic (125°) 150 - 210(μm) diameter glass beads. However, for the first, second and fourth parabolas, air bubbles were observed in the formed oil droplet which affected the experimental observations. In the third parabola (*parabola 3*), an oil droplet of approximately 6mm in diameter was formed in microgravity and thereafter subjected to retraction. As a result of the hydrophobic nature of the particles, the particles were expected to be in the silicone oil phase. Figures 5.3 show the behaviour of the droplet in microgravity when subjected to retraction.

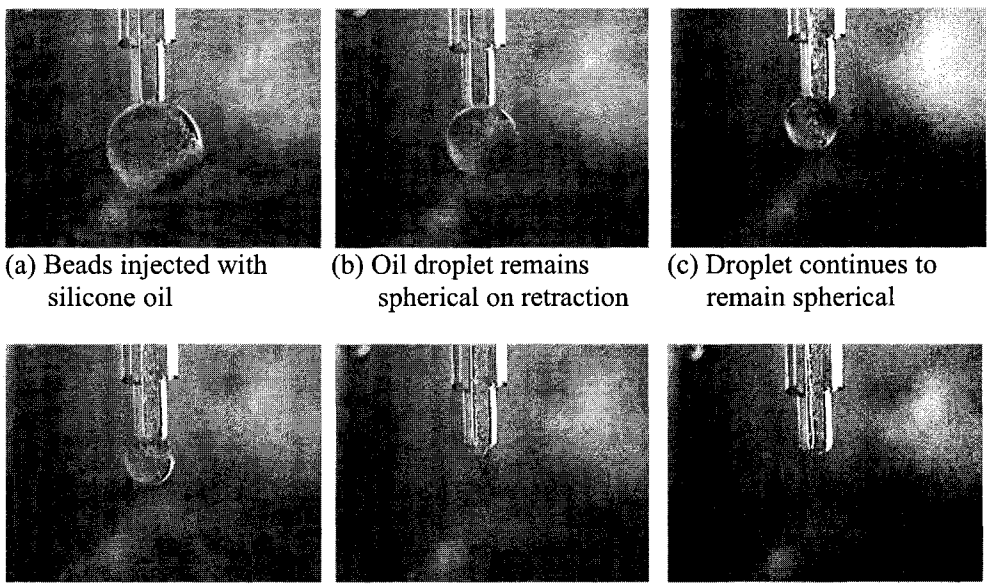

(a) Beads injected with silicone oil

(b) Oil droplet remains spherical on retraction

(c) Droplet continues to remain spherical

(d) Droplet continues to remain spherical

(e) Beads sucked in with silicone oil

(f) Beads completely sucked in with silicone oil

Fig.5.3: Subsequent stages of drop retraction for a 500 cSt silicone oil droplet in microgravity with hydrophobic (125°) 150 - 210 (μm) diameter glass beads, in water.

From Figure 5.3, it is seen that the droplet was initially spherical and the particles clearly in the silicone oil. The beads were also observed to be on one side of the silicone oil droplet. On retraction, the droplet remained spherical and the beads were completely sucked into the capillary with oil as retraction continued.

5.2.5 Observations from Microgravity Flight 5

For the fifth flight campaign, silicone-oil-droplet-in-water experiments were performed with hydrophilic (45°) 150 - 210 (μm) diameter glass beads. Only two parabolas were conducted for the fifth flight. As a result of the hydrophilic nature of the particles, the particles were expected to be on the water side of the interface and sticking out of the oil droplet.

For the first parabola (*parabola 1*), an oil droplet approximate 8mm in diameter was formed in microgravity and subsequently subjected to retraction. On retraction, the beads which were clearly observed to be on the interface were being sucked into the capillary however the camera focus was lost during the experiment.

For the second parabola (parabola 2), an oil droplet of approximately 8mm in diameter with hydrophilic (45°) 150 - 210 (μm) diameter beads was formed and then subjected to retraction. Figure 5.4 show the behaviour of the droplet during the retraction.

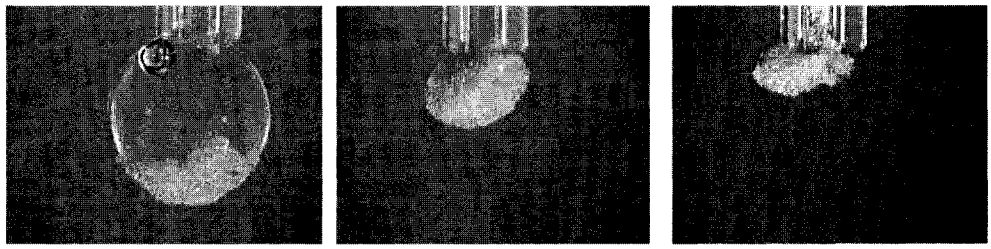

(a) Silicone oil droplet injected with water

(b) Drop starts to deform on retraction

(c) Drop completely deformed on retraction

Fig.5.4: Subsequent stages of drop retraction for a 500 cSt silicone oil droplet in microgravity with hydrophilic (45°) 150 - 210 (μm) diameter glass beads, in water.

It is seen from Figure 5.4 that the drop was initially spherical and deformed on retraction.

5.2.6 Observations from Microgravity Flight 6

For the sixth microgravity flight campaign, a water-drop-in-silicone-oil experiment was performed with the hydrophobic (125°) 150 - 210 (μm) diameter glass beads. However rather than injecting the beads with water, the beads were placed in the silicone oil continuous phase at the bottom of the test cell. Prior to microgravity, a small drop of water was formed and lowered to the bottom of the test cell to pick up some beads. The drop was then enlarged in microgravity prior to retraction. Only one parabola was conducted for the sixth flight campaign.

A water droplet of approximately 2mm in diameter was formed prior to microgravity and lowered to pick up some beads. During microgravity, more water was injected to increase the drop size to approximately 6mm and the

droplet was then subsequently subjected to contraction. The particles were clearly on the interface and what seemed to be a little necking (though not clearly visible) was observed during the retraction. Unfortunately, no clear image of the droplet was captured as the camera focus was lost during the experiment.

5.3 Discussion of Results from Microgravity Experiments

The objective of the microgravity experiment was to perform similar experiments to that on ground in a reduced gravity environment, where interfacial tension force dominates and the gravitational force is minimal. This was necessary to determine to role of viscous drag and in particular the gravitational or buoyancy force on the drop detachment and necking instabilities observed in the ground based studies.

From the experimental observations discussed in section 5.2, it was seen that for water droplet in the 500 cSt silicone oil experiments with hydrophilic beads, the water droplet remained spherical on retraction and the beads were sucked in with water. This same result was observed in the ground based experiments.

However for water drop is silicone oil experiments with the hydrophobic (125^{o}) glass beads, the particles were mostly in the water phase and did not get to the interface as expected. The particles were soaked in water for at least 2hrs prior to the microgravity experiments and this could have affected the surface treatment of the particles as discussed in literature [2]. It is believed that particles treated with trimethylchlorosilane to change their surface wetting properties,

could lose their surface hydrophobicity when exposed to air or water for a prolonged period. This may explain why the supposedly hydrophobic particles behaved more like hydrophilic particles.

For silicone oil droplet in water experiments with hydrophilic (45^{o}) glass beads, it was seen that the beads were clearly on the interface as expected and the droplet deformed on retraction. While for silicone oil in water with hydrophobic (125^{o}) glass beads, the beads were clearly on the interface and the beads were sucked in with silicone oil on retraction.

5.4 Conclusions from Microgravity Experiments

The microgravity experiments did not clearly provide us with more analysis as a result of experimental problems such as, an inability to retract droplet, the short experimental time (20sec) available for microgravity experiments and motion sickness, encountered during the microgravity experiments. No concrete conclusion could thus be made from the microgravity experiments.

5.5 References

[1] R. Chiang, "Development of a macroscopic model of solids-stabilized emulsion", M. Sc Thesis, University of Alberta, Fall 2003.

[2] P. Blake and J. Ralston, "Controlled methylation of quartz particles", Colloids and Surfaces, 15 (1985) 101.

CHAPTER 6

CONCLUSIONS

This research study was divided basically into two parts: theoretical and experimental studies. Theoretically, the effect of gravity on systems with varying three-phase line length was studied and specifically the effect of interface deformation due to gravity on the interpretation of line tension measurements by the conical capillary rise method was determined. Experimental studies were focused on the positioning and behaviour of particles at interfaces and specifically a parametric study was performed of the effect of particles on the behaviours of a retracting drop in the presence of gravity and in a reduced gravity environment.

The objective of the theoretical study was to analyze the conical capillary rise method of line tension measurements and the effect of the deformation due to gravity on the interpretation of line tension measurements by the conical capillary rise method.

For the experimental studies, the objective was to observe and explain the behaviour of a model retracting liquid-in-liquid pendant droplet, with adsorbed particles at the interface, as a function of the size of the particles, their wettability, the viscosity of the continuous phase and the radius of the capillary introducing the drop. Attempts will then be made to apply knowledge gained from this model system to real bitumen emulsion systems.

Below is a summary of the conclusions made from both the theoretical and experimental studies.

6.1 Conclusions on the Analysis of Line Tension Measurements by the Conical Capillary Rise Method - The Effect of Interface Deformation Due to Gravity

An analysis of the conical capillary rise method of line tension measurement indicated that the assumption of spherical liquid-vapour interface (that is neglecting the effect of gravity) used in the interpretation of line tension measurements, by Jensen and Li, was inadequate. The following conclusions can be made on the theoretical analysis of the effect of interface deformation due to gravity on the interpretation of line tension from the conical capillary rise method of measurement.

1. By including the effect of the deformation due to gravity on the shape of the liquid-vapour interface in the conical capillary analysis, as has been done in this work, the line tension values inferred from the experimental data of the conical tube method were not only reduced by about fifty percent (50%) but compare better with those of other methods described in the literature.
2. The conical capillary rise method of line tension has been advanced and provides a simple and reliable means of measuring line tension.

6.2 Conclusions on the Experimental Study of the Behaviour of Droplets with Particles at Liquid-Liquid Interfaces

The behaviour of a model retracting liquid-in-liquid pendant droplet, with adsorbed particles at the interface, was studied as a function of the size of the particles, their wettability, the viscosity of the continuous phase and the radius of the capillary introducing the drop both in the presence of gravity and in reduced gravity. The following conclusions can be made from the experimental studies.

4. Interface crumpling on retraction was clearly visible with the smallest 13 micron diameter silica particles of intermediate wettability and the interface crumpling was reversible.
5. The necking instability accompanied by droplet detachment was observed with the larger particles (< 105 microns silica particles and the 150 - 210 microns glass beads) and the more viscous silicone oil.
6. The observed necking instability and subsequent drop detachment can be explained by an analysis of the forces (capillary, gravitational or buoyancy force and the viscous drag) acting on the droplet at the point of detachment. Both gravitational force and viscous drag were responsible for the observed necking instability and the subsequent drop detachment.
7. The behaviour of a retracting liquid-in-liquid pendant droplet with adsorbed particles depends on: the size of the particles, their

wettability, the viscous effects in the continuous phase and is independent of the radius of the capillary introducing the droplet.

8. Interface crumpling observed in real bitumen emulsion systems may be attributed to the very small size and the hydrophobic nature of the interfacial adsorbed aggregates whether they are solid particles or perhaps asphaltenes.

9. No concrete conclusion could be made from the microgravity experiments as a result of experimental problems such as, inability to retract droplet, short experimental time (20s) available for microgravity experiments and motion sickness, encountered during the microgravity experiments.

10. Further more, in relation to the study of real bitumen emulsion systems, the important factors, which must necessarily be considered, in understanding the behaviour of real bitumen emulsion systems stabilized by solid particles include: the size of the interfacial adsorbed particles, the particles' wettability, and also the viscosity of the continuous phase.

6.3 Recommendations for Future Work

Future studies should be extended to smaller particles and possibly nano-size particles and particles of different shapes (other than spherical) in the experimental studies. More experimental studies should also be performed with

real bitumen as well as de-asphaltened bitumen while the use of surfactants and chemical modification of the aqueous phase should also be considered for future studies.

APPENDICES

Appendix A

Algorithm and Program for Numerical Solution

Appendix A.1: Algorithm to solve the differential equation describing the conical capillary interface

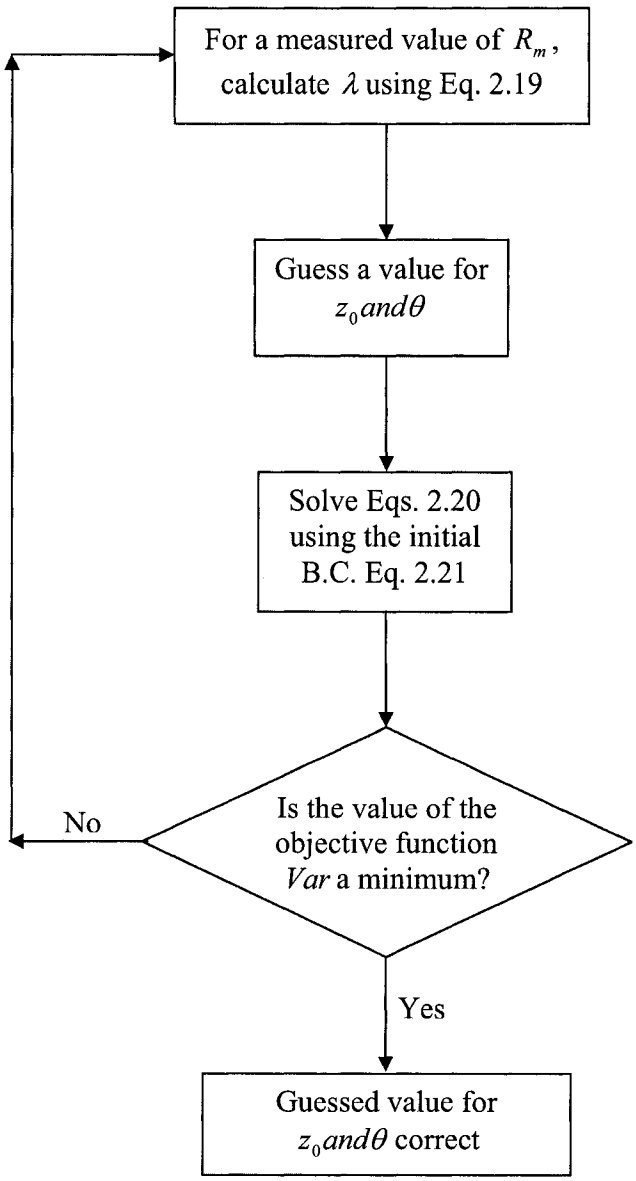

Appendix A.2: Matlab Script to solve the differential equation describing the conical capillary interface

MAIN SCRIPT

```
Clear all

format long;

Define global variable

global u Zm v J

Input parameters

Del_Rho = 773; % density difference.

g = 9.81; % acceleration of gravity.

ST = 27.60e-3; % Liquid surface tension.

Beta = 1.443; % cone angle.

D = 3.220e-3; % measured diameter.

Rm = D/2; % measured radius.

H = 0.688e-3; % measured height of interface.

Zm = H/Rm;

J = (Del_Rho*g*Rm^2)/ST;

Define initial value of parameters theta and z_guess for the iteration

p = [0.2; 0.5]; % initial values of theta and z_guess.
```

Optimize the iteration using the Matlab *FMINSEARCH* tool

***FMINSEARCH* uses the *Nelder - Mead* simplex (*direct search*) method**

v = fminsearch (@var, p); % *finds a minimum of the objective function at p.*

theta = v (1);

z_guess = v (2);

Display result.

display (theta)

display (z_guess)

SCRIPT FILE FOR THE DIFFERENTIAL EQUATION SOLVER

function du = functn (ga_mma, u)

global J

du = zeros (2, 1); % *a column vector*

Q = J*u (2) - (sin (ga_mma)/u (1));

du (1) = cos (ga_mma)/Q;

du (2) = sin (ga_mma)/Q

SCRIPT FILE FOR CALCULATING THE SUM OF SQUARE OF ERRORS

function si_gma = var (p)

```
global u Zm v J

Beta = 1.443;

v = p;

[ga_mma, u] = ode45 (@functn,[0 (Beta-v(1))],[0.0000001 v(2)]);

n = length (u);

si_gma = (1-u (n, 1)) ^2 + (Zm-u (n, 2)) ^2; % objective/optimization equation.

fprintf ('at v = [%1.5f %1.5f] the sum of the square of errors

                is: %1.8f\n', v (1), v (2),si_gma);
```

Appendix B

Experimental Pictures

Appendix B.1

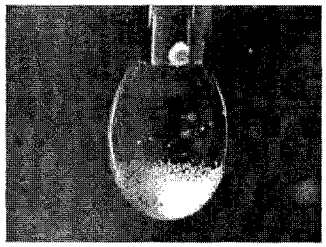

(a) Particles injected with water

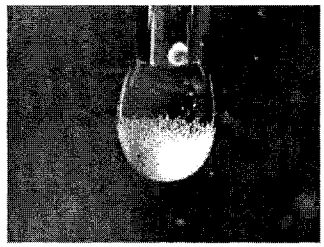

(b) Drop remained spherical on retraction

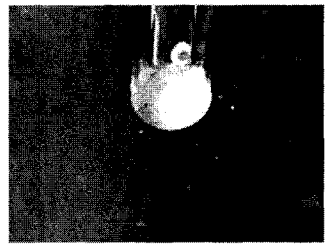

(c) Droplet continues to remain spherical

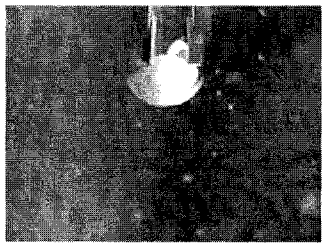

(d) Particles sucked in with water

Fig.B.1: Subsequent stages of drop retraction for a water droplet, with hydrophilic (45°) < 105 (μm) diameter silica particles, in 500 cSt silicone oil

Appendix B.2

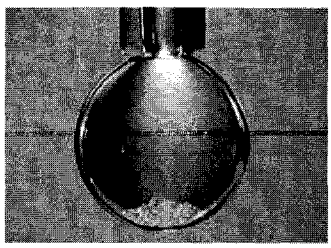

(a) Beads injected with water

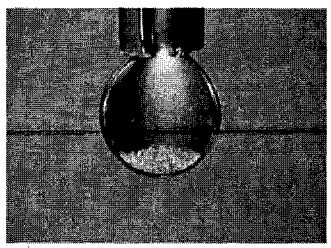

(b) Water droplet remained spherical on retraction

(c) Droplet continues to remain spherical

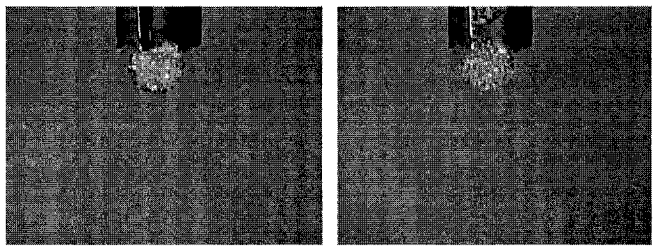

(d) Beads moved into syringe

(e) Beads can no longer be sucked in

Fig.B.2: Subsequent stages of drop retraction for a water droplet, with hydrophilic (45°) 150 - 210 (μm) diameter glass beads, in 500 cSt silicone oil

Appendix B.3

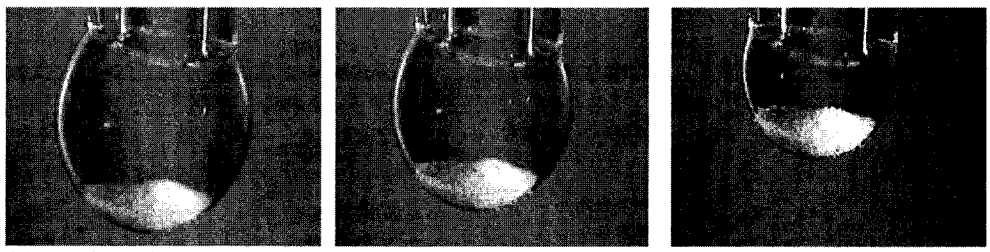

(a) Particles injected with water

(b) Water droplet remains spherical on retraction

(c) Droplet continues to remain spherical

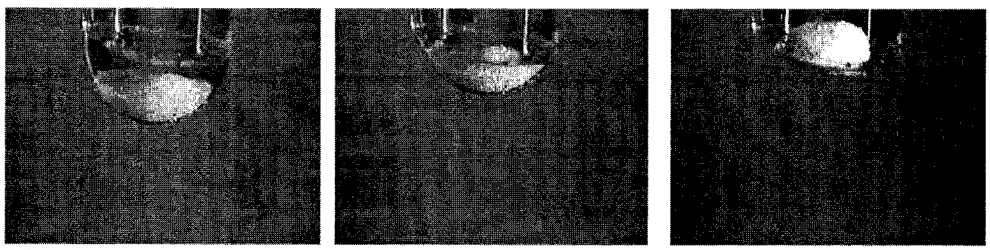

(d) Droplet continues to remain spherical

(e) Particles sucked in with water

(f) Particles completely sucked in with water

Fig.B.3: Subsequent stages of drop retraction for a water droplet, with hydrophilic (45°) < 105 (μm) diameter silica particles, in 5 cSt silicone oil

Appendix B.4

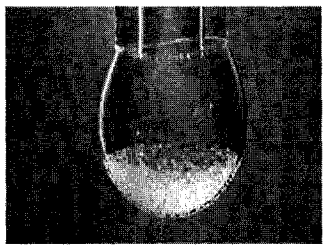

(a) Particles injected with water

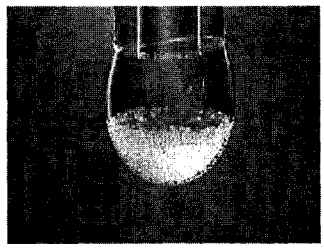

(b) Water droplet remains spherical on retraction

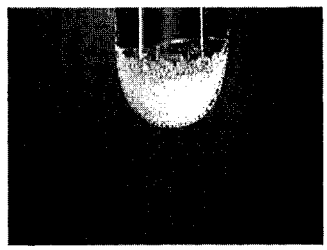

(c) Droplet continues to remain spherical

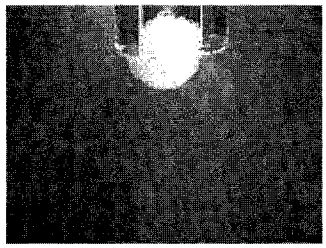

(d) Particles sucked into syringe

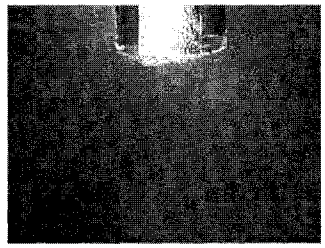

(e) Particles sucked in completely

Fig.B.4: Subsequent stages of drop retraction for a water droplet, with hydrophilic (45°) 150 - 210 (μm) diameter glass beads, in 5 cSt silicone oil

Appendix B.5

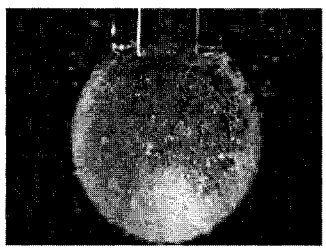

(a) Particles injected with water

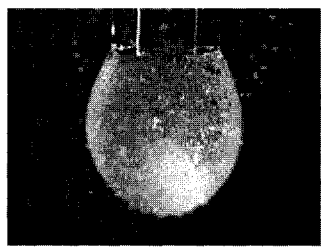

(b) Water droplet remains spherical on retraction

(c) Droplet starts to crumple on retraction

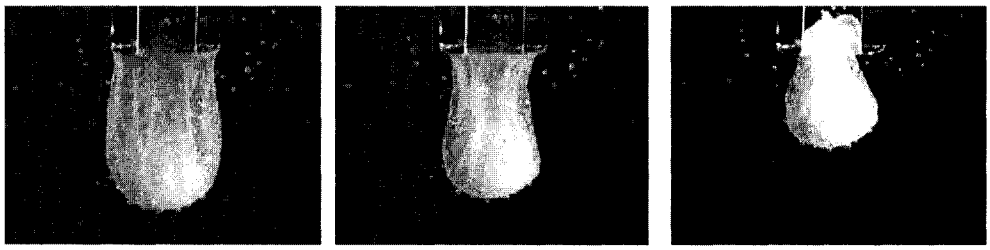

(d) Droplet continues to crumple on retraction

(e) Crumpling clearly visible

(f) Drop completely crumpled like a paper bag

(g) Crumpled droplet after retraction

(h) Water droplet slowly being expanded

(i) Droplet continues to expand to original shape

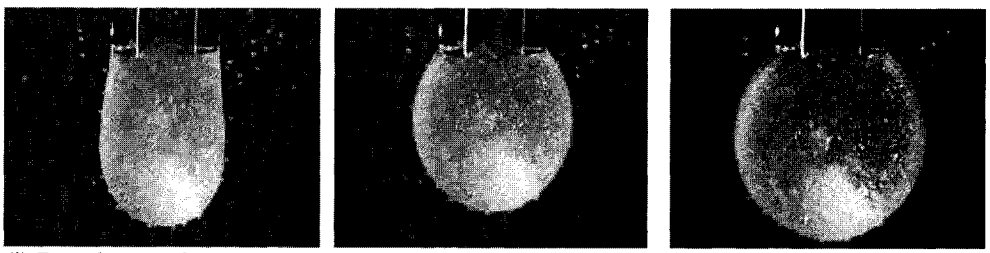

(j) Droplet continues to expand

(k) Water droplet continues to expand

(l) Droplet back to original shape

Fig.B.5: Subsequent stages of drop retraction and expansion for a water droplet, with hydrophobic (125°) c.a. 13 (μm) diameter silica particles, in 500 cSt silicone oil (Large capillary)

Appendix B.6

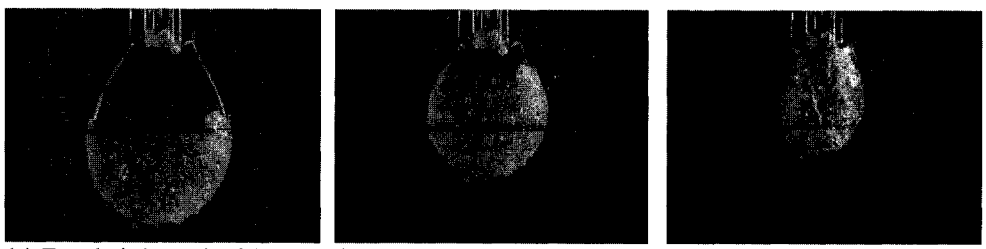

(a) Beads injected with water

(b) Water droplet remains spherical on retraction

(c) Droplet starts to crumple on retraction

(d) Droplet continues to crumple on retraction | (e) Crumpling clearly visible | (f) Drop falls off tip of capillary

Fig.B.6: Subsequent stages of drop retraction for a water droplet, with hydrophobic (125°) <105 (μm) diameter silica particles, in 500 cSt silicone oil

Appendix B.7

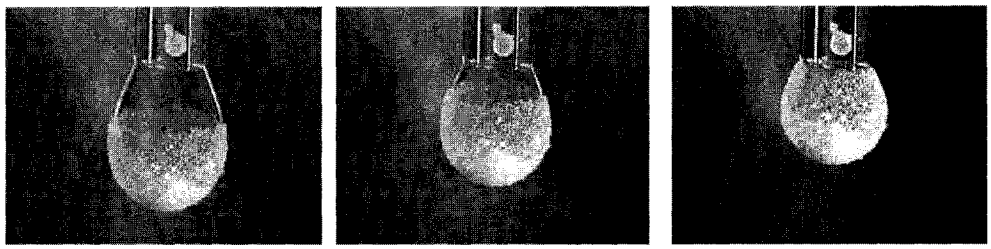

(a) Particles injected with water | (b) Water droplet remains spherical on retraction | (c) Droplet continues to remain spherical

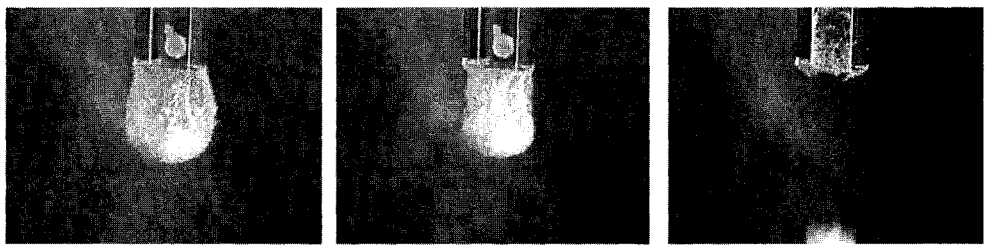

(d) Droplet starts to crumple on retraction | (e) Crumpling clearly visible | (f) Drop falls off tip of capillary

Fig.B.7: Subsequent stages of drop retraction for a water droplet, with hydrophobic (125°) <105 (μm) diameter silica particles, in 5 cSt silicone oil

Appendix B.8

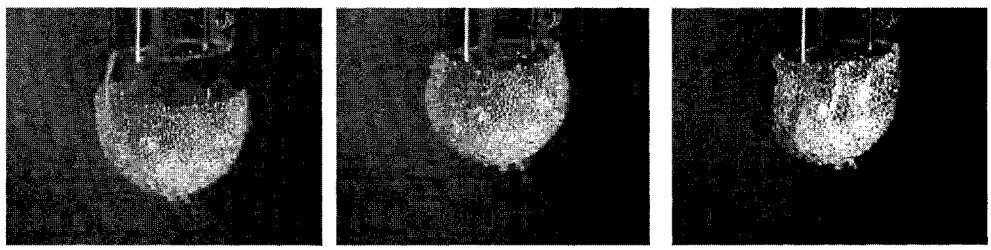

(a) Beads injected with water

(b) Water droplet remains spherical on retraction

(c) Droplet starts to crumple on retraction

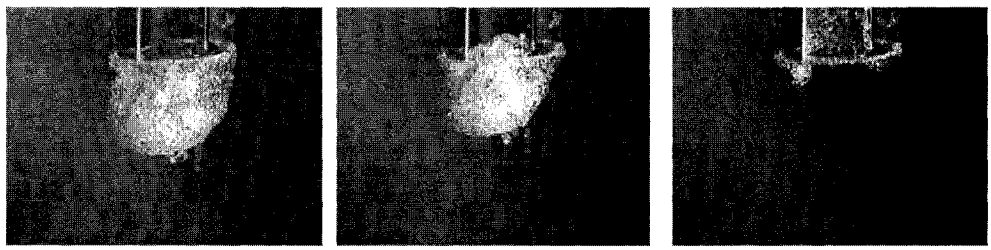

(d) Droplet continues to crumple on retraction

(e) Crumpling clearly visible

(f) Drop falls off tip of capillary

Fig.B.8: Subsequent stages of drop retraction for a water droplet, with hydrophobic (125°) 105 - 210 (μm) diameter glass beads, in 5 cSt silicone oil

Appendix B.9

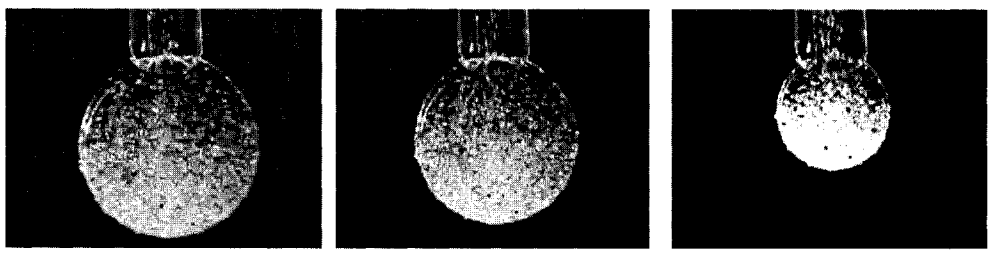

(a) Particles injected with silicone oil

(b) Oil droplet remains spherical on retraction

(c) Droplet continues to remain spherical

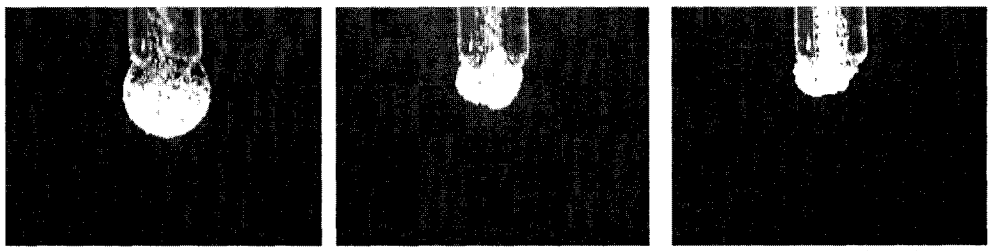

(d) Droplet continues to remain spherical

(e) Particles sucked in with some deformation

(f) Drop sucked in with silicone oil

Fig.B.8: Subsequent stages of drop retraction for a 500 cSt silicone oil droplet, with hydrophilic (45°), <105 (μm) diameter silica particles, in water

Appendix C

Drop Detachment Calculations

Calculations were based on the analysis discussed in Section 3.6 and using Equations 3.1 through 3.9. Calculations were done using an ***Excel Spreadsheet.***

Formulae and definition of terms

Formulae	Definition of terms
$z = R_c / V_d^{1/3}$	
$\varphi = z[0.50832 + z\{1.5257 + z(-1.2462 + z\,0.60642)\}] - 0.0115$	*Correction factor*
$F_\gamma = 2\pi R_c \gamma \varphi$	*Interfacial tension force*
$V_d = 4/3 \times \pi R_d^3$	*Volume of drop*
$V_p = 4/3 \times \pi R_p^3$	*Volume of a particle*
$V_{filled} = 1/3 \times \pi h^2 (3R_d - h)$	*Volume of drop filled with particles to height h*
$Np = 0.74\, V_{filled} / (4/3 \times \pi R_p^3)$	*Number of particles in filled drop*
$F_B = (\rho_p - \rho_{cp})\, 0.5\, V_p N_p g + (\rho_p - \rho_d)\, 0.5\, V_p N_p g + (\rho_d - \rho_{cp})\, V_d g$	*Force due to buoyancy*
$F_{VD} = 6\pi\mu R_d v$	*Force due to drag*

Case 1: Water droplet in 500 cSt (more viscous) silicone oil with hydrophobic 150 - 210 micron diameter glass beads

Parameters	Values	comment
R_c - Radius of capillary (m)	3.80E-04	*inner diameter of small capillary = 0.076 cm*
R_d - Radius of drop (m)	1.50E-03	*approximate drop diameter of 3 mm*
R_p - Radius of a particle (m)	9.00E-05	*150 - 210 microns diameter glass beads*
ρ_d - Density of drop (kg/m^3)	1000	*density of water*
ρ_p - Density of particle (kg/m^3)	2500	*density of glass beads*
ρ_{cp} - Density of continous phase (kg/m^3)	975	*heavier silicone oil 500 cSt*
μ - Viscosity of continous phase (kg/m.s)	4.88E-01	*heavier silicone oil 500 cSt*
γ - interfacial tension (N/m)	2.11E-02	*heavier silicone oil 500 cSt*
v - velocity of retraction (m/s)	7.33E-05	*average retraction velocity*
h - height covered by particles on drop (m)	5.00E-04	*< one-fourth the droplet diameter was covered*
g - acceleration of gravity (m/s^2)	9.81E+00	

Calculations

π	V_d	V_p	h	V_{filled}	z	φ	N_p	F_γ	F_B	F_{VD}
3.1416	1.41E-08	3.05E-12	5.00E-04	1.05E-09	0.1572	0.1016	2.54E+02	5.12E-06	1.50E-05	1.01E-06

Case 2: Water droplet in 5 cSt (less viscous) silicone oil with hydrophobic 150 - 210 micron diameter glass beads

Parameters	Values	comment
R_c - Radius of capillary (m)	3.80E-04	*inner diameter of small capillary = 0.076 cm*
R_d - Radius of drop (m)	1.50E-03	*approximate drop diameter of 3 mm*
R_p - Radius of a particle (m)	9.00E-05	*150 - 210 microns diameter glass beads*
ρ_d - Density of drop (kg/m^3)	1000	*density of water*
ρ_p - Density of particle (kg/m^3)	2500	*density of glass beads*
ρ_{cp} - Density of continous phase (kg/m^3)	915	*lighter silicone oil 5 cSt*
μ - Viscosity of continous phase (kg/m.s)	4.58E-03	*lighter silicone oil 5 cSt*
γ - interfacial tension (N/m)	1.97E-02	*lighter silicone oil 5 cSt*
v - velocity of retraction (m/s)	7.33E-05	*average retraction velocity*
h - height covered by particles on drop (m)	5.00E-04	*< one-fourth the droplet diameter was covered*
g - acceleration of gravity (m/s^2)	9.81E+00	

Calculations

π	V_d	V_p	h	V_{filled}	z	φ	N_p	F_γ	F_B	F_{VD}
3.1416	1.41E-08	3.05E-12	5.00E-04	1.05E-09	0.1572	0.1016	2.54E+02	4.78E-06	2.35E-05	9.49E-09

Case 3: Water droplet in 500 cSt (more viscous) silicone oil with hydrophobic 13 micron diameter silica particles

Parameters	Values	comment
R_c - Radius of capillary (m)	3.80E-04	*inner diameter of small capillary = 0.076 cm*
R_d - Radius of drop (m)	1.50E-03	*approximate drop diameter of 3 mm*
R_p - Radius of a particle (m)	6.50E-06	*13 microns diameter silica particles*
ρ_d - Density of drop (kg/m^3)	1000	*density of water*
ρ_p - Density of particle (kg/m^3)	2650	*density of silica particles*
ρ_{cp} - Density of continous phase (kg/m^3)	975	*heavier silicone oil 500 cSt*
μ - Viscosity of continous phase (kg/m.s)	4.88E-01	*heavier silicone oil 500 cSt*
γ - interfacial tension (N/m)	2.11E-02	*heavier silicone oil 500 cSt*
v - velocity of retraction (m/s)	7.33E-05	*average retraction velocity*
h - height covered by particles on drop (m)	5.00E-04	*< one-fourth the droplet diameter was covered*
g - acceleration of gravity (m/s^2)	9.81E+00	

Calculations

π	V_d	V_p	h	V_{filled}	z	φ	N_p	F_Y	F_B	F_{VD}
3.1416	1.41E-08	1.15E-15	5.00E-04	1.05E-09	0.1572	0.1016	6.74E+05	5.12E-06	1.61E-05	1.01E-06

Case 4: Water droplet in 500 cSt (more viscous) silicone oil with hydrophobic 150 - 210 microns glass beads

Parameters	Values	comment
R_t - Radius of capillary (m)	3.80E-04	*inner diameter of small capillary = 0.076 cm*
R_d - Radius of drop (m)	1.50E-03	*approximate drop diameter of 3 mm*
R_p - Radius of a particle (m)	6.50E-06	*13 microns diameter silica particles*
ρ_d - Density of drop (kg/m^3)	1000	*density of water*
ρ_p - Density of particle (kg/m^3)	2650	*density of silica particles*
ρ_{cp} - Density of continous phase (kg/m^3)	915	*lighter silicone oil 5 cSt*
μ - Viscosity of continous phase (kg/m.s)	4.58E-03	*lighter silicone oil 5 cSt*
γ - interfacial tension (N/m)	1.97E-02	*lighter silicone oil 5 cSt*
v - velocity of retraction (m/s)	7.33E-05	*average retraction velocity*
h - height covered by particles on drop (m)	5.00E-04	*< one-fourth the droplet diameter was covered*
g - acceleration of gravity (m/s^2)	9.81E+00	

Calculations

π	V_d	V_p	h	V_{filled}	z	φ	N_p	F_γ	F_B	F_{VD}
3.1416	1.41E-08	1.15E-15	5.00E-04	1.05E-09	0.1572	0.1016	6.74E+05	4.78E-06	2.47E-05	9.49E-09